IMPROVING THE PERFORMANCE OF DAMAGED FBECR IN CHLORIDE-CONTAMINATED CONCRETE

BY

MOHAMMED ISMAIL

A Thesis Presented to the

DEANSHIP OF GRADUATE STUDIES

KING FAHD UNIVERSITY OF PETROLEUM & MINERALS

DHAHRAN, SAUDI ARABIA

In Partial Fulfillment of the
Requirements for the Degree of

MASTER OF SCIENCE

In

CIVIL ENGINEERING

MARCH 2005

KING FAHD UNIVERSITY OF PETROLEUM AND MINERALS
DHAHRAN 31261, SAUDI ARABIA

DEANSHIP OF GRADUATE STUDIES

This thesis, written by **MOHAMMED ISMAIL** under the direction of his Thesis Advisor and approved by his Thesis Committee, has been presented to and accepted by the Dean of Graduate Studies, in partial fulfillment of the requirements for the degree of **MASTER OF SCIENCE IN CIVIL ENGINEERING.**

Thesis Committee

Dr. Ahmad Saad Al-Gahtani (Advisor)

Dr. Mohammed Maslehuddin (Member)

Prof. Omar S. Baghabra Al-Amoudi (Member)

Prof. Hamad I. Al-Abdul Wahhab
Department Chairman

Dr. Mohammad Abdul Aziz Al-Ohali
Dean of Graduate Studies

Date 28-11-2005

Dedicated to My Parents,

Brother and Sisters

ACKNOWLEDGEMENTS

All the praises and thanks be to Almighty Allah, Subhana-wa-taala, the most Merciful; the most Benevolent, for bestowing me with the health, knowledge, opportunity, courage and patience to complete this research. May the peace and blessings of Allah (SWT) be upon Prophet Mohammed (Sal allahu alahi wa sallam).

I acknowledge, with deep gratitude and appreciation, the inspiration, encouragement, valuable time and guidance given to me by my thesis Committee Chairman, Dr. Ahmad S.Al-Gahtani. Thereafter, I am deeply indebted and grateful to Dr. Mohammed Maslehuddin, my committee member, my unrestrained appreciation and gratitude goes for his constant assistance and guidance, an overt acknowledgement is dedicated for his ideas and interest in this research, Inspite of his busy schedule. I am also grateful to my other committee member Dr. Omar S. B. Al-Amoudi for his constructive guidance, valuable advices and cooperation.

I also acknowledge the sincere and untiring efforts to Engr. Mukarram Khan and Mr. Hassan Zakaria who assisted me during all stages of my experiments and also helped me in preparing the experimental set-up utilized in this study. Thanks are due to the department secretaries, Mr.Mumtaz and Mr.Solano for their help and assistance.

My heartfelt appreciation and gratefulness are dedicated to my mother, father, sisters, brother and uncles for their constant prayers, guidance, encouragement and support through out my career. They are the source of power, inspiration, and confidence in me.

Thanks are due to my senior colleagues at the university, Mr.Ibrahim, Mr.Shameem, Mr.Akber and Mr.Imran Ali for their valuable advices. My distinctive acknowledgements are dedicated to my friends Hameed, Ayub Azher, Moied, Asif, Siraj, Muqtader, Jaffer, Anees and Ayub. Special thanks are due to Shafi, Junaid, Atif, Mujahed and Abbas who were always there to help me. This chain of acknowledgments is incomplete without expressing the contributions of entire Indian community at KFUPM for affable guidance, and support which they imparted to me.

TABLE OF CONTENTS

LIST OF FIGURES

LIST OF TABLES

LIST OF PLATES

THESIS ABSTRACT (ENGLISH)

Name: Mohammed Ismail

Title: Improving the Performance of Damged FBECR in Chloride-Contaminted Concrete

Major Field: Civil Engineering

Date of Degree: March 2005

This study was conducted to evaluate the effect of surface damage on corrosion-resistance of fusion bonded epoxy coated (FBEC) steel bars cast in plain and blended cement concretes. The effect of exposure temperature (23±2°C, 35±2°C and 48±2°C) on the rate of corrosion was also evaluated. The effect of these parameters on the corrosion of FBEC bars was compared with the corrosion of mild steel bars by exposing the concrete specimens prepared with them and measuring corrosion potentials and corrosion current density at regular intervals. The corrosion current density measurements indicated that the defect-free FBEC bars were in a passive condition in all blended cements concrete specimens with up to 2% chloride, by weight of cement, even when they were exposed to 48°C. The corrosion current density in concrete specimen with black and damaged FBEC steel bars increased with an increase in the exposure temperature and the chloride contamination. The long-term performance of FBEC steel bars exposed to 48 °C was satisfactory in the silica fume cement concrete specimens admixed with up to 2% chloride, by weight of cement.

MASTER OF SCIENCE

KING FAHD UNIVERISTY OF PETROLEUM AND MINERALS

Dhahran, Saudi Arabia

March 2005

THESIS ABSTRACT (ARABIC)

الاسم : محمد إسماعيل

العنوان : تحسين أداء قضبان الحديد المطلية في بيئة كلور خرسانية

القسم : الهندسة المدنية

تاريخ منح الدرجة : مارس ٢٠٠٥

تم إجراء هذه الدراسة لتحديد اثر الخدوش على طبقة طـلاء قـضبان حديـد التسليح المطلية بمادة الأيبوكسي عند استخدام خرسانة اسمنت عادي وخرسانة اسمنت مخلوط بمواد إضافية مثل سليكافيوم، فلاي أش و بلاست فرنس سلاق. أيضا تم تحديد اثر التعرض لدرجات الحرارة المختلفة (٢٣±٢، ٣٥±٢، و٤٨±٢ درجة مئوية) على معدل تآكل الحديد. تمت مقارنة التآكل نتيجة لصدأ الحديـد فـي القـضبان المطليـة ومقارنة بالتآكل في القضبان الغير مطلية بواسطة قياس شدة الجهد الكهربائي للتيـار الناتج عن الصدأ وأيضا شدة التيار الكهربائي خلال فترات زمنية منتظمة. أظهـرت نتائج قياس شدة التيار ان القضبان التي لم تتعرض لخدوش في سطح الطلاء كانـت خاملة في كل بيئات الكلور حتى نسبة تركيز ٢% و تعريضها لدرجـة حـرارة ٤٨ درجة مئوية. بيمنا وجد إن الصدأ في القضبان التي تعرضت لخدوش في الطلاء يزيد بزيادة كمية الخدوش و درجة الحرارة وتركيز الكلور في العينة. وقـد وجـد إن أداء القضبان المطلية بالأيبوكسي كان مرضي في درجة الحرارة ٤٨ درجة مئوية وحتـى نسبة تركيز ٢% من الكلور في خلطة الخرسانة.

ماجستير العلوم
جامعة الملك فهد للبترول والمعادن
الظهران، المملكة العربية السعودية
مارس ٢٠٠٥

CHAPTER 1

INTRODUCTION

2.1 CONCRETE DURABILITY IN AGGRESSIVE ENVIRONMENT

Reinforced concrete has proved to be an efficient and durable construction material for structures over a long period of time. Its low cost, ecologically favorable profile and excellent strength and stiffness properties coupled with its ease of manufacture at the construction site are among the important factors that have established it as a major construction material.

Although concrete is the most widely used construction material, it has its own limitations. It deteriorates rapidly in conditions where moisture and temperature are high and more so, when it is exposed to aggressive media. The reduction in the useful service-life of reinforced concrete construction, mainly due to reinforcement corrosion, in North America, Europe and the coastal regions of the world is of great concern to the construction industry. Considerable resources have to be diverted towards the repair and rehabilitation of the deteriorated concrete structures. While reinforcement corrosion in the temperate climatic conditions is mainly attributed to the use of deicer salts; in the arid and semi-arid regions, deterioration is attributed to the following: (i) severe climatic and geomorphic conditions, (ii) inappropriate materials specifications, and (iii) inadequate construction practices [22]. In such environments, the construction practices need to be modified to be compatible with the exposure conditions. The concrete construction in

such environments should be designed for durability in addition to strength and workability. In these regions, concrete quality should be specified in terms of chloride diffusion and water permeability indices Shameem et al. [1].

2.2 CONCRETE PROTECTION

A variety of solutions have been proposed to protect the reinforcing steel from corrosion in order to minimize concrete deterioration. However, it is postulated that good quality fusion-bonded epoxy-coated (FBEC) steel bars perform better than galvanized steel, concrete coated with water-proofing membranes, latex-modified concrete, corrosion inhibitors and silane and methacryalate coatings Malasheski et al. [2] and Pfeifer et al. [3].

FBEC bars have been used worldwide for more than two decades to enhance the useful service-life of reinforced concrete structures in aggressive environments. In Saudi Arabia, many organizations, such as Saudi Aramco, Royal Commission for Jubail and Yanbu, Saudi Arabian Basic Industries Corporation, use the coated bars in new construction projects, particularly in substructures. Nowadays, the use of FBEC bars by the private sector is increased in Saudi Arabia. However, there is a main concern with regard to the use of bars with damages on the coating film and their subsequent effect on the corrosion resistance, especially in the aggressive exposures of the Arabian Gulf environmental conditions.

Field observations indicate that handling and fabrication of FBEC bars create significant damages on the coating as a result of lack of supervision and skilled labors in construction sites Al-Gahtani et al. [4]. In order to improve the concrete quality, silica

fume, fly ash and blast furnace slag will be used as mineral admixture with Portland cement. The durability of concrete structures through the use of mineral admixtures with FBECR has not been investigated within the Arabian Gulf environment.

2.3 NEED FOR THIS RESEARCH

Data are lacking on the performance of FBEC reinforcing steel bars in the environmental conditions of the Arabian Gulf. Moreover, there is no enough information in the literature regarding the degree of damage that is vulnerable for corrosion in the context of chloride contamination and concrete protection improved by the concomitant use of mineral admixture (i.e. silica fume, fly ash and blast furnace slag) with FBEC rebars. In addition, the effect of exposure temperature, particularly in hot climatic conditions of Arabian Gulf, is in need of further investigation.

2.4 OBJECTIVES

The broad objectives of this research were to evaluate the performance of damaged FBEC steel bars in combination with supplementary cementing materials in improving the durability of reinforced concrete construction. The specific objectives were as follows:

1. To evaluate the effect of coating damage on corrosion of FBEC bars embedded in chloride-contaminated concrete,

2. To evaluate the combined effect of FBEC bars and supplementary cementing materials in improving concrete durability,

3. To evaluate the effect of exposure to high temperature on the performance of FBEC bars in chloride-contaminated concrete, and

4. To provide guidelines on the allowable coating damage with respect to chloride contamination in plain and blended cement concretes under varying temperature conditions.

CHAPTER 2

LITERATURE REVIEW

2.1 PROTECTION OF REINFORCING STEEL

Portland cement concrete provides both chemical and physical protection to the reinforcing steel. The chemical protection is provided by the highly alkaline nature of the pore solution (pH >13). At this high pH, steel is passivated in the presence of oxygen, presumably due to the formation of a sub-microscopically thin gamma-ferric oxide (γ-Fe_2O_3) film Pourbaix [5].

According to Page [6], the lime-rich layer, which is observed at the steel-concrete interface, provides further protection to the steel. This was confirmed by Leek and Poole [7] who reported that the interfacial layer surrounding the steel bars consists of an aggregate free zone of portlandite [$Ca(OH)_2$] of variable thickness (5 to 15 μm) disrupted by inclusion of calcium-silicate-hydrate (C-S-H) gel. This layer is thought to screen most of the surface of the steel from the aggressive ions and to act as an alkaline buffer to pH reduction resulting from the hydrolysis of corrosion products. According to Sagoe-Crentsil and Glasser [8], both $Ca(OH)_2$ and C-S-H gel form a buffering pair, and a high pH is readily maintained by C-S-H as well as $Ca(OH)_2$. The physical protection to steel is provided by the dense and impermeable structure of concrete, which retards the diffusion of the aggressive species, such as chlorides, carbon dioxide, oxygen and moisture, to the steel-concrete interface.

2.2 MECHANISMS OF REINFORCEMENT CORROSION

The most common form of reinforcement corrosion is electrochemical. It requires an anode (where oxidation of steel takes place), a cathode (where reduction of oxygen occurs), an electrical conductor (steel reinforcement) and an electrolyte (concrete). At the anode, metallic iron goes into solution by oxidation (loss of electrons) as follows:

$$Fe \rightarrow Fe^{++} + 2e^{-} \qquad \text{(Oxidation of steel)} \qquad (1.1)$$

At the cathode, dissolved oxygen in the pore water that has diffused to the steel surface is reduced by the electrons supplied by the anodic reaction to form hydroxyl ions:

$$\frac{1}{2}O_2 + H_2O + 2e^{-} \rightarrow 2OH^{-} \qquad \text{(Reduction of oxygen)} \qquad (1.2)$$

The OH^{-} ions flow back to the anode through the concrete to complete the circuit. The rate of this transfer depends on the temperature, moisture content, ionic concentration and electrical resistivity of concrete. The OH^{-} ions at the anode combine with the Fe^{++} cation to form a fairly soluble ferrous hydroxide, $Fe(OH)_2$ as follows:

$$Fe^{++} + 2OH^{-} \rightarrow Fe(OH)_2 \qquad (1.3)$$

The above explanation is diagrammatically shown in Figure 2.1.

If sufficient oxygen is available, this product can be further oxidized to form insoluble hydrated red rust. This rust can have a volume 2 to 14 times of the parent iron from which it is formed (see Figure 2.2). The rust product can exert tensile stresses of the

order of 4000 psi, which is about 10 times the tensile strength of normal concrete. This excessive pressure causes the concrete cover to crack leading to its eventual spalling off at an advanced stage of the corrosion process leading to a reduction in the cross-sectional area of the structural member.

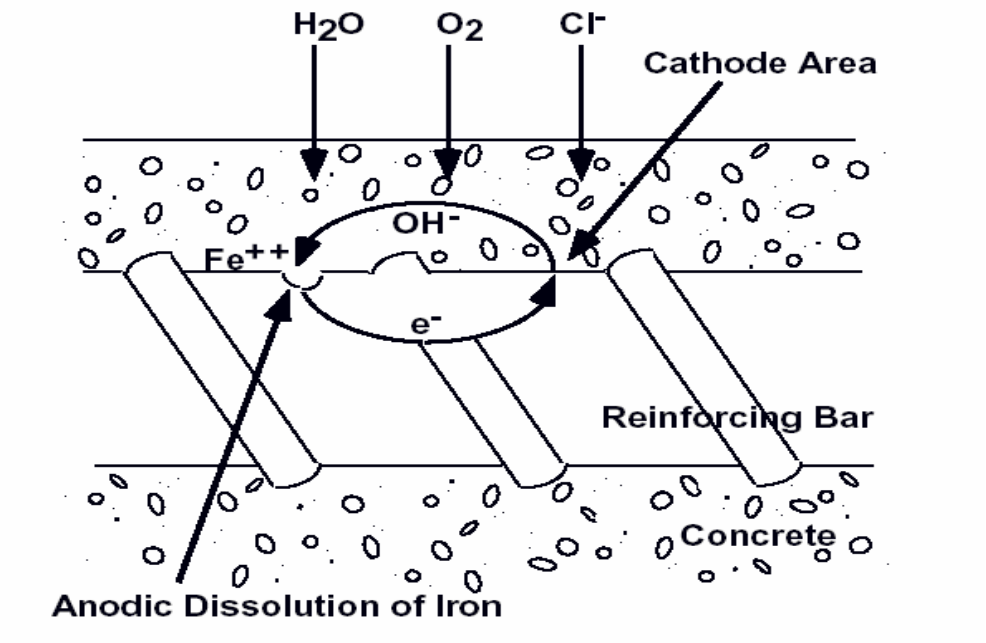

Figure 2.1: Schematic representation of the mechanics of reinforcement corrosion.

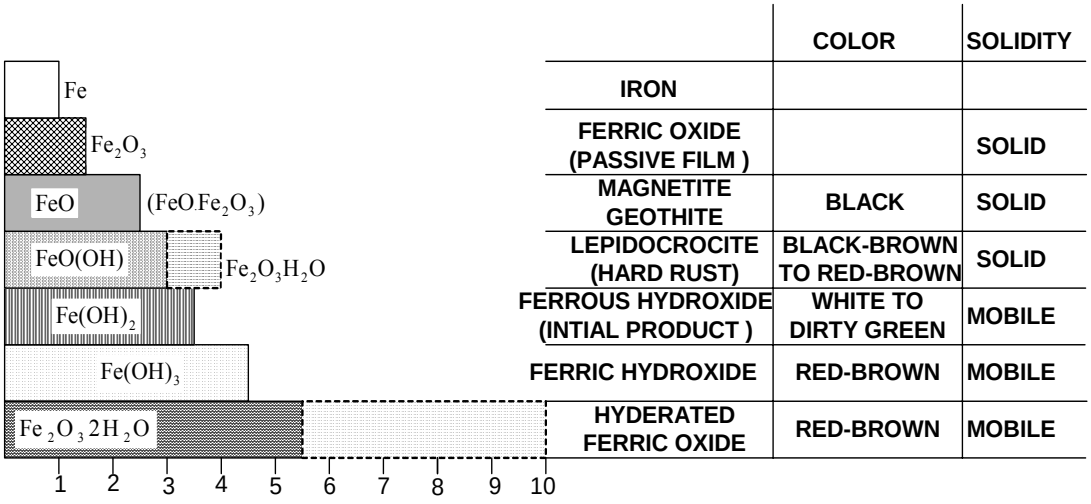

	COLOR	SOLIDITY
IRON		
FERRIC OXIDE (PASSIVE FILM)		SOLID
MAGNETITE GEOTHITE	BLACK	SOLID
LEPIDOCROCITE (HARD RUST)	BLACK-BROWN TO RED-BROWN	SOLID
FERROUS HYDROXIDE (INTIAL PRODUCT)	WHITE TO DIRTY GREEN	MOBILE
FERRIC HYDROXIDE	RED-BROWN	MOBILE
HYDERATED FERRIC OXIDE	RED-BROWN	MOBILE

Figure 2.2: Volume of various oxides formed due to corrosion of iron.

Hence, it can be noted that oxygen and moisture are the most important ingredients for reinforcement corrosion to occur and the ingress of these elements through the concrete must be controlled to avoid corrosion.

2.3 CHLORIDE-INDUCED REINFORCEMENT CORROSION

As mentioned in Section 2.1, a thin insoluble film of γ-Fe_2O_3 is formed on the steel bars, which prevents the Fe^{++} cations from entering into solution and also acts as a barrier to prevent oxygen anions from contacting the steel surface. This passivity is disrupted by the ingress of chloride and carbonation to the steel surface.

Corrosion of steel in concrete proceeds at a far greater rate in the presence of chloride ions. The chloride ions act as a catalyst in the corrosion reactions. Most researchers believe that the chloride ion initiates the corrosion reaction by depassivating

the natural oxide film on the steel surface, allowing the iron to dissolve into solution. On reaching the iron substrate, the chloride ion oxidizes the iron to form $FeCl_3$ and draws its unstable ferrous ion into solution, where it reacts with the available hydroxyl ions to form $Fe(OH)_2$. This release the Cl^- ion back into the solution and consumes hydroxyl ions, as seen in the following reactions:

$$2Fe + 6\,Cl^- \rightarrow 2FeCl_3{}^- + 4e^- \quad (1.4)$$

$$FeCl_3{}^- + 2OH^- \rightarrow Fe(OH)_2 + 3Cl^- \quad (1.5)$$

The electrons released in the oxidation reaction, as shown in Equation 1.4, flow through the steel to the cathode. This process results in an increase in the concentration of the chloride ions and a reduction of the pH at the points of corrosion initiation, probably accounting for the process of pitting corrosion. Equation 1.5 indicates that 3 chloride ions are released as a by-product of steel corrosion indicating that once the chloride ion reaches the metal surface, no further chloride ions are required and depending on the electrical resistivity of concrete either general or local corrosion proceeds. It can also be noted that even for the chloride-induced reinforcement corrosion to occur, the presence of moisture and oxygen is necessary.

2.4 CARBONATION OF CONCRETE

Reinforcement corrosion may also be caused by carbonation of concrete. Carbonation involves a reaction of carbon dioxide, CO_2, with $Ca(OH)_2$, in the cement gel to form insoluble $CaCO_3$ and water:

$$CO_2 + Ca(OH)_2 \xrightarrow{\text{moisture}} CaCO_3 + H_2O \quad (1.6)$$

This reaction results in a reduction in the pH of the electrolyte to less than 8.5 due to the removal of hydroxyl ions from the pore water. At this low pH, steel is no longer passive and corrosion can occur. Factors influencing carbonation of concrete and the subsequent corrosion of embedded steel include concrete mix design, depth of reinforcement cover, improper curing, moisture conditions and temperature.

Steel corrosion due to carbonation of concrete is mainly observed in the old structures and in industrial environments. The environmental conditions in the coastal areas of the Arabian Gulf (Temperature: 35°C to 45°C; relative humidity: 45 to 60%) are conducive for the acceleration of carbonation of concrete and the resulting depassivation of the reinforcing steel. Carbonation depths of more than the concrete cover were measured in reinforced concrete structures located in industrial environment in a survey conducted by King Fahd University of Petroleum and Minerals [9].

Depassivation of the reinforcing steel occurs by the reduction of the pore solution pH to less than 8.5, due to carbonation or by ingress of chloride ions to the steel–concrete interface. A number of mechanisms by which chlorides break down the passive layer have

been proposed, e.g., the chemical dissolution of the film [10-11], the build-up of pinholes at the film-substrate interface [12] and due to high chloride concentrations at the iron oxide-pore solution interface that leads to local acidification and pitting [13].

Chloride ions play a dominant role in the initiation of reinforcement corrosion. From this perspective, ACI 318 limits the water-soluble chlorides to 0.15% by weight of cement. ACI Committee 224, adopting a more conservative approach, has suggested that the acid-soluble chloride content should not be more than 0.2% by weight of cement. The British Standard, BS 8110, allows a maximum chloride content of 0.4%. The Norwegian Code, NS 3474, allows an acid–soluble chloride content of 0.6%. RILEM permits 0.4% and the revised Australian Standard for Concrete Structures, AS 3600, allows an acid-soluble chloride content of 0.8 kg/m^3 of concrete. Rasheeduzzafar et al. [14] indicated that the chloride threshold limits for cements with up to 8% C_3A agree very well with the ACI 318 limit of 0.15% water-soluble chlorides. They also reported that the ACI, BS and Australian code limits appeared to be conservative for concrete prepared with high C_3A cements.

Recent research findings have shown that cement alkalinity also significantly influences the chloride binding and hence the volume of free chlorides [15-18]. Taking into account the concomitant effect of chlorides and alkalinity, Hausmann suggested that the critical Cl^-/OH^- ratio is about 0.6 [19]. Gouda [20] indicated that the Cl^-/OH^- ratio was 0.3 based on the pH values of the electrolyte representative of the concrete pore solution.

Mangat and Moloy [21] indicated that a universal threshold Cl^-/OH^- ratio is not applicable to different cement concretes. In their investigation, reinforcing steel corrosion was observed in the control matrix when the pore fluid Cl^-/OH^- was 13. Al-Amoudi et al. [22] reported minimal reinforcement corrosion in silica fume and blast furnace slag cement mortar specimens placed in the aggressive environment of sabkha, even at Cl^-/OH^- ratios of 3.3 and 6.5, respectively.

Chloride ions are often unintentionally inducted into the concrete through the constituent materials like salt-contaminated aggregates or water and sometimes intentionally in the form of chemicals to accelerate the setting of concrete. Moreover, they may penetrate the hardened concrete when exposed to aggressive environment. While the chlorides contributed by the constituent materials can be controlled by strict adherence to improved construction practices, the ingress of chloride ions from the service environment can only be controlled by producing a good quality concrete and/or coating with impermeable membranes.

2.5 FUSION-BONDED EPOXY-COATED REINFORCEMENT

2.5.1 Epoxy Coating Material

Generally, the epoxy material used for coating the reinforcing steel bars is a bisphenol-amine powder formulation [23-26]. This epoxy resin is diglycidyl ether which is a thermosetting material belonging to the polyaddition plastics family [27-28]. The functional chemical groups forming the epoxy consist of carbon and oxygen atoms arranged in various possible structures. The epoxy groups are also termed epoxides –more frequently in Europe- in recognition of their nature as oxides [29].

Epoxies are classified as thermosetting materials because their cure process is accelerated by heat [30]. Upon full curing, they retain their shape up to their decomposition temperatures. Thus, changes in temperature do not readily cause a change in their physical properties [27]. Liquid epoxy paints, on the other hand, are classified as thermoplastic materials [31]. Exposure to heat may significantly change their physical properties.

Epoxy systems usually consist of two components: an epoxy resin and a curing compound. However, when in powder form, the two components are contained within each powder particle [30]. Therefore, mixing of epoxy powders is unnecessary. Fillers, pigments and flow control agents can be added in various quantities to the epoxy. The type and quantity of each of these constituents, as well as the blend process, significantly affect the properties of the final product [27]. The fusion blend process (melt mix), in

which the solid ingredients of the epoxy are integrated into each particle, yields a product with high potential for good performance.

The epoxy powder is usually applied to the reinforcing steel bars in a process known as fusion bonding. Epoxy fusion bonding is a heat-catalyzed chemical reaction by which the epoxy transforms from a hard brittle material into a tough elastic-like material [30-31]. This thermostatic process is an irreversible chemical reaction [32]. It develops molecular or polar bonding between the epoxy and the steel [33]. As a result to this chemical bonding, heating the cured coating will not cause it to soften. In addition to the chemical bonding, physical roughness on the steel surface provides a mechanical anchorage to increase the bond between the epoxy and the steel bar.

2.5.2 Epoxy Material Characteristics

Epoxy coating materials have been known for their excellent characteristics. Some of the most desirable features are [27, 29-30, 35]:

- Excellent adhesion;
- Ease of cure;
- Mechanical strength;
- High electrical insulation;
- Resistance to solvents and chemicals;
- High ductility;
- Low shrinkage upon polymerization;
- Good heat resistance; and
- Low oxygen and chloride ion permeability.

The epoxy coating materials have also some undesirable features. The most pronounced ones are water absorption and water permeability [36, 27-29]. Moisture permeation through the epoxy coating has been recognized a long time ago. Exposure of the epoxy coatings to moisture greatly reduces the adhesion between the epoxy and the steel. Loss of adhesion, however, does not automatically cause corrosion of the metal. Another undesirable feature is the tendency of the epoxy-coated bars to slip in concrete when subjected to elevated temperature exceeding 100°C (212°F) [36]. Slipping may occur although the epoxy coating can tolerate a temperature increase of to about 200°C (392°F).

2.5.3 Function of Epoxy Coating

The primary function of epoxy coating, as a barrier-type, is to prevent chloride ions from coming in contact with steel [37-39]. However, it has been reported in literature that epoxy coating works as an isolator for the steel from coming in contact with oxygen, moisture, and chloride ions [40-43]. While it has been proven experimentally that the epoxy coating is essentially impermeable to chloride ions and to oxygen diffusion, its resistance to moisture penetration has not been established.

The epoxy coating offers corrosion protection to steel in concrete by three main mechanisms: (i) protect the steel from chloride ions; (ii) increasing the electrical resistance along the corrosion cell path; and (iii) retarding the cathodic reduction process. Epoxy coating on the steel, inherently, increases the macro-corrosion cell resistive path [27, 34, 39, 44]. As a result, the flow of corrosion current between adjacent coated steel locations is greatly reduced. As long as this feature is maintained, the risk of developing

destructive macrocell action is kept low. The epoxy coating prevents the cathodic reactions (mainly oxygen reduction) from taking place on the underlying steel, thereby hindering the corrosion process [34, 44].

In short, the epoxy coating is effective if it abates the driving force for corrosion created by a potential difference in a corrosion cell, and sustained by continuous cathodic reactions. Even if corrosion were to occur, the total metal lost in the concealed iron would be greatly reduced and the risk of concrete deterioration would be minimized.

The ability of epoxy-coated steel to perform well depends on the properties of the epoxy material as well as the characteristics of the coated steel as a finished product to the following requirements [36, 45]:

- High coating strength, toughness, and long-term durability;
- High adhesive strength to steel substrate;
- High resistance to alkaline concrete, carbonized concrete, chloride-contaminated concrete;
- High resistance to oxygen and water vapor diffusion; and
- High resistance to normal low and elevated temperatures.

In addition, the coated bars should contribute to satisfactory structural behavior of the concrete members.

2.6 EVOLUTION OF EPOXY-COATED REINFORCEMENT

When corrosion-induced reinforcement deterioration was recognized on bridge decks, research was launched on determining the mechanism of distress and methods of prevention. Efforts were concentrated upon investigation and trial use of moisture barrier systems to prevent the ingress of chloride ions to the embedded reinforcing steel. Other methods or systems to accomplish the same purpose were also identified. Nonmetallic coatings were the primary alternatives. The first use of organic coating to protect against corrosion was reported in the 1950's [34]. The successful applications of epoxy coatings on underground transmission pipes for corrosion prevention encouraged the industry to focus on epoxy resins. Pipe coatings were electrostatically applied with powder epoxies.

In March 1973, the Federal Highway Administration (FHWA) initiated the National Experimental and Evaluation Program (NEEP) Project No.16, Epoxy-Coated Reinforcing Steel. Under this project, the National Bureau of Standards (NBS) and the FHWA, Office of Research and Office of Development, conducted extensive research. Based on NBS preliminary tests and evaluation, four epoxy products were pre-qualified for use in the NEEP 16 Project. The project then encouraged highway agencies to construct experimental projects to evaluate the coated reinforcement. Information was disseminated to insure that the coated bars used in these projects were equivalent to those that had passed stringent research tests [46-48].

At that time, the use of epoxy-coated bars came in lieu of the moisture barrier systems required on new bridge deck constructions. Reinforcing bar coating was done by several companies scattered throughout the USA. These companies were specialized in

pipe coating therefore, they modified their equipment for reinforcing bar coating [47]. The first epoxy powder specifically formulated for reinforcement coating was put in the market in 1976 [42]. The industry of coating reinforcing steel grew fast. In 1982, approximately 20 coating application companies were established in the United States and Canada [33]. Because of the special needs of the development material, many of the applicators provided a fabrication service, and some were directly involved in field installation of the coated bars.

Recently, the application of epoxy-coated reinforcement on bridge decks and other concrete structures became very widespread. Discussions are almost exclusively limited to non-prestressed type of reinforcement. However, epoxy coated prestressing strands are also commercially available [40].

2.7 CORROSION OF EPOXY-COATED REINFORCING STEEL

Unfortunately, instances of premature failure of the epoxy coating and significant corrosion of steel substrate have occurred recently. The premature deterioration of the substructures of the Florida Keys bridges in the late 1980's was the first major incident whereby four bridge substructures in the Florida Keys deteriorated significantly after about 6 to 10 years in service. Corrosion was noted on both straight and bent coated bars. It is likely that the high water salinity and high temperature in Florida promoted corrosion, but several other factors were raised as possible causes of that failure. Damage and debonding of epoxy coating prior to concrete placement were among the major factors.

Other corrosion problems related to epoxy failure were also reported in Oregon and New York [27]. Three bridge decks and one noise barrier wall constructed with epoxy-coated bars were identified, with at least a portion of each structure suffering from reinforcement corrosion or corrosion-related distress, or both [50]. These structures were subjected to both freeze-thaw cycles and deicing salt application.

In the Middle East, some epoxy-coated bars stored outdoors for over six months exhibited cracking and debonding as well as under film corrosion [31]. The coating was discolored and debonded on one side of the bar. Fine cracking of the substrate, in addition to crystalline deposits, were discovered beneath the coating. The major cause of coating failure was attributed to inadequate surface preparation.

Inspite of these incidents, there is no published evidence to date of any corrosion-related damage in bridge decks incorporating coated bars within the US. Apparently, the coated bars provide a high degree of protection in chloride-contaminated bridge decks [51]. However, it has been debated whether the generally good corrosion performance of sampled coated bars from bridge decks was due to epoxy coating or to improved concrete quality and deeper cover [50].

The deterioration of bridge substructures in Florida has raised concerns about the effectiveness of the epoxy coatings to prevent chloride-induced corrosion of reinforcement in highly corrosive environments. The concern over performance of coated bars was heightened after new observations regarding the propensity of the coated reinforcement to lose its protection.

Clear [52, 53] has reported that fusion-bonded epoxy coatings will not be effective in providing long-term (50 years or more) protection to reinforcement in salt-contaminated concrete. It has been said that an unexpected failure mechanism involving progressive loss of coating adhesion and under-film corrosion occurs even in high quality coated bars. A highly corrosive environment can cause a pattern of debonding, blistering, and cracking of the epoxy film.

2.8 HISTORICAL REVIEW OF THE USE OF FBEC BARS IN CONCRETE

In most cases coating of the reinforcement serves as a means of isolating the embedded steel from the surrounding environment. Thus, an intact coating shields the steel from the various adverse conditions occurring at the concrete-steel interface which can cause corrosion of the steel and subsequent failure of the structure. In general, the coatings can be said to shield the steel from corrosive solutions and water; to greatly reduce the area of exposed steel and consequently lower the probability that an area of exposed steel coincides with an area of protection failure by the concrete; and to increase the resistance of the steel to stray current corrosion, stress corrosion cracking, and hydrogen embitterment. More specifically, coating of reinforcing steel is generally used to eliminate the effect of some anticipated factors which promote corrosion of the embedded steel.

Research on epoxy coatings for deformed reinforcing steel bars was initiated in the 1960s by the Federal Highway Administration, U.S.A; the organic coating being one of many innovative concepts that were studied to address the rapidly increasing serious

problem of bridge deck deterioration. The corrosion resulted in expansion forces that delaminate the concrete decks and led to even more serious structural problems.

A major contract research study was first conducted at the National Bureau of Standards to evaluate different types of coatings applied by different means, using corrosion, bending (around pins), and pullout tests. The results of this test program clearly indicated that the only impervious and touch/bendable coatings were the epoxy 'powder' coatings that were applied by the electrostatic spray fusion-bonding process that had been developed to coat steel pipes for the pipeline industry.

The first major field application of epoxy-coated reinforcement bars was in a Pennsylvania bridge deck in 1973. Fusion-bonded epoxy-coated reinforcement reached the commercial market in 1976, and fusion-bonded epoxy-coated welded wire fabric reached the market in 1984. In 1981, an ASTM standard specification for epoxy-coated reinforcing steel bars was issued, permitting a range of epoxy thickness between 5 to 12 mils (103 and 300 μm) [54].

Field construction practices relative to epoxy-coated reinforcement have become fairly well standardized. Generally, shop fabrication (bending) of epoxy-coated reinforcing bars is performed after the bars are coated. Acceptable field practice with nonmetallic or coated reinforcing bars includes handling with nylon slings, supported with nonmetallic or coated wire supports (chairs), and in place epoxy touch-up to damaged coating.

Although the original trend was to use epoxy-coated reinforcement only in the top layers of reinforcement in bridge decks, the present trend is to use epoxy-coated bars in

both the top and bottom layers of bridge-deck reinforcement. There have been notably successful applications of epoxy-coated reinforcing bars in continuously reinforced concrete highway pavements as well [55].

Many investigations have been carried out to determine the effectiveness of epoxy coating for reinforcing steel in concrete. Weyers and Candy [56] reported that epoxy coating for reinforcing steel does provide a level of corrosion protection in the field against the deterioration of concrete caused by corroding reinforcing steel. Treadaway and Davis [57] showed that slabs made with epoxy-coated bars showed no cracks while galvanized steel performed adequately in poor quality, carbonated concrete, but could not resist substantial chloride contamination. In another study, Swamy [58] showed that, irrespective of concrete cover and epoxy film thickness, the epoxy-coated bars remained totally unaffected by rust. All bars remained unpitted, and there was practically no sign of corrosion in any of the test specimens. Results after two years of accelerated exposure, however, indicated the presence of isolated blisters in the 100 μm (3.9 mils) coating but even then they remained unpitted.

McKenzie [42] evaluated the effect of defects in commercially produced epoxy-coated reinforcing steel. The conditions investigated included uncoated ends, repaired ends and bent bars. The results of that study indicated a lower cracking and severity of cracking in specimens made with epoxy-coated reinforcement compared with those containing uncoated reinforcement over a two-year period. Reinforcement corrosion, observed beneath the epoxy coating, was of light surface without loss in the bar section, or peeling or blistering of the coating, whilst there was noticeable loss in the bar section due to corrosion of the uncoated bar.

Zayed et al. [26] evaluated the effect of different surface and mechanical condition on the corrosion behavior of epoxy-coated reinforcing steel exposed to a marine environment. The effects of degree of bend, epoxy damage, surface condition of the steel, and presence of cracks in concrete and manufacturing sequence were evaluated. The results of that study indicated that after 300 days of exposure, the corrosion in bent epoxy-coated steel appeared to be in the order of magnitude lower than that of the bare bent steel. Fabrication bending resulted in loss of adherence of the epoxy, and corrosion was observed in the resulting disbonded area.

Erdogdu et al. [67] evaluated the effects of different degrees of damage on the plain and epoxy coated bars in laboratory for that plain and epoxy coated reinforcing steel bars were cast in concrete slabs and exposed in the laboratory to 3% sodium chloride solution. The concrete slabs had a water to cement ratio of 0.6 and steel reinforcement had 20 mm concrete cover. The epoxy-coated bars were with no damage, 1% and 2% damage to the coating. They monitored the experiment on a regular basis using linear polarization and open-circuit potential techniques. After 2 year monitoring program, they indicated that the corrosion current density was negligible for epoxy-coated bars with no damage to the coating regardless of the exposure conditions and that the undamaged epoxy-coated bars provided excellent performance in preventing reinforcement corrosion in reinforced concrete structures subjected to a chloride environment. Similarly, rebar with damaged epoxy coating gave no evidence that sufficient rust had accumulated at the steel/concrete interface to cause the concrete cover to crack.

Sagues and Powers [59] evaluated the mechanisms of coating disbondment by exposing regularly-produced epoxy-coated rebars to liquid solutions of calcium

hydroxide, sodium chloride, and calcium hydroxide with sodium chloride. The tests were conducted under freely corroding conditions and also under anodic and cathodic polarized conditions. The results indicated that the adherence of the coating remained unaffected by exposure to the saturated calcium hydroxide solution over the exposure time and potential range tested. Delamination of the coating characteristics of cathodic disbondment was observed after exposure to 3.5% sodium chloride solution at the freely corroding and lower potentials. However, exposure under anodic polarization resulted in pitting but little disbondment. Exposure to the mixed calcium hydroxide and sodium chloride environment did not result in extensive disbondment at the cathodic potentials. However, exposure under anodic polarization resulted in both pitting and delamination.

Elleithy et al. [68] conducted a study to evaluate the effect of holidays and damage to fusion-bonded epoxy-coating (FBEC) on reinforcement corrosion in chloride-contaminated concrete. They compared the effect of these parameters on the corrosion of FBEC bars with corrosion of mild steel by measuring the corrosion potentials and corrosion current density at regular intervals. Corrosion current density measurements indicated that the defect-free FBEC bars were in a passive condition in the concrete specimens with up to 2% chloride by weight of cement. The long-term maintenance-free performance was not assured in the concrete specimens with chloride concentration of 1% and above and made with FBEC bars having >1% surface damage. The long-term performance of FBEC bars with up to two pinholes (ASTM A 775 limit) was satisfactory in the concrete specimens with up to 2% chlorides, by weight of cement. The authors reported that, surface damage to the FBE coating is more critical compared to holidays, in chloride-bearing concrete from corrosion point of view.

In a study conducted by the U.S. Naval Facilities Engineering Services Center (NFESC), concrete specimens reinforced with FBEC or zinc-coated (galvanized) bars were evaluated after seven years of exposure to different marine environments [60]. The specimens were exposed to inter-tidal zone at Bermuda; Key West, Florida, Port Huenene and California. The findings of that study indicated that epoxy-coated rebars and zinc-coated rebars can extend the life expectancy of reinforced concrete structures in a marine environment [61].

In an investigation conducted by Sakai and Shinichi [62], pre-cracked reinforced concrete specimens were exposed to a marine environment in Japan. After ten years of exposure, there was evidence of corrosion in some of the epoxy-coated bars. The authors attributed the corrosion to an inadequate hardening of the coating, building of the reinforcing bars, and partial lack of coating thickness, all of which reflected inadequate manufacturing technology for the epoxy-coated reinforcing bars at the early stages of that industry in Japan. They further reported that the bars were coated in 1980, and the problems with coating technology were thereafter solved [62].

While several studies, quoted in the preceding section, have reported the beneficial effect of using FBECR, concern has recently been raised regarding their effectiveness in preventing rebar corrosion and extending the useful service life of structure [63]. In Key West, Florida, reinforced concrete bridges built using epoxy-coated reinforcement exhibited signs of steel corrosion within 10 years [64]. The Canadian Strategic Highway Research Program (C-SHRP) sponsored a research project to determine the effectiveness and long-term (50 years or more) performance of FBECR in preventing corrosion of reinforcement in highway structures exposed to environments representative of the

Canadian conditions [53]. The field and laboratory results suggested that FBEC bars will not be effective in providing long-term corrosion protection to reinforcing steel in salt-contaminated concrete. Clear [53] reported that the increase in the life of epoxy-coated rebar structures over those constructed with uncoated bars will be in the range of only 3 to 6 years; rather that above 40 years as was previously estimated.

Rasheeduzzafar et al. [65] evaluated the corrosion-resistance performance of bare (i.e. uncoated), galvanized, epoxy-coated and stainless-clad reinforcing steel. These bars were cast in concrete specimens contaminated with 0.6, 1.2 and 4.8% chloride ions by weight of cement and exposed to the environmental conditions of eastern Saudi Arabia. After 7 years of exposure, severe corrosion was observed in the uncoated bars while in the concrete specimens made with galvanized bars, there was a delay in onset of cracking. The epoxy-coated bars performance was exceedingly well as a corrosion-resistant steel in the specimens contaminated with 0.6% and 1.2% chloride. No reinforcement corrosion and concrete cracking was observed in these specimens. However, in the specimens contaminated with 4.8% chlorides, significant corrosion of the substrate under the coating was noted, indicating a finite chloride tolerance by the epoxy coating. The stainless-clad reinforcing bars exhibited the best performance.

Sagues [66] evaluated the mechanism of corrosion of epoxy-coated rebar in reinforced concrete used in marine bridge substructures. The work examined the mechanism of corrosion, its prediction and a form of corrosion control. From the results of this study, the corrosion in the field was viewed as resulting from the normally present production imperfections which were later aggravated by fabrication, handling and a severe construction environment. This investigation indicated that epoxy-coated rebars are

susceptible to modes of deterioration commonly present in Florida substructure service environments.

Darwin et al. [69] studied the performance of FBEC rebars in a poor quality concrete by subjecting the specimens to a cyclic wet/dry exposure (monthly) using either 3.5% NaCl or dematerialized water over a period of 12 months. On-going measurements of half-cell potentials were made together with regular visual observations. They reported that the FBECR provided a significant improvement in corrosion resistance that was further enhanced by the presence of chromate conversion coating.

Al-Amoudi et al. [70] conducted long-term research to evaluate the effect of holidays, surface damage, and chloride contamination on corrosion of FBEC steel bars. They concluded that the surface damage is more deleterious to FBEC steel bars than the pinholes in terms of corrosion. No significant variation was observed in the corrosion current density of the steel bars with the number of pinholes in the coating while it increased with an increase in the degree of damage to the coating. Similarly, the corrosion activity increased with an increase in the chloride concentration.

The above literature indicates that FBECR is an effective method for inhibiting reinforcement corrosion. However, a few cases have been reported in the literature, such as the Florida Keys Bridges, where concrete spalling was observed in less than 10 years of service. The explanation forwarded for such a failure is that the coating technology was not properly developed at that stage and the application was probably not appropriate. Irrespective of the causes for such a failure, it should be noted that corrosion of epoxy-coated reinforcing steel might be caused by the combined effect of several factors such as

damage to the coating during fabrication, handling, transportation, storage, placement and concrete operations, in addition to the aggressivity of the environments.

However, data are lacking on the performance of FBEC reinforcing steel in the environmental conditions of the Arabian Gulf. Moreover, there is no enough information in the literature regarding the degree of damage/holidays that is vulnerable to corrosion in the context of chloride contamination and concrete protection improved by the use of mineral admixtures (i.e. silica fume, fly ash and blast furnace slag). In addition, there is a need to evaluate the effect of exposure temperature on the performance of FBEC bars.

2.9 EFFECT OF POZZOLANS ON REINFORCEMENT CORROSION

2.9.1 Pozzolanic Materials

Pozzolanic materials can be either natural, like pozzolana, or artificial, like fly ash or silica fume [71]. They are mainly glassy siliceous materials that may contain aluminous compounds but have low lime (calcium hydroxide) content. In themselves, they do not have binding properties, but acquire them at normal ambient temperature in the presence of lime giving rise to hydration products similar to Portland cement.

The reaction between pozzolanic materials, lime and water is known as the pozzolanic reaction:

$$\text{Pozzolana} + Ca(OH)_2 \rightarrow \text{C-S-H} + H_2O \qquad (2.1)$$

In cements containing pozzolanic additions, the lime needed to react with pozzolana is provided by the hydration of Portland cement. The hardened cement paste (compared to that obtained with Portland cement only) has a lower lime content and higher silica content of C-S-H. The amount of pozzolanic addition to Portland cement generally ranges from 20 to 40% of the total cement content: it should be adjusted according to the lime produced in the hydration of Portland cement. Any excess of pozzolanic addition will not react and thus behave as an inert addition [71].

2.9.2 Natural Pozzolans

This is a sedimentary material, usually of piroclastic origin, that is derived from sediment of volcanic eruptions that have produced incoherent deposits that have been chemically transformed with time (such as Italian pozzolana, which was used by the Romans). Pozzolanic materials may also have other origin, such as diatomaceous earth composed of siliceous skeleton of microorganisms. The pozzolanic activity of these materials is related to their siliceous components in the vitreous state and to their fineness. There are also pozzolans that are obtained by calcination of natural substances [71].

2.9.3 Blast Furnace Slag

Ground granulated blast furnace slag (GGBS) is a waste product in the manufacture of pig iron, about 300 kg of slag being produced for each ton of pig iron. Chemically, slag is a mixture of lime, silica and alumina, that is, the same oxides that make up Portland cement but not in the same proportions. There exist also non-ferrous slags; their use in concrete may become common in the future [71].

Blast furnace slag varies greatly in composition and physical structure depending on the processes used in their production and on the method of cooling of the slag. For use in the manufacture of blast furnace cement, the slag has to be quenched so that it solidifies as glass, crystallization being largely prevented. This rapid cooling by water results also in fragmentation of the material into a granulated form. Palletizing, which requires less water, can also be used.

The specific gravity of GGBS is about 2.9, which is somewhat lower than the specific gravity of Portland cement (that is 3.15) [71].

2.9.4 Fly Ash

Fly ash, known also as pulverized-fuel ash, is the ash precipitated electro-statically or mechanically from the exhaust gases of coal-fired power stations; it is the most common artificial pozzolana. The fly ash particles are spherical (which is advantageous from the water requirement point of view) and have a very high fineness: the vast majority of particles have a diameter between less than 1 μm and 100 μm, the specific surface of fly ash is usually between 250 and 600 m^2/kg, using the Blaine Method. The high specific surface area of the fly ash means that the material is readily available for reaction with calcium hydroxide.

The American classification of fly ash, given in ASTM C 618, is based on the type of coal from which the ash originates. The most common fly ash derives from bituminous coal, is mainly siliceous, and is known as Class F fly ash. Sub-bituminous coal and lignite result in high-lime ash, known as Class C fly ash.

2.9.5 Silica Fume

Silica fume was originally introduced as an active pozzolana. However, its action in concrete is not only that of a very reactive pozzolana but is also beneficial in other respects though it is expensive [71]. Silica fume is also referred to as microsilica or condensed silica fume, but the term 'silica fume' has become generally accepted. It is a by-product of the manufacture of silicon and ferrosilicon alloys from high-purity quartz and coal in a submerged arc electric furnace. The escaping gaseous SiO oxidizes and condenses in the form of extremely fine spherical particles of amorphous silica (SiO_2), hence it is given of the name silica fume. Silica fume in the form of glass (amorphous) is highly reactive, and the smallness of the particles speeds up the reactions with calcium hydroxide produced by the hydration of Portland cement. The very small particles of silica fume can enter the space between the particles of cement, and thus improve packing. When the furnace has as efficient heat recovery system, most of the carbon is burnt so that silica fume is virtually free from carbon and is light in color. Furnaces without a full heat recovery system leave some carbon in the fume, which is therefore dark in color.

The specific gravity of silica fume is generally around 2.20, but it is very slightly higher when the silica content is lower. This value can be compared with the specific gravity of Portland cement, which is 3.15. The particles of silica fume are extremely fine, most of them having a diameter ranging between 0.03 and 0.3 μm; the median diameter is typically below 0.1 μm. The specific surface of such fine particles cannot be determined using the Blaine method; nitrogen adsorption indicates a specific surface of about 20,000

m^2/kg, which is 13 to 20 times higher than the specific surface of other pozzolanic materials, determined by the same method [71].

Such a fine material as silica fume has a very low bulk density: 200 to 300 m^2/kg (12 to 19 lb/ft^3). Handling this light powder is difficult and expensive. For this reason, silica fume is available in the densified form of micro pellets, that is agglomerates of the individual particles (produced by aeration), with a bulk density of 500 to 700 kg/m^3. Another form of silica fume is slurry of equal parts by mass of water and silica fume. The density of the slurry is about 1300 to 1400 kg/m^3.

2.10 EFFECT OF POZZOLANS ON REINFORCEMENT CORROSION

Pozzolans and industrial by-products, such as fly ash, blast furnace slag, and silica fume, are increasingly used in concrete to improve its durability. These materials, which are aluminous and siliceous in composition, react with calcium hydroxide (CH) liberated in the hydration of the tricalcium silicate (C_3S) and dicalcium (C_2S) in the Portland cement to form secondary calcium silicate hydrate [72]. The secondary C-S-H phase, although less dense than the primary C-S-H formed in the plain cements, nevertheless effectively fills up the large voids in the hydrated Portland-pozzolan cement concretes. Feldman [73] attributes the superior durability performance of pozzolan-cement concretes to an apparent discontinuous pore structure that renders: (i) low permeability and (ii) a relatively low content of CH. Mehta [74] suggest that the decrease in the permeability of pozzolanic concretes is due to the effect of these pozzolans on the transition zone. Mehta [74] indicated that sufficient replacement of cement with mineral admixtures, such as fly

ash, blast furnace slag and silica fume reduces the ultimate permeability of Portland cement paste. Of these materials, silica fume is the most effective in reducing permeability at early ages. Several researchers [75-77] have shown that mortars and concretes incorporating silica fume are less permeable than plain cement specimens. They attributed this reduction to a decrease in the number of coarse pores of the cement-silica fume paste system; although the total porosity remains nearly the same as in the neat cement paste [75-77]. Studies conducted by Manmohan et al. [78] and Nyame et al. [79] have shown that, in concrete, it is the pore size distribution rather than the total porosity that governs the penetration of aggressive species into concrete. Research conducted by Hussain [80] showed that the average pore radius is reduced from 285 Å to 181 Å with 10% silica fume blending. Similar results were obtained by Kumar et al. [81] for a paste prepared with 0.4 water to binder ratio, the median pore size was reduced from 15 nm to 7.5 nm and the coefficient of chloride diffusion was reduced from $227x10^{-13}$ m^2/s to $22x10^{-9}$ m^2/s for 10% silica-fume blended cement paste. It has been indicated that the diffusion of aggressive agents, chloride ion in particular, is affected not only by the pore structure of the materials but also by the diffusion mechanism [82]. According to them [82], a reduction in the chloride transport also occurs due to a change in the chemical composition beyond that caused by physical factors. It is assumed that because of the pozzolanic reaction, a significant amount of gel is produced during hydration in the pozzolanic materials; the critical point is that the gel-type hydrates are located to block the pores instead of just forming a layer on the solid pore surfaces. The lower amount of $Ca(OH)_2$ in the pozzolanic cement pastes, and their higher silica and alumina contents, are of benefit for these kinds of cementitious materials to minimize the penetration of chloride ion. Further, the pore channels in these cements have a high tortuosity compared to plain

cement pastes. Also, the chloride ions may be the inhibited by the interaction of these secondary hydrates formed by the pozzolanic reactions with other ions as they pass through the pores.

The dense pore structure of blended cements also impedes the flow of moisture and oxygen to the steel-concrete interface, thereby retarding the anodic reaction. Moreover, the electrical resistivity of blended cements being higher than that of plain cements propagation of corrosion current will be hampered in these cements as compared with plain cements, The lower corrosion activity in blended cements as compared with plain cements may be attributed to the dense micro-structure, lower oxygen and moisture diffusion, and increased electrical resistivity.

Several studies conducted in the Arabian Gulf and elsewhere, have shown the superior durability performance of cement concrete specimens incorporating these materials. This superior performance of blended cements is mainly attributed to the increase in denseness of concrete due to the formation of the secondary C-S-H gel leading to pore refinement. Several researchers have also reported increased chloride binding capacity in fly ash and BFS cements compared to SRPC and OPC. Kawamura et al. [83] studied the effect of fly ash addition on the pore solution concentration in cement mortar specimens contaminated with NaCl and $CaCl_2$. A marginal decrease in the chloride ion concentration was recorded due to the incorporation of fly ash in mortar specimens contaminated with NaCl and $CaCl_2$. Kawamura et al. [83] reported the formation of Friedel's salt, detected by DTA, in both plain and fly ash cements. Greater chloride-binding in the fly ash and slag cements compared to OPC has also been reported by Hussain [80]. It is understood that the chloride- binding in the slag cements takes place by

mechanisms other than the formation of Friedel's salt, possibly the slag itself is capable of binding some of the chlorides. It is also probable that the chloride ions are adsorbed on the C-S-H gel in the slag cements: the chloride being more loosely bound than that bound with the C_3A. This was confirmed in a recent study conducted by Khan [84] that indicated that the water-soluble chloride concentration in the blast furnace slag cement (slag constituted 70% of the total cementitious material) was more than that in the OPC paste specimens.

Maslehuddin et al. [85] reported results of experiments conducted to evaluate the compressive strength development and corrosion resisting characteristics of concrete mixtures in which fly ash was used as sand replacement for cement. Concrete specimens were partially immersed in a 5% sodium chloride solution for a period of about four years. Results indicated that the addition of fly ash as an admixture increased the early age compressive strength and the long-term corrosion resisting characteristics of concrete. The authors [85] concluded that the superior performance of the fly ash cements concrete was attributable to the densification of the paste structure due to the pozzolanic reaction. Byfors [86] conducted investigations on the chloride diffusion characteristics of paste samples prepared from silica fume and fly ash cement blends. The author [86] reported that silica fume and fly ash inclusion considerably reduced the chloride diffusion rate. He suggested that there are other factors of major importance for that enhance the capacity of the cement paste to bind more chlorides chemically. By conducting measurements of pH, in extracted pore solutions, he concluded that although the mineral additions reduce the pH the addition of silica fume or fly ash, inappropriate quantities could extend the initiation time for diffusion controlled and chloride reinforcement corrosion.

The performance of blended cements in resisting reinforcement corrosion exposed to chloride-sulfate environments was evaluated in a recent study conducted by Al-Amoudi et al. [87]. In this study, the concrete specimens were exposed to a simulated sabkha environment. The chloride and sulfate concentrations used were typical of the groundwater salinity in the coastal area of the Arabian Gulf (Cl^- = 15.7% and $SO4^{--}$ = 0.55%). The reinforcement corrosion activity was evaluated by monitoring the corrosion potentials and measuring the corrosion current density on the steel after 425 days of exposure to the test solution. The data indicated lower corrosion activity in the blended cements compared with OPC concrete specimens. The corrosion current density on steel in fly ash, blast furnace slag, and silica fume cement concrete specimens was, 13, and 120 times lower than that in the ordinary Portland cement concrete specimens. The superior performance of blended cements compared to OPC was attributed to dense microstructure of these cements. The dense micro-structure of the blended cements impedes the diffusion of oxygen and moisture that are necessary for the cathodic reaction. Further, the electrical resistivity of blended cements, being considerably higher than that of the OPC, the flow of corrosion current from anodic to the cathodic sites and vice versa is reduced.

2.11 EFFECT OF TEMPERATURE ON REINFORCEMENT CORROSION

High temperature causes great differences in the degree of attack in concrete and reinforcement corrosion. The penetration of aggressive substances such as chloride ions, and carbon dioxide, proceeds more rapidly. Studies carried out by Uhlig [88] on the effect of temperature and humidity on the corrosion process showed that when circumstances are such that corrosion can occur, its rate is increased by high temperature and high

humidity. The rate of corrosion appears to be sharply increased by an increase in temperature in size range of 20º C to 40ºC, especially at high humidity. In studies carried out by Maslehuddin et al. [89], the corrosion current density on steel increased with the exposure temperature, the corrosion current density on steel in the specimens exposed to 25ºC and 40ºC was more or less similar. However, these values increased almost linearly for exposure temperatures of more than 40ºC. The corrosion current density on steel in the specimens exposed to 25ºC was 1.05 $\mu A/cm^2$, whereas it was 2.0 $\mu A/cm^2$ on steel in specimens exposed to 70ºC. The augmentation in the corrosion activity due to increasing temperature may be attributed to the acceleration of the electrochemical reactions. The chemical reactions are known to be doubled when exposure temperature is increased from 20ºC to 40ºC [88-90]. In the studies conducted by Benjamin et al. [91-92], pitting potential was observed to decrease with exposure temperature. This trend was observed in both steel placed in saturated calcium hydroxide solutions and ordinary Portland cement mortar. Schieβl et al. [93] also reported an increase in the corrosion current density when the temperature was increased from 15ºC to 20ºC. The mean value of this acceleration factor was reported to be 1.4. Moreover, the corrosion rate of steel in the carbonated concrete was observed to increase two times for each 10ºC rise in temperature. Maslehuddin et al. [89] also investigated the effect of temperature and chloride contamination on the electrochemical behavior of mild steel placed in an electrolyte representing the concrete pore solution. The potentio-dynamic curves for the uncontaminated specimens, showed a decrease in the pitting potential with temperature. The authors attributed the pitting to the small amount of chloride of about 180 to 300 ppm, preset in the solution. Baumel et al. [94] also indicated that in a saturated calcium hydroxide solution, chloride concentration as small as 22 ppm, could compromise steel

passivity. The polarization resistance (Rp) value for the specimens exposed to the uncontaminated saturated calcium hydroxide solution at 25ºC was 147 k-Ω.cm^2; where as it was 25 and 18 k-Ω.cm^2 for specimens exposed to 40ºC and 70ºC, respectively [89]. The potentio-dynamic curves for mild steel placed in an alkaline solution contaminated with chloride and exposed to temperatures in the range of 25ºC to 70ºC indicated an increase in the corrosion activity with temperature. While there was a marginal increase in the corrosion current density when the temperature was increased from 25ºC to 40ºC, the increase in the corrosion current density when the exposure temperature was increased from 40ºC to 55ºC was substantial. No significant difference in the corrosion current density was observed when the temperature was increased from 55ºC to 70 ºC. Pitting corrosion was indicated in all the specimens exposed to this environment. Investigations conducted by Henriksen [95] on the electrochemical behavior of steel in $Ca(OH)_2$ solution containing 0.1 NaCl indicated a linear variation in the pitting potential with a change of 25 mV for every 10 ºC. Similarly, the corrosion rate, measured as the current needed to maintain the passive potential on the specimen, increased linearly up to 50 ºC, with the rate doubling for every 10ºC, but between 50 ºC and 65ºC the change in the corrosion rate decreased.

2.12 EFFECT OF CHLORIDE IONS ON REINFORCEMENT CORROSION

Almost all researchers agree that the chloride ions act as an essential catalyst in the corrosion reaction. The precise role that the chloride ions plays in the corrosion process, however, is not agreed upon. Most researchers believe that the chloride ions initiate the

corrosion reaction by depassivating the natural oxide film on the steel surface, allowing the iron to dissolve into solution. However, depassivation of steel does not necessarily occur through a direct reduction of alkalinity in the electrolyte by the chloride-induced reaction. Some researchers now believe that the chloride ions also react directly by migrating through the film [96]; the actual mechanism of migration, however, is not very well understood or agreed upon. Ogura et al. [97] suggested that nucleation sites are related to microscopic inclusions and grain boundaries on the metal surface.

Chloride ions also cause a shift of potential of the steel. Non-uniform penetration of chloride ions to the level of the steel produces differences in potential and leads to the formation of "macro" corrosion cells. Non-uniform penetration is a general occurrence, and results from such factors as variations in concrete cover and local differences in concrete quality. On reaching the iron substrate, the chloride ions act as a catalyst for the oxidation of iron by taking an active part in the reaction. According to Uhlig [98], chloride ions oxidize the iron to form $FeCl_3$ and draw its unstable ferrous ion into solution, where it reacts with the available hydroxyl ions to form $Fe(OH)_2$. This releases the Cl^- ions back into solution, as seen in the following reactions:

$$Fe + 3Cl^- \rightarrow FeCl_3 + 3e^- \tag{2.2}$$

$$FeCl_3 + 3OH^- \rightarrow Fe(OH)_3 + 3Cl^- \tag{2.3}$$

The electrons released in the oxidation reaction (Eq.2.2) flow through the steel to the cathode. This process results in an increase in the concentration of chloride ions and a reduction of the pH at the points of corrosion initiation. The lowered pH at these sites contributes to the continual breakdown of the passive oxide film. Equation 2.3 indicates

that three chloride ions are released as a byproduct indicating that once the chloride ion reaches the metal surface, no further chlorides are required for further corrosion and depending on the electrical resistivity of concrete either general or local corrosion proceeds.

Further, concrete acting as a conducting medium has a wide variation in its electrical resistivity. Resistivity values ranging from about 10 to 10,000 k.Ω have been reported by researchers studying concrete with different moisture-induced ionic elements. An increase in temperature or addition of moisture and ions, such as chloride ions, to the hydrated concrete results in a large drop in the resistivity. High water-cement ratio, chloride-bearing saturated concrete provides the lowest resistivity to corrosion current, while low water-cement ratio, well-cured, dry concrete provides the highest.

CHAPTER 3

METHODOLOGY OF RESEARCH

This Chapter outlines the materials and experimental test methods utilized to achieve the objectives of this investigation. Whenever applicable, relevant standard ASTM or BS test methods were adopted

3.1 MATERIALS

3.1.1 Steel Bars

Deformed mild steel bars of 20 mm diameter produced by the Saudi Iron and Steel Company (Hadeed) were used. The bars were coated by a specialist local coating company. The coating was applied by electrostatic spraying as required by ASTM A 775/A 775M. Plate 3.1 shows uncoated and fusion-bonded epoxy-coated deformed bars used in this study.

Though there is not enough information in the literature about the degree of surface damage, ASTM A 775 specifies a maximum damage of 1% [54]. Therefore, surface damages of 1.5% and 3% were selected to assess the influence of this parameter on corrosion of FBEC bars.

Plate 3.1: Coated and uncoated steel bars used in this study.

The prescribed levels of surface damages were achieved by intentionally damaging the coating till the steel surface was visible. This was done by using a scriber. Plate 3.2 shows fusion-bonded epoxy-coated steel bars with 3% and 1.5% surface damage.

Plate 3.2: Fusion-bonded epoxy-coated steel bars with 3% and 1.5% surface damage.

3.1.2 Aggregates

Crushed limestone from Abu-Hadriyah was used as coarse aggregate and dune sand as fine aggregate. Coarse aggregates were first sieved into different sizes and then washed with potable water to remove dust and salt contamination. It was then dried for 24 hours and, thereafter, stored. Tables 3.1 and 3.2 show the specific gravity and average absorption of coarse and fine aggregates, respectively.

The coarse aggregate was proportioned to confirm to ASTM C33 grading limits of size 7. Table 3.3 shows the grading of coarse aggregates used in this study.

Table 3.1: Absorption and specific gravity of coarse aggregates.

Aggregates	Absorption (%)	Specific Gravity
Lime Stone (Abu-Hadriyah)	1.8	2.6

Table 3.2: Absorption and specific gravity of fine aggregates.

Absorption (%)	Specific Gravity
0.4	2.67

Table 3.3: Grading of the coarse aggregates used in preparing the concrete specimens.

Size	Passing, %
1/2” (12.5 mm)	35
3/8” (9.5 mm)	35
3/16” (4.75 mm)	20
3/32” (2.36 mm)	10

3.2 EXPERIMENTAL VARIABLES

The variables included in this experimental work were:

- Extent of the damage on the coated bars (0%, 1.5% and 3%).
- Plain and blended cements (incorporating silica fume, fly ash, and blast furnace slag).
- Different percentages of chloride addition in the mix (0%, 1%, 2%).
- Exposure temperature (23 ± 2ºC, 35 ± 2ºC, 48 ± 2ºC).

Test specimens were cast with an effective water to cementitious materials ratio of 0.5, gross water- cementitious materials ratio of 0.565 and cementitious materials content of 370 kg/m^3.

3.3 SPECIMEN PREPARATION

A total of 432 reinforced concrete specimens were cast to cover the experimental variables detailed in Sec 3.2. In each mix, 36 reinforced concrete specimens, 75 mm in diameter and 150 mm high, were cast. From the total 432 samples, 144 samples were placed in 5% NaCl solution at room temperature, and 144 samples each were kept in 5% NaCl solution at the other two temperatures (35 and 48°C).

3.4 DESIGNATION OF THE SPECIMENS

Four different types of bars used in the present study were designated as A through D, where A stands for Black Bar, B stands for Epoxy Coated Bar, C stands for Epoxy Coated Bar with 1.5% surface damage and D stands for Epoxy Coated Bar with 3% surface damage.

The specimens were designated based on the mix, the type of reinforcement and the specimen number. As an example, specimen in the designation 1A1: 1 indicates the mix number, A indicates the type of reinforcement (black bar), and 1 indicates the sample number.

Figure 3.1 depicts a typical concrete specimen utilized to evaluate the reinforcement corrosion. The steel rods used in the specimen were coated with epoxy paint at the top (25 mm), i.e. half was in the concrete and half was exposed to the air or solution as shown in the figure, and at bottom (12.5 mm). The steel bars were coated at the bottom due to break down of the passive film and at top due to change in the medium the chances of initiation of corrosion from both places are high. Table 3.4 shows the specimen designation used in this study.

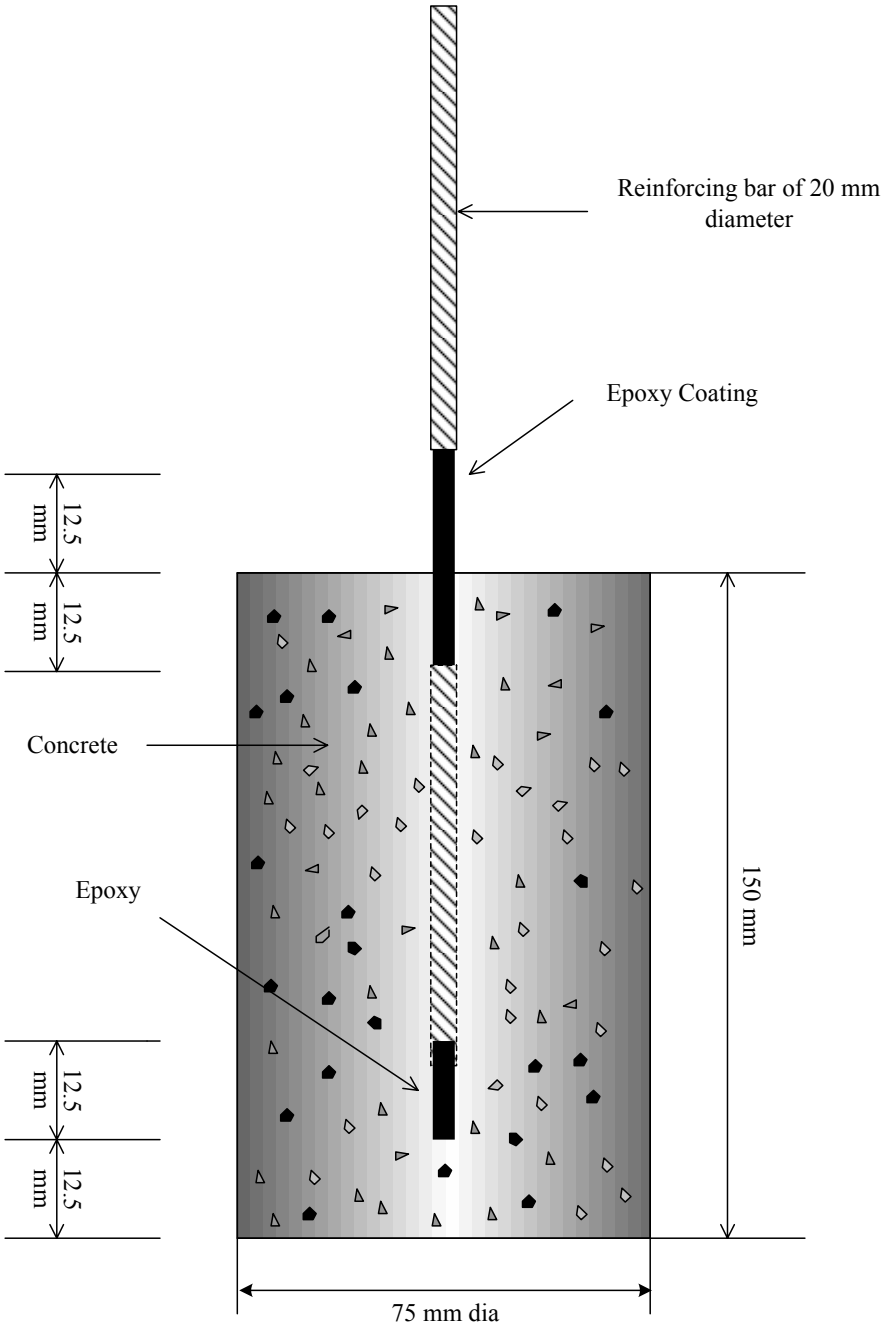

Figure 3.1: Concrete specimen utilized to evaluate reinforcement corrosion.

Table 3.4: Details of Specimen Designation.

Series Number	Mix	Tank B (35 ± 2ºC)	Tank B (35 ± 2ºC)	Tank C (48 ± 2ºC)
1	OPC	1A1 1A2 1A3	1A4 1A5 1A6	1A7 1A8 1A9
		1B1 1B2 1B3	1B4 1B5 1B6	1B7 1B8 1B9
		1C1 1C2 1C3	1C4 1C5 1C6	1C7 1C8 1C9
		1D1 1D2 1D3	1D4 1D5 1D6	1D7 1D8 1D9
2	OPC	2A1 2A2 2A3	2A4 2A5 2A6	2A7 2A8 2A9
	1% Cl	2B1 2B2 2B3	2B4 2B5 2B6	2B7 2B8 2B9
		2C1 2C2 2C3	2C4 2C5 2C6	2C7 2C8 2C9
		2D1 2D2 2D3	2D4 2D5 2D6	2D7 2D8 2D9
3	OPC	3A1 3A2 3A3	3A4 3A5 3A6	3A7 3A8 3A9
	2% Cl	3B1 3B2 3B3	3B4 3B5 3B6	3B7 3B8 3B9
		3C1 3C2 3C3	3C4 3C5 3C6	3C7 3C8 3C9
		3D1 3D2 3D3	3D4 3D5 3D6	3D7 3D8 3D9
4	Silica Fume	4A1 4A2 4A3	4A4 4A5 4A6	4A7 4A8 4A9
		4B1 4B2 4B3	4B4 4B5 4B6	4B7 4B8 4B9
		4C1 4C2 4C3	4C4 4C5 4C6	4C7 4C8 4C9
		4D1 4D2 4D3	4D4 4D5 4D6	4D7 4D8 4D9
5	Silica fume	5A1 5A2 5A3	5A4 5A5 5A6	5A7 5A8 5A9
	1% Cl	5B1 5B2 5B3	5B4 5B5 5B6	5B7 5B8 5B9
		5C1 5C2 5C3	5C4 5C5 5C6	5C7 5C8 5C9
		5D1 5D2 5D3	5D4 5D5 5D6	5D7 5D8 5D9
6	Silica fume	6A1 6A2 6A3	6A4 6A5 6A6	6A7 6A8 6A9
	2% Cl	6B1 6B2 6B3	6B4 6B5 6B6	6B7 6B8 6B9
		6C1 6C2 6C3	6C4 6C5 6C6	6C7 6C8 6C9
		6D1 6D2 6D3	6D4 6D5 6D6	6D7 6D8 6D9
7	Blast furnace slag 70%	7A1 7A2 7A3	7A4 7A5 7A6	7A7 7A8 7A9
		7B1 7B2 7B3	7B4 7B5 7B6	7B7 7B8 7B9
		7C1 7C2 7C3	7C4 7C5 7C6	7C7 7C8 7C9
		7D1 7D2 7D3	7D4 7D5 7D6	7D7 7D8 7D9
8	Blast furnace slag 70%	8A1 8A2 8A3	8A4 8A5 8A6	8A7 8A8 8A9
	1% Cl	8B1 8B2 8B3	8B4 8B5 8B6	8B7 8B8 8B9
		8C1 8C2 8C3	8C4 8C5 8C6	8C7 8C8 8C9
		8D1 8D2 8D3	8D4 8D5 8D6	8D7 8D8 8D9

Table 3.4 Contd…

9	Blast furnace slag	9A1 9A2 9A3	9A4 9A5 9A6	9A7 9A8 9A9
	2% Cl	9B1 9B2 9B3	9B4 9B5 9B6	9B7 9B8 9B9
		9C1 9C2 9C3	9C4 9C5 9C6	9C7 9C8 9C9
		9D1 9D2 9D3	9D4 9D5 9D6	9D7 9D8 9D9
10	Fly ash 30%	10A1 10A2 10A3	10A4 10A5 10A6	10A7 10A8 10A9
		10B1 10B2 10B3	10B4 10B5 10B6	10B7 10B8 10B9
		10C1 10C2 10C3	10C4 10C5 10C6	10C7 10C8 10C9
		10D1 10D2 10D3	10D4 10D5 10D6	10D7 10D8 10D9
11	Fly ash 30%	11A1 11A2 11A3	11A4 11A5 11A6	11A7 11A8 11A9
	1% Cl	11B1 11B2 11B3	11B4 11B5 11B6	11B7 11B8 11B9
		11C1 11C2 11C3	11C4 11C5 11C6	11C7 11C8 11C9
		11D1 11D2 11D3	11D4 11D5 11D6	11D7 11D8 11D9
12	Fly ash 30%	12A1 12A2 12A3	12A4 12A5 12A6	12A7 12A8 12A9
	2% Cl	12B1 12B2 12B3	12B4 12B5 12B6	12B7 12B8 12B9
		12C1 12C2 12C3	12C4 12C5 12C6	12C7 12C8 12C9
		12D1 12D2 12D3	12D4 12D5 12D6	12D7 12D8 12D9

3.4.1 Preparation of Assembly for Corrosion Monitoring

Some special racks were fabricated for the placement of specimens in the exposure tanks. These stainless steel racks were placed on the bottom of the tanks so as to raise the specimens above the bottom of the tanks to ensure proper circulation of solution and heat around the specimens. These racks were then coated with epoxy to avoid corrosion by the NaCl solution. The steel meshes kept on these racks to support the specimens were also coated. Connections of the wires to the specimens were done through soldering by first grooving the reinforcing rods so as to ensure perfect connection throughout the experimental period for corrosion potential and corrosion current density measurements.

Control panels with wiring and switch for each specimen were separately assembled and the samples were connected to the control panel, which were used to obtain corrosion potentials and corrosion current density values. Figure 3.2 through 3.4 shows concrete specimen in two tanks.

3.5 EXPOSURE

Specimens were partially immersed in the 5% NaCl solution in each tank. The solution in the first tank was maintained at room temperature (23 ± 2ºC), while in the second and third tanks, the temperature was maintained at 35 ± 2ºC and 48 ± 2ºC, respectively.

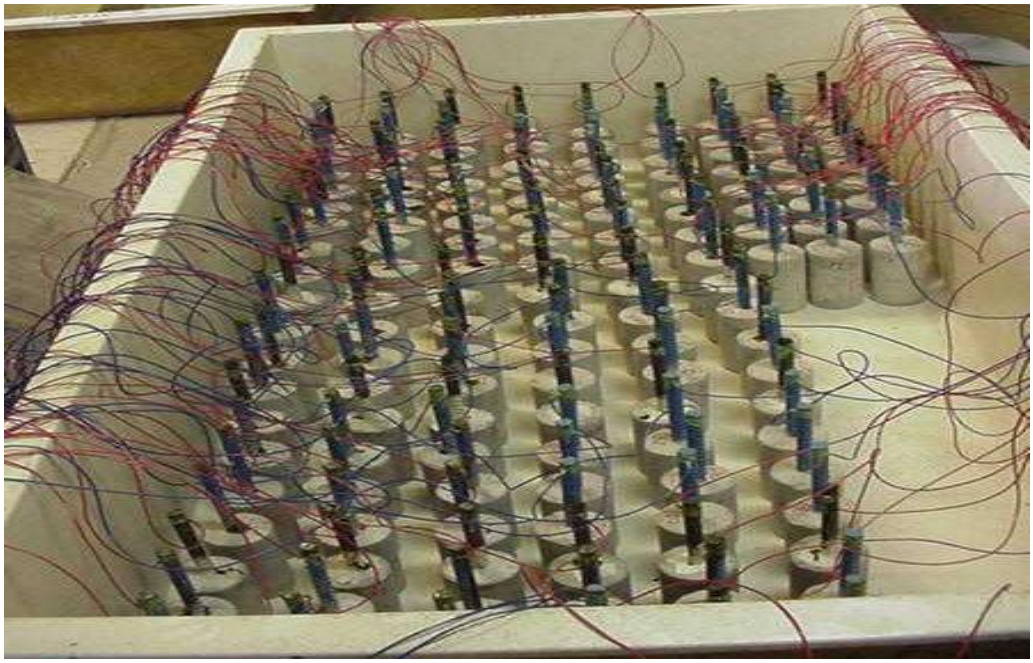

Figure 3.2: Concrete specimens in Tank A (Temperature: 23 ± 2ºC).

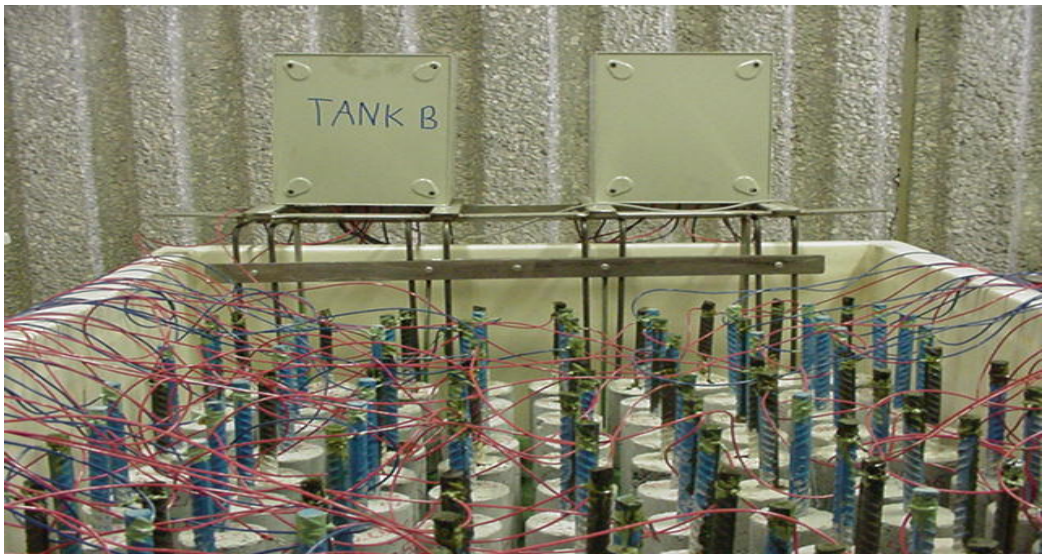

Figure 3.3: Concrete specimens in Tank B (Temperature: 35 ± 2ºC).

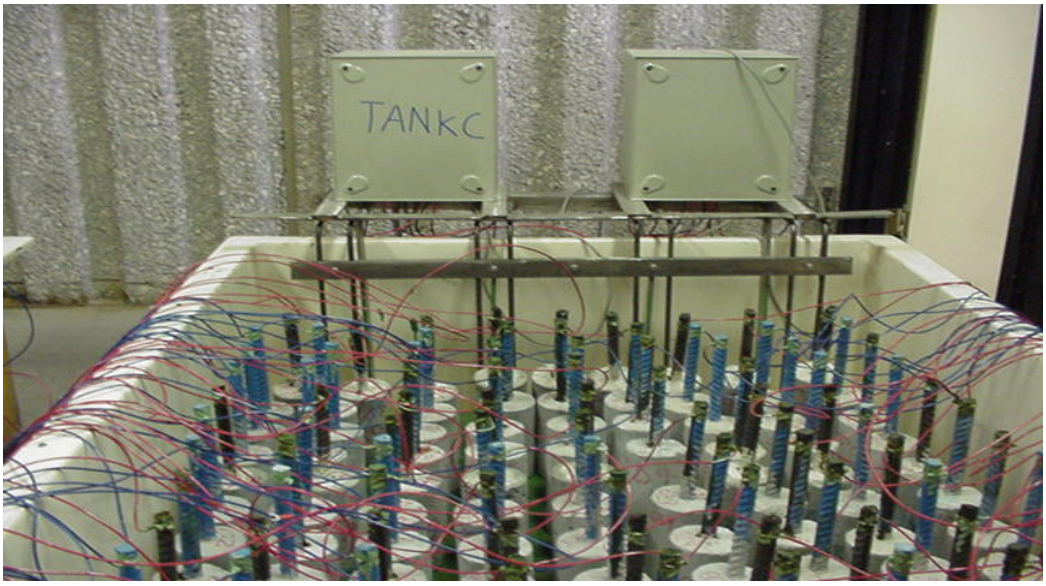

Figure 3.4: Concrete specimens in Tank C (Temperature: 48 ± 2ºC).

3.6 MEASUREMENTS

3.6.1 Corrosion Potentials

Corrosion potential measurements provide a means of monitoring the corrosion activity of epoxy-coated bars. Corrosion potentials (also referred as half-cell potentials) demonstrate the thermodynamic behavior of reinforcing steel in concrete. Potential readings may indicate if the steel is in a passive, active, or unstable active-passive condition. According to ASTM C 876 [99], the probability of corrosion of uncoated steel in concrete is determined by the half-cell potential criteria shown in Table 3.5. Caution is required in the interpretation of half-cell potential measurements with epoxy-coated steel bars. The reason for caution is that the coating is non-conductive and may affect the

readings. In the absence of a more reliable criterion for evaluation of the potentials measured on epoxy-coated bars, those displayed in Table 3.5 will be used in this study for comparison of performance of the tested steel bars. Potential readings may also be useful in indicating the time to corrosion, which is marked by a significant drop in the potential value. After corrosion has started, the state of corrosion activity may be monitored by observing the changes in the potential readings.

The main drawback with the corrosion potential measurements is that it shows the thermodynamics, but not the kinetics, of the corrosion process. This means that the potentials are useful in indicating the probability of active corrosion occurring on the steel. However, they do not indicate the rate of corrosion [100].

Table 3.5: Interpretation of Half-Cell Potentials based on ASTM C876.

Corrosion Potential		Probability of Corrosion
Copper/Copper Sulfate, CSE (mV)	Saturated Calomel, SCE (mV)	
< -200	< -120	Less than 10%
Between -200 and -350	Between -120 and -270	Uncertain
> -350	> -270	More than 90%

3.6.2 Corrosion Current Density

Linear polarization resistance technique is used to measure the rate of corrosion of steel reinforcement [101-102]. The test procedure is based on the Stern-Geary characterization of the typical polarization curve for the corroding metal. Here, a linear relationship is described mathematically for a region on the polarization curve in which slight changes in the current applied to the corroding metal in an ionic solution cause corresponding changes in the potentials of the metal. In other words, if a large current is required to change the potentials by a given amount, the corrosion rate is high and on the other hand, if only a small current is required, the corrosion rate is low [103].

In this test, three electrodes were used to measure the resistance to polarization (Rp) using a Potentiostat\Galvanostat. The steel rod was connected to the working electrode terminal while a steel plate and a reference electrode were connected to the respective terminals of the potentiostat. The steel was polarized by applying a potential of ± 10 mV of the open circuit potential and the resulting current between the counter and the working electrodes was measured. The potentials were changed at a rate of 6 mV/min and the resulting current was measured. Figure 3.5 shows the general view of the experimental setup.

Figure 3.5: Experimental setup for corrosion current density measurements.

The slope of the potential-current curve is the resistance to polarization (R_p). The corrosion current density is then calculated using the following relationship [103]:

$$I_{corr} = B/R_p$$

Where, I_{corr} = corrosion current density, $\mu A/cm^2$

R_p = resistance to polarization resistance, $\frac{\Delta E}{\Delta I}$, Ωcm^2

$$B = \frac{\beta_a \beta_c}{2.3(\beta_a + \beta_c)}$$

β_a = Anodic tafel constant, mV

β_c = Cathodic tafel constant, mV.

The Tafel constants can be determined by polarizing the steel to ± 250 mV of the corrosion potential. In the absence of sufficient data on tafel constants, a value of 120 mV is used both for anodic and cathodic Tafel constants are for steel in a highly resistant medium [105]. A good correlation between the weight loss determined by the gravimetric weight loss and the linear polarization resistance technique was observed by Gonzalez et al. [106] by using a B = 26 mV for steel in the active state and B = 52 mV in the passive state. In our investigation, $\beta a = \beta c = 120$ mV was used throughout, which corresponds to B = 26 mV. Such values have been found to be useful in the corrosion experiments conducted at KFUPM.

3.6.3 Visual Observation

It is often difficult to detect the extent and severity of corrosion of embedded reinforcement. To trace corrosion activity, concrete specimens are often surveyed for special signs, such as staining and cracking. Concrete specimens incorporating epoxy-coated reinforcement may not show such obvious clues because corrosion could be localized (at breaks in the epoxy film, or beneath the coating) without associated manifestation.

Cracks that are parallel to the direction of the reinforcing bars are more serious than those in the transverse direction. They may evolve corrosion, or may be produced because of corrosion. Crack monitoring, if possible, helps identify the cause of cracking and the crack relation to possible corrosion activity. In more advanced corrosion cases, spalling or large-scale delamination emanates at the bars.

3.6.4 Chloride Profile

The chloride concentration at the level of reinforcement in concrete is an important indicator of the corrosivity of the environment surrounding the steel. Extraction of chloride ions from concrete can be either by acid or water. In the acid extraction analysis, acid-soluble chlorides are isolated from concrete. In the water extraction test, water-soluble chlorides are removed.

Concrete powder samples were taken by drilling with a 5-mm diameter masonry drill bit along the reinforcing steel bars at various incremental depths, i.e. 5, 10, 15, 20 mm. A total of 48 powder samples were collected from the 12 mixes with four depths in each specimen. These powder samples were analyzed for water-soluble chloride concentration according to ASTM C 1218 to determine the chloride profile.

CHAPTER 4

RESULTS AND DISCUSSION

This Chapter is devoted to present the results obtained in this study and their discussion. Reinforced concrete specimens with epoxy coated bars and with varying surface damage and chloride contamination were tested. The results obtained from the experiments conducted in this study were discussed in the following sections.

4.1 RESULTS

4.1.1 Corrosion Potentials

Reinforced concrete specimens were partially immersed in 5% NaCl solutions and the corrosion potentials were measured periodically using multimeter and saturated calomel reference electrode (SCE). The corrosion potential curves were utilized to assess the time to initiation of reinforcement corrosion. For this purpose, ASTM C 876 criterion was utilized. According to this criterion, if the corrosion potentials are numerically less than -270 mV SCE, then there is 90% probability of reinforcement corrosion (Table 3.5).

At the beginning of exposure, the potentials were not stable. However, the readings after 15 days of exposure were found to be comparatively stable. Previous research [107] has also indicated that days, weeks and even months are required for reinforced concrete

specimens to shift from a potential of approximately -100 mV SCE to a more stable potential of -600 mV SCE.

The time-corrosion potential curves for plain, silica fume, blast furnace slag and fly ash cement concrete specimens with increasing chloride contamination, i.e., 0%, 1%, and 2% and exposed to temperatures of 23 ± 2°C, 35 ± 2°C and 48 ± 2°C are shown in Figures 4.1 through Figure 4.36.

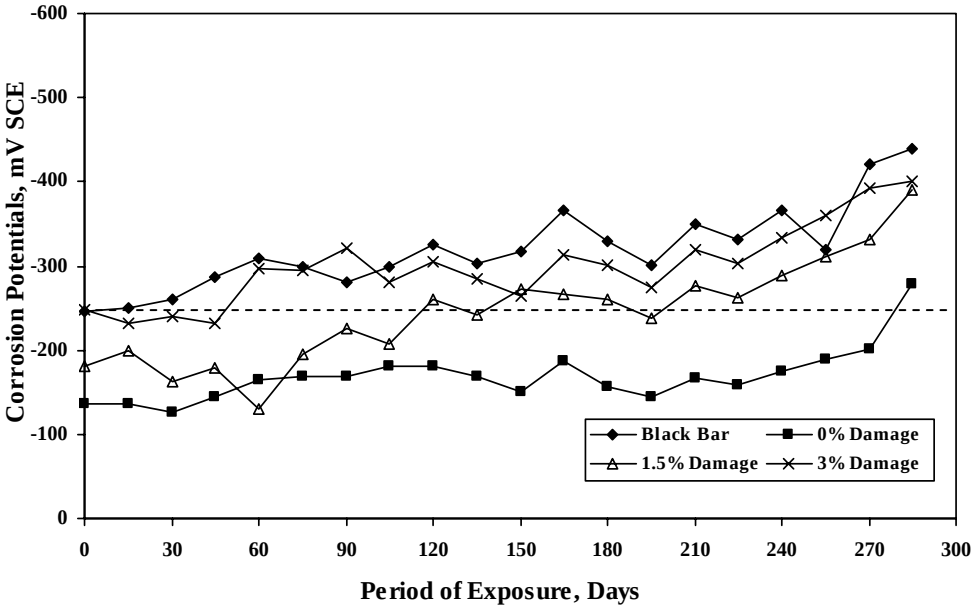

Figure 4.1: Corrosion Potentials on Uncoated and Coated Bars in Uncontaminated Plain Cement Concrete Specimens (Temp: 23°C).

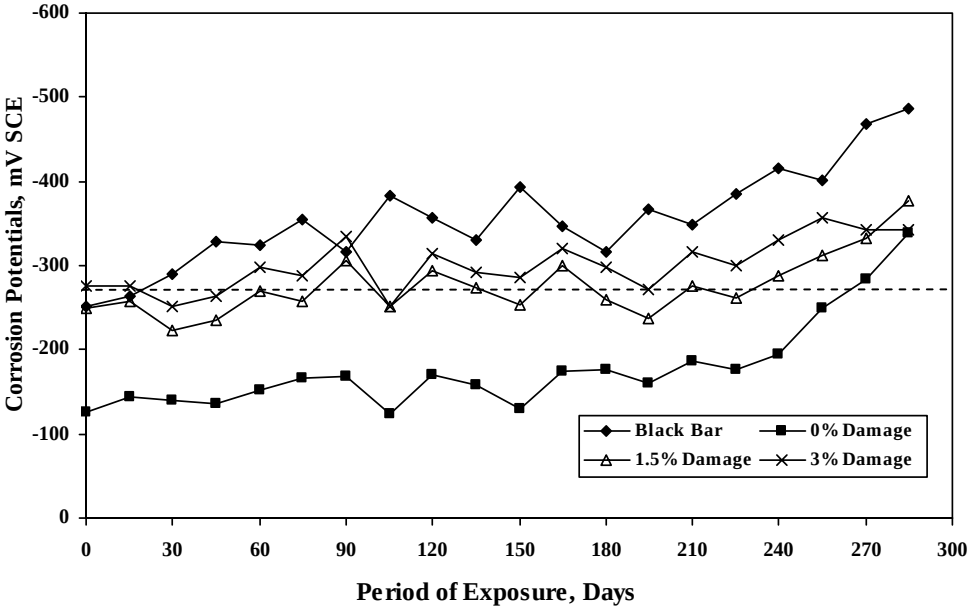

Figure 4.2: Corrosion Potentials on Uncoated and Coated Bars in Plain Cement Concrete Specimens Contaminated with 1% chloride (Temp: 23°C).

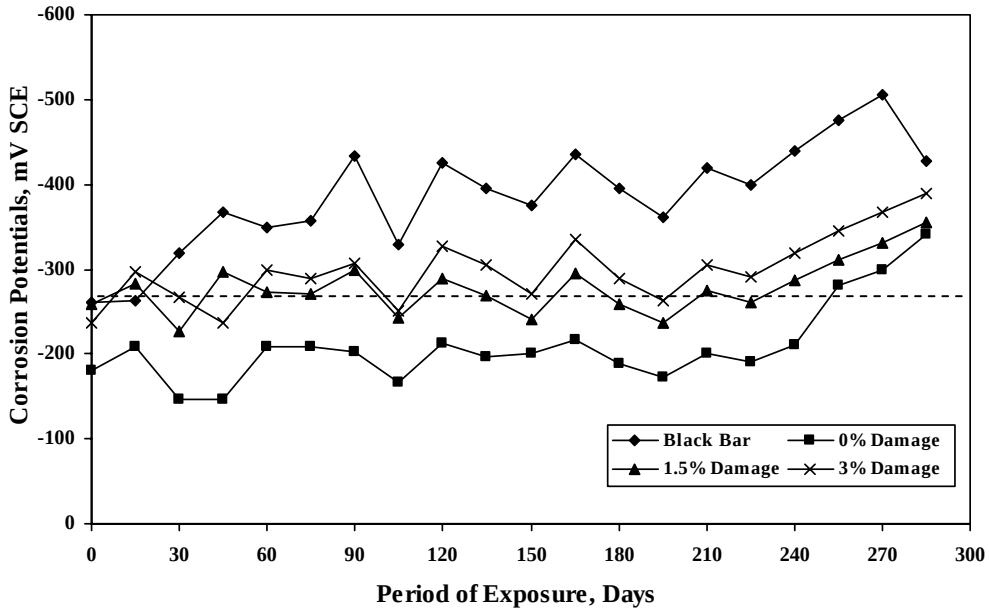

Figure 4.3: Corrosion Potentials on Uncoated and Coated Bars in Plain Cement Concrete Specimens Contaminated with 2% chloride (Temp: 23°C).

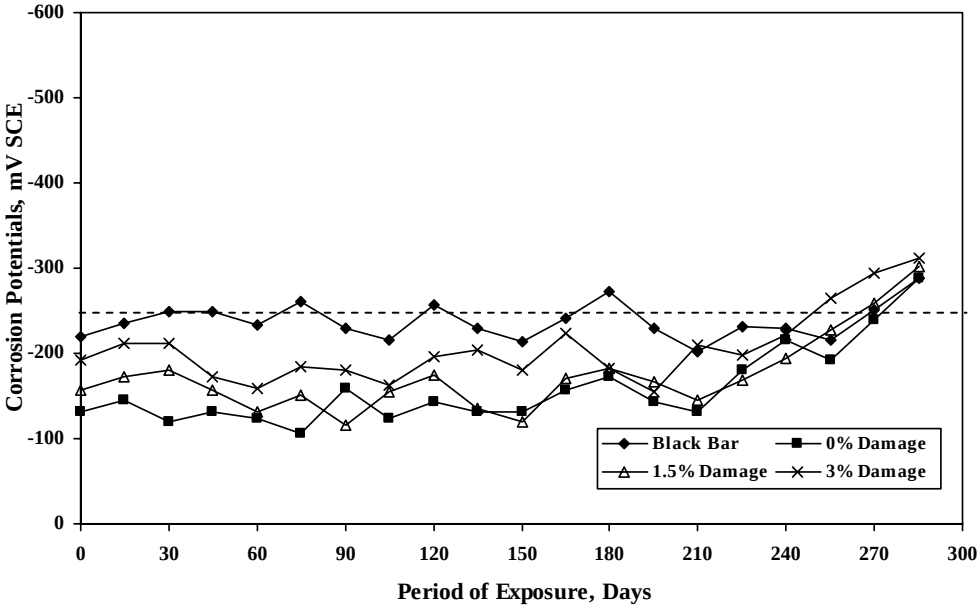

Figure 4.4: Corrosion Potentials on Uncoated and Coated bars in Uncontaminated Silica Fume Cement Concrete Specimens (Temp: 23°C).

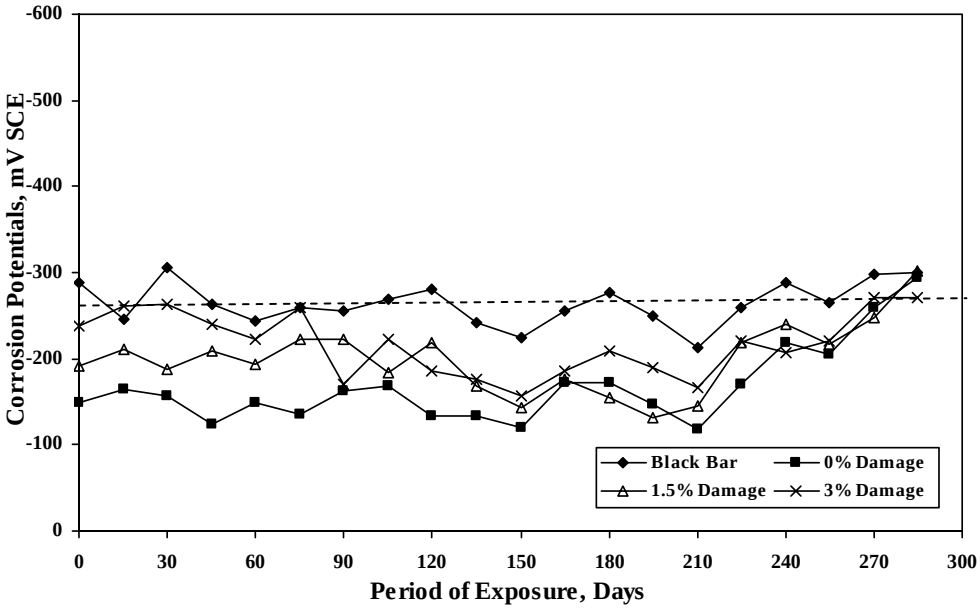

Figure 4.5: Corrosion Potentials on Uncoated and Coated Bars in Silica Fume Cement Concrete Specimens Contaminated with 1% chloride (Temp: 23°C).

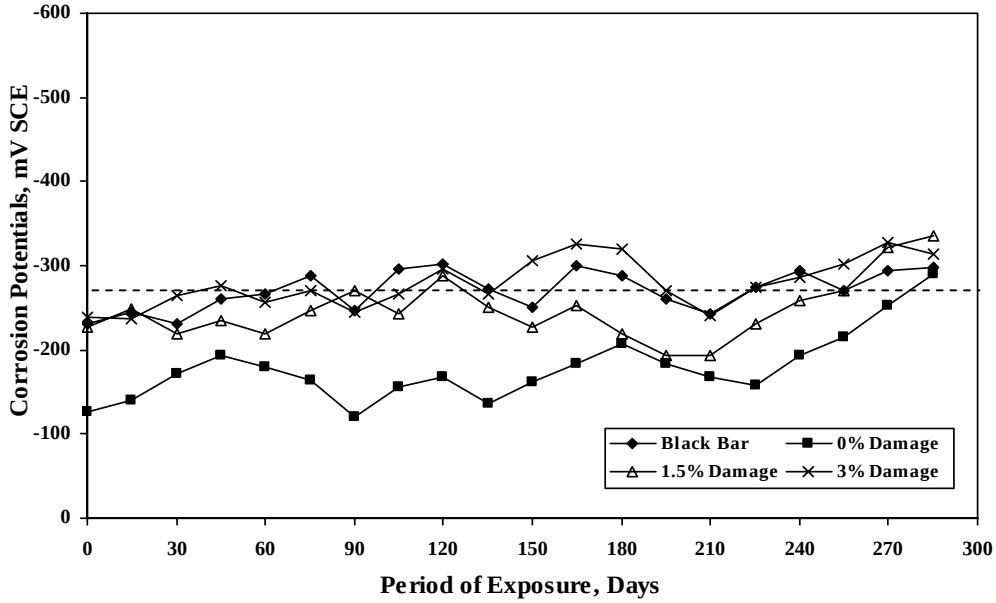

Figure 4.6: Corrosion Potentials on Uncoated and Coated Bars in Silica Fume Cement Concrete Specimens Contaminated with 2% chloride (Temp: 23°C).

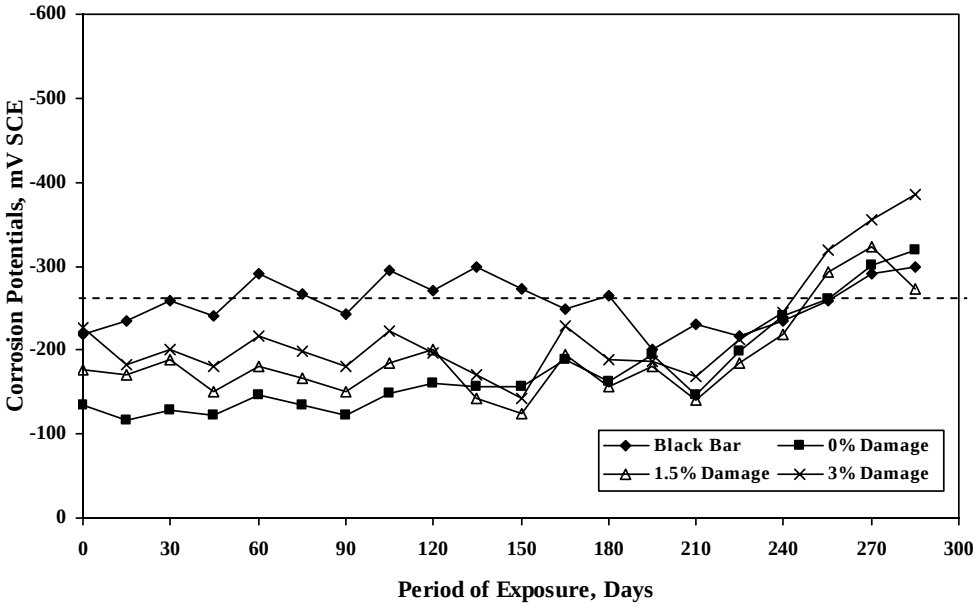

Figure 4.7: Corrosion Potentials on Uncoated and Coated Bars in Uncontaminated Blast Furnace Slag Cement Concrete Specimens (Temp: 23°C).

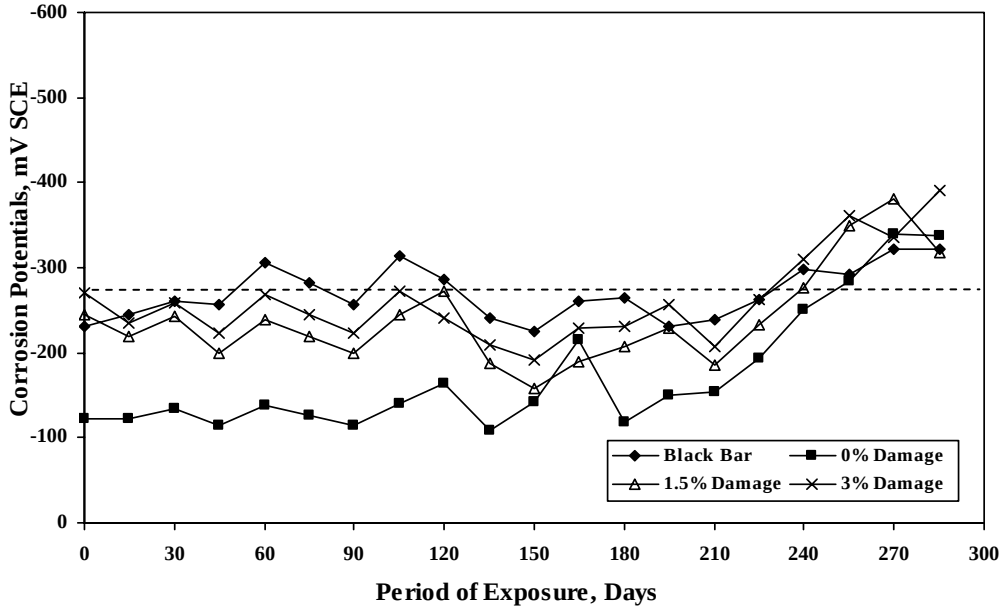

Figure 4.8: Corrosion Potentials on Uncoated and Coated Bars in Blast Furnace Slag Cement Concrete Specimens Contaminated with 1% chloride (Temp: 23°C).

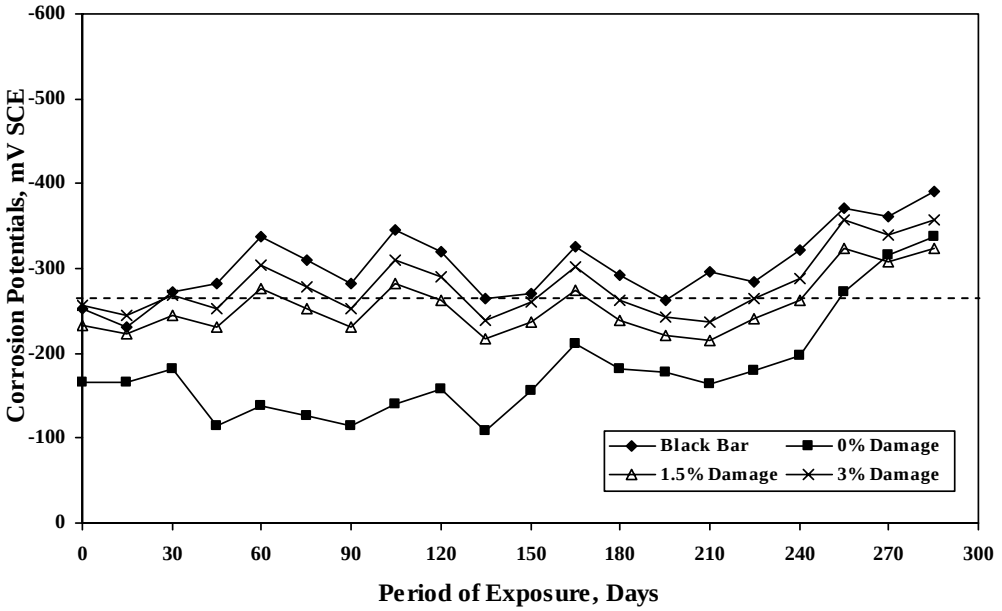

Figure 4.9: Corrosion Potentials on Uncoated and Coated Bars in Blast Furnace Slag Cement Concrete Specimens Contaminated with 2% chloride (Temp: 23°C).

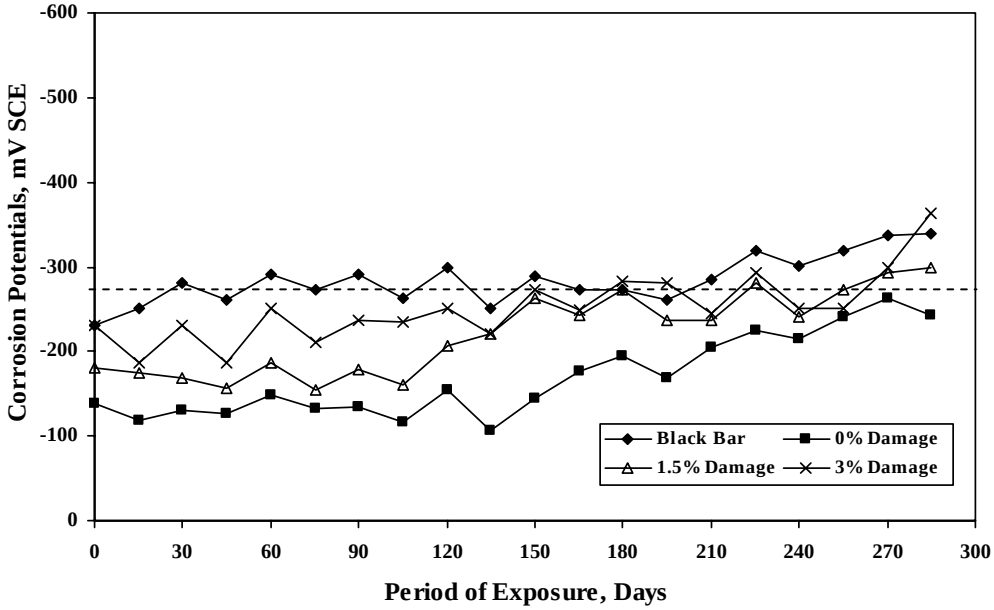

Figure 4.10: Corrosion Potentials on Uncoated and Coated Bars in Uncontaminated Fly Ash Cement Concrete Specimens (Temp: 23°C).

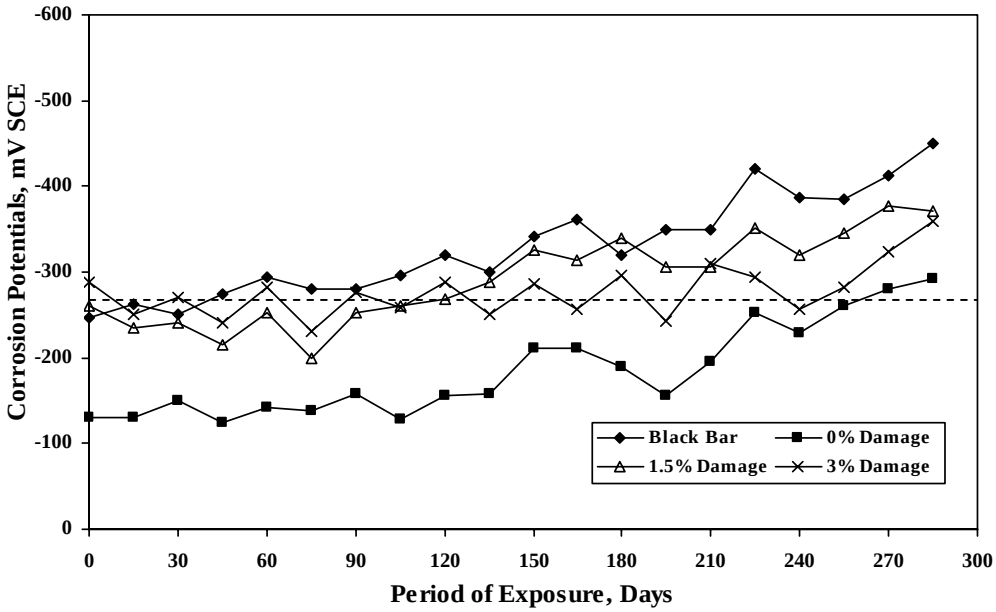

Figure 4.11: Corrosion Potentials on Uncoated and Coated Bars in Fly Ash Cement Concrete Specimens Contaminated with 1% chloride (Temp: 23°C).

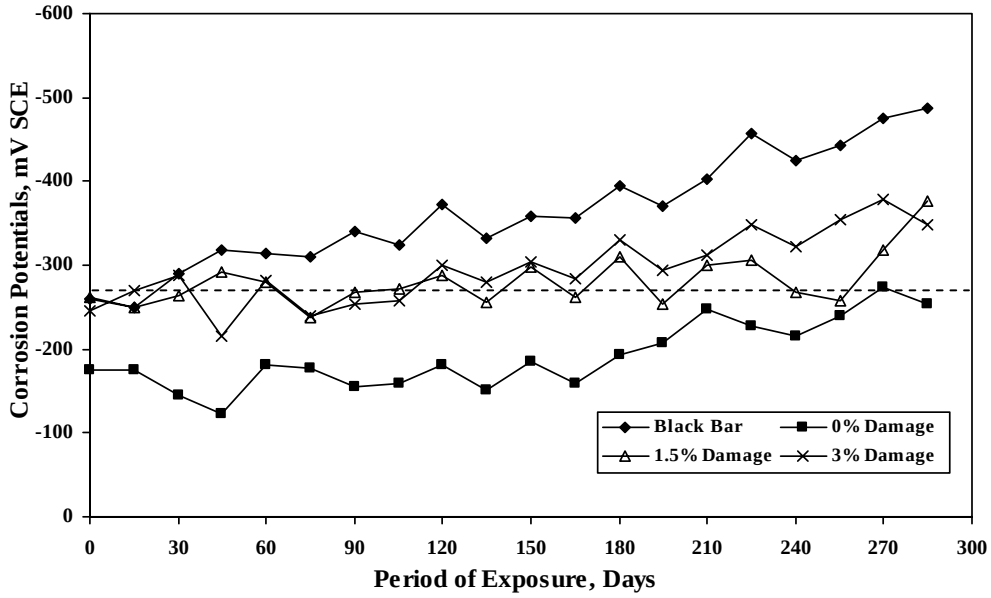

Figure 4.12: Corrosion Potentials on Uncoated and Coated bars in Fly Ash cement Concrete Specimens Contaminated with 2% chloride (Temp: 23°C).

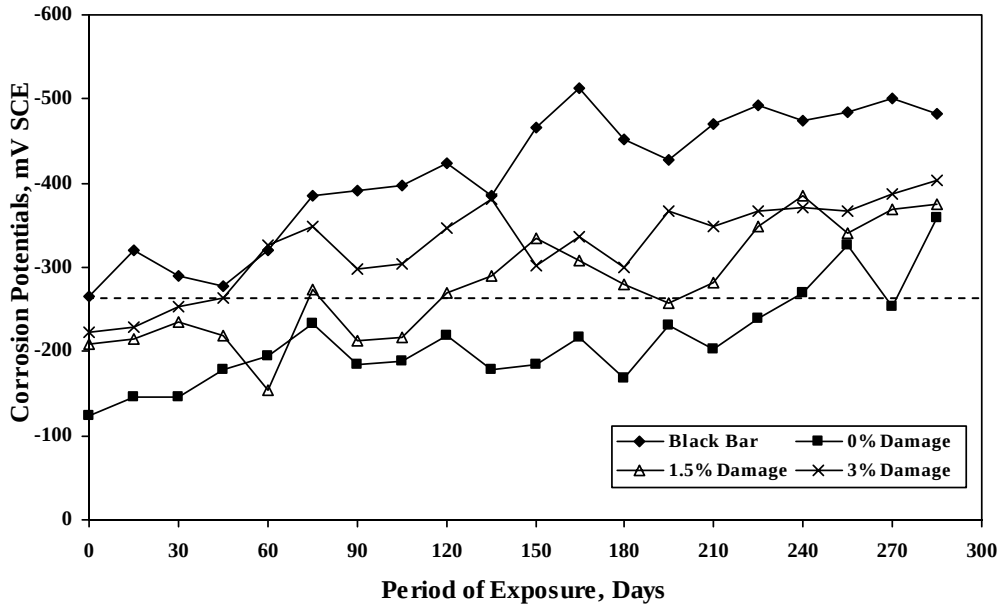

Figure 4.13: Corrosion Potentials on Uncoated and Coated Bars in Uncontaminated Plain Cement Concrete Specimens (Temp: 35°C).

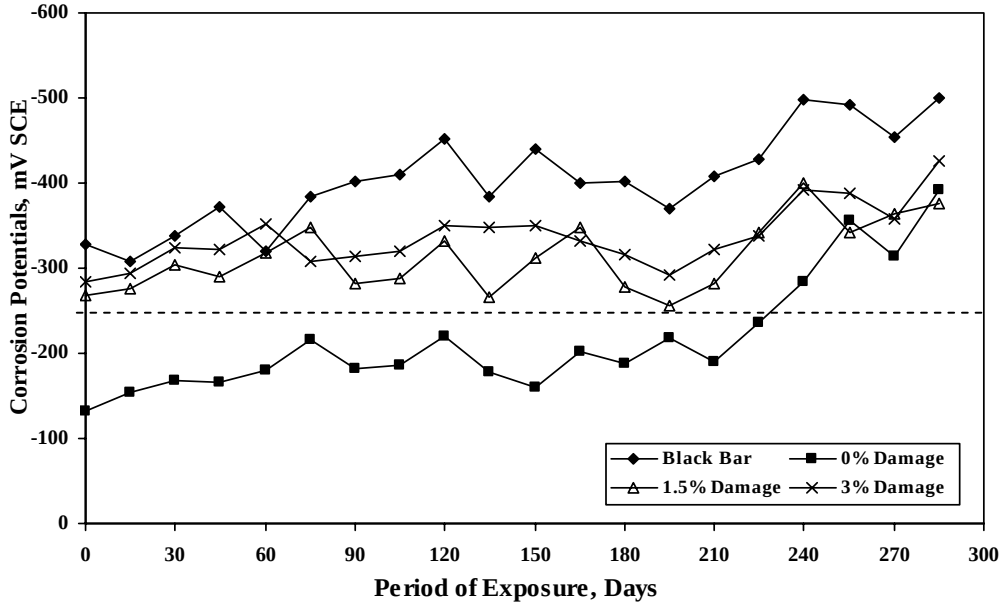

Figure 4.14: Corrosion Potentials on Uncoated and Coated bars in Plain Cement Concrete Specimens Contaminated with 1% chloride (Temp: 35°C).

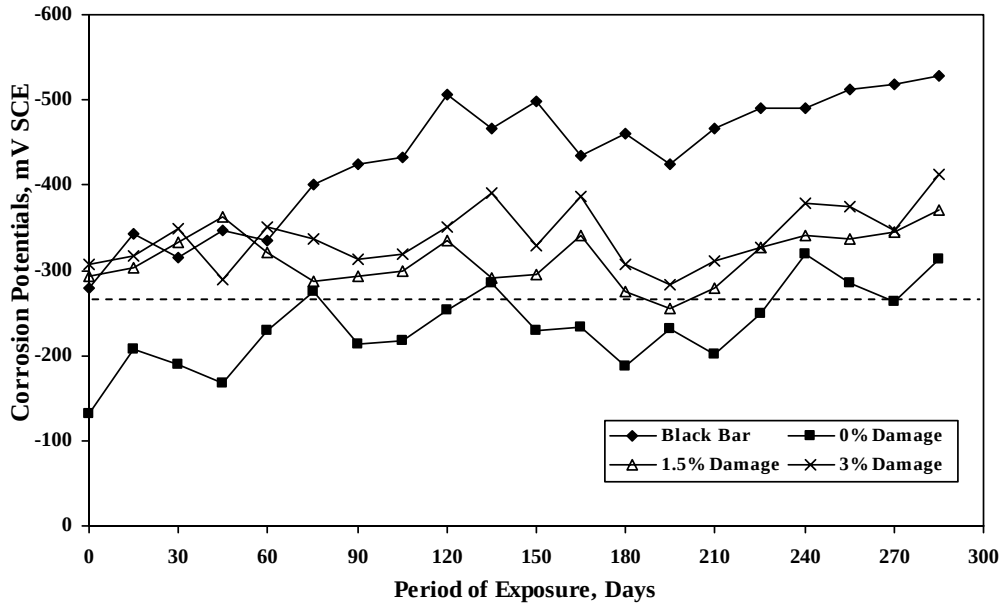

Figure 4.15: Corrosion Potentials on Uncoated and Coated Bars in Plain Cement Concrete Specimens Contaminated with 2% chloride (Temp: 35°C).

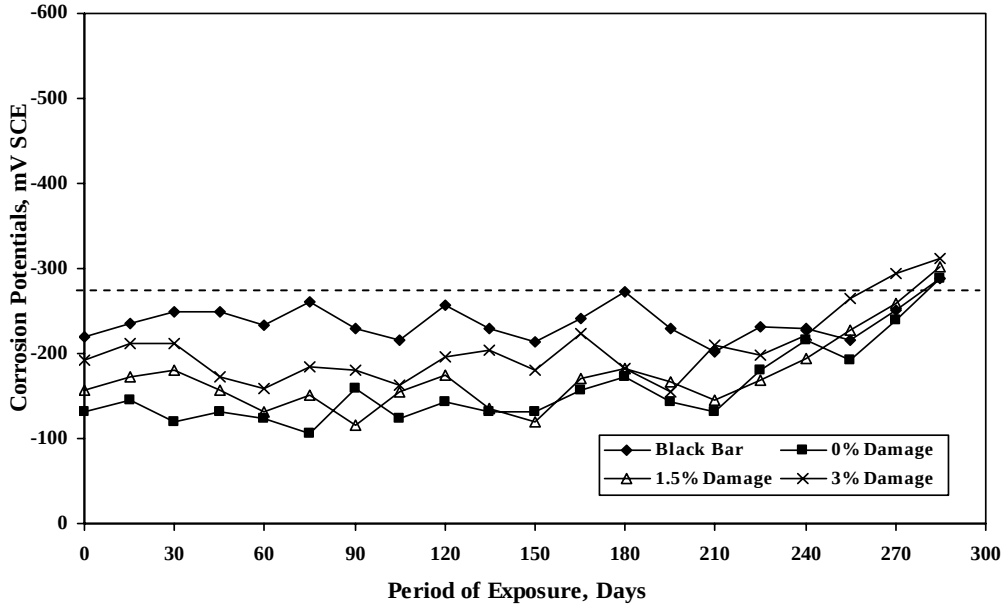

Figure 4.16: Corrosion Potentials on Uncoated and Coated Bars in Uncontaminated Silica Fume Cement Concrete Specimens (Temp: 35°C).

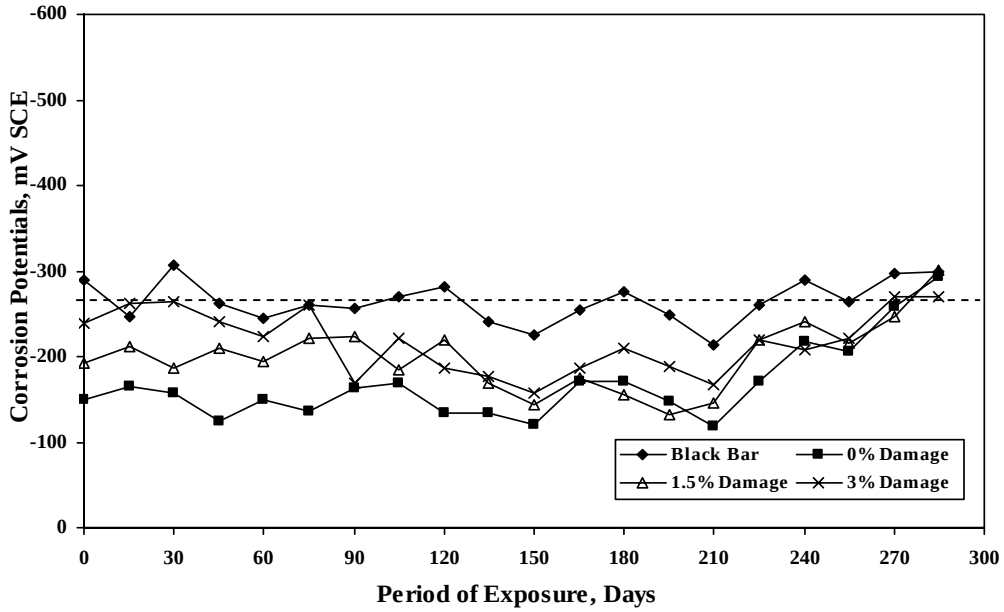

Figure 4.17: Corrosion Potentials on Uncoated and Coated Bars in Silica Fume Cement Concrete Specimens Contaminated with 1% chloride (Temp: 35°C).

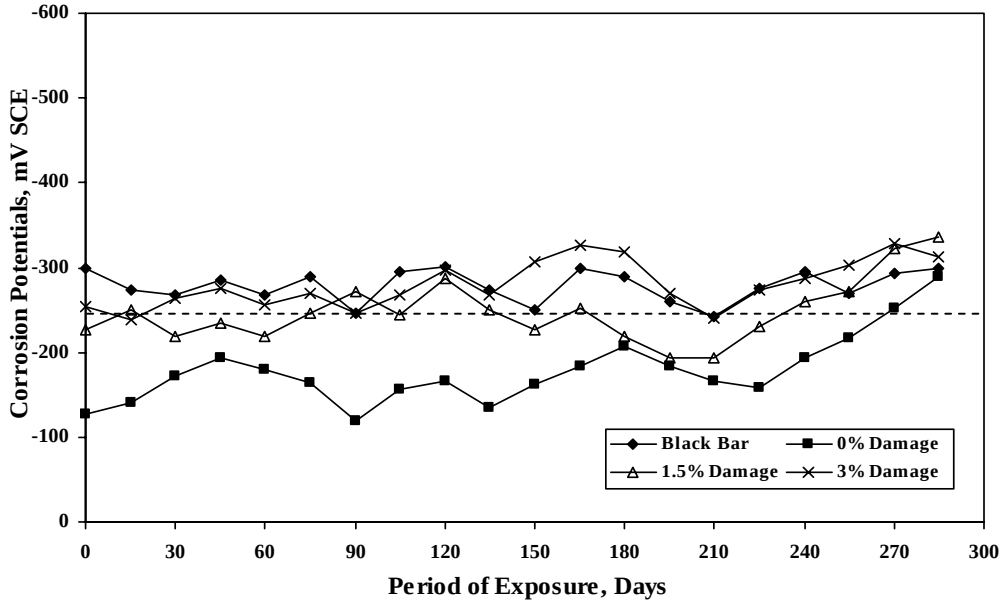

Figure 4.18: Corrosion Potentials on Uncoated and Coated Bars in Silica Fume Cement Concrete Specimens Contaminated with 2% chloride (Temp: 35°C).

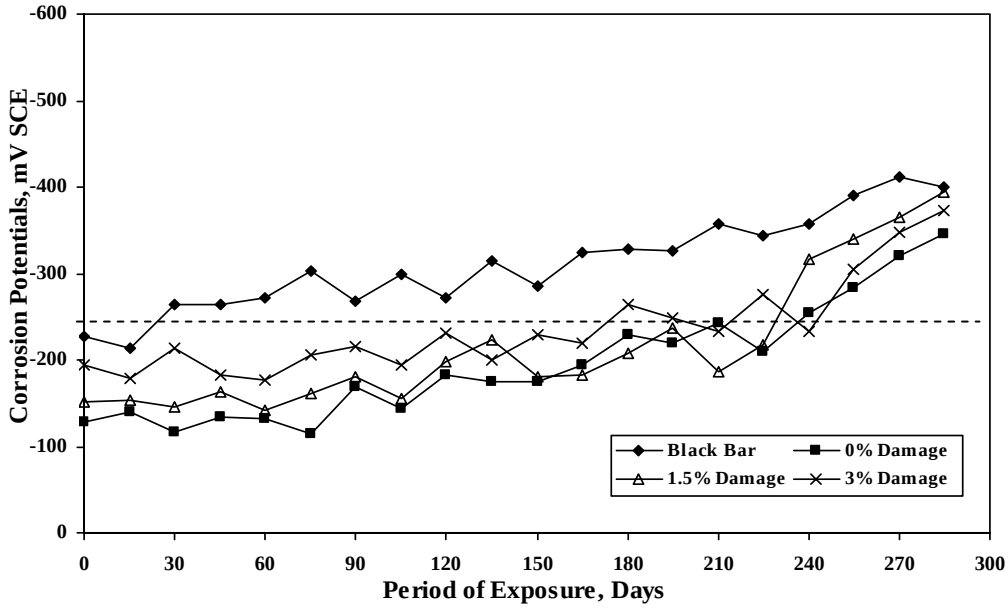

Figure 4.19: Corrosion Potentials on Uncoated and Coated Bars in Uncontaminated Blast Furnace Slag Cement Concrete Specimens (Temp: 35°C).

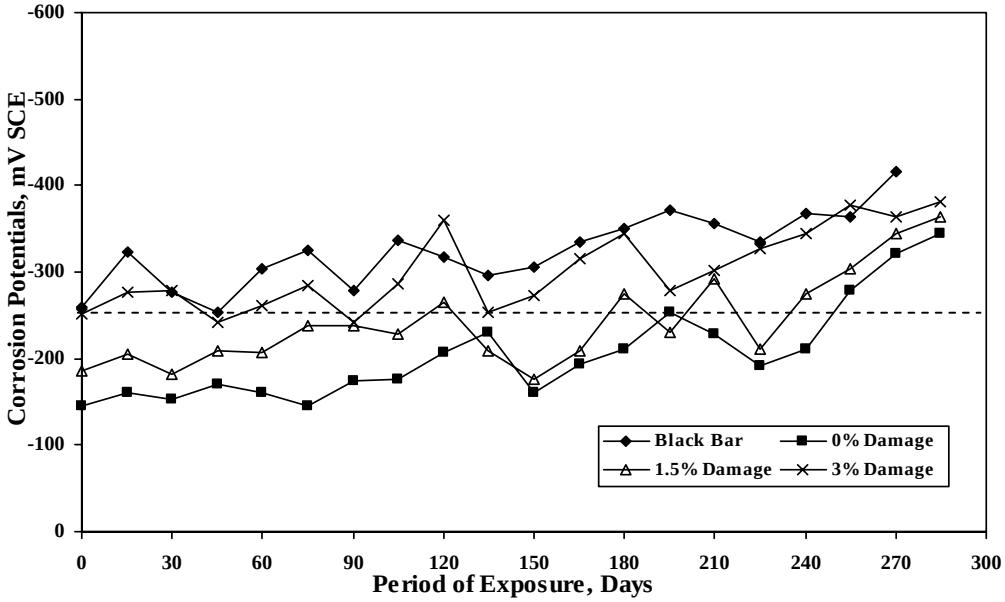

Figure 4.20: Corrosion Potentials on Uncoated and Coated Bars in Blast Furnace Slag Cement Concrete Specimens Contaminated with 1% chloride (Temp: 35°C).

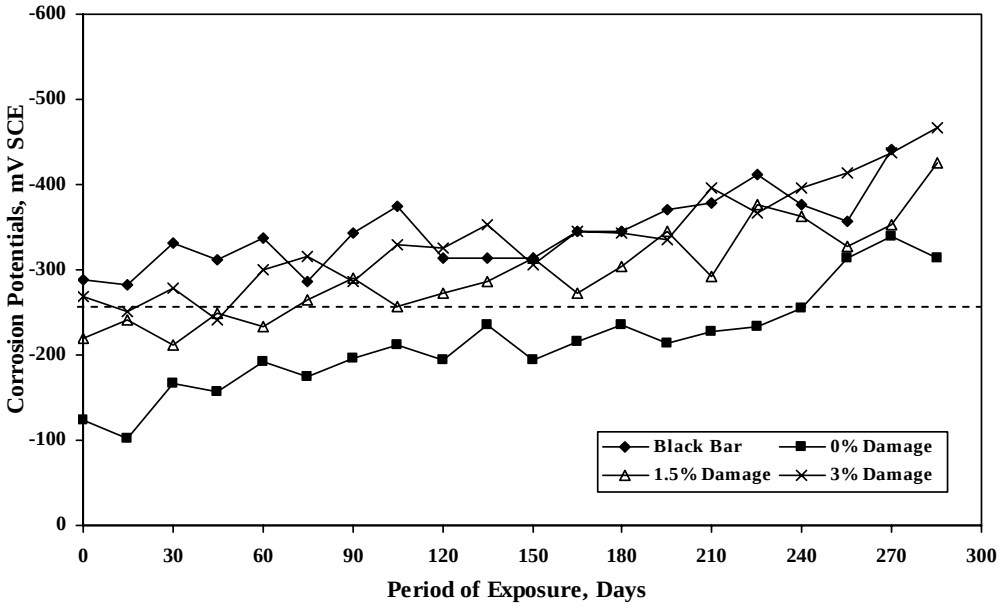

Figure 4.21: Corrosion Potentials on Uncoated and Coated Bars in Blast Furnace Slag Cement Concrete Specimens Contaminated with 2% chloride (Temp: 35°C).

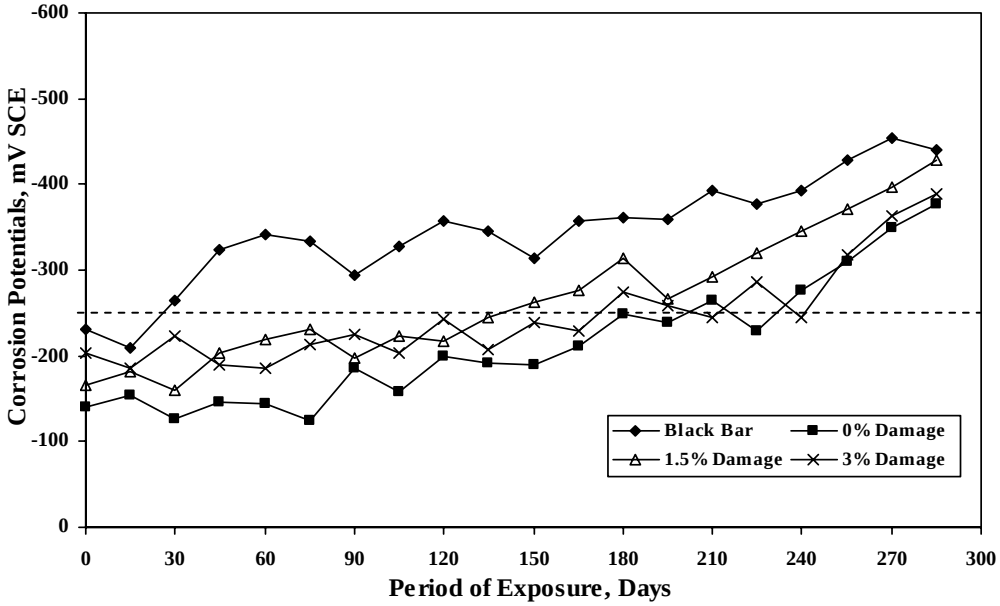

Figure 4.22: Corrosion Potentials on Uncoated and Coated Bars in Uncontaminated Fly Ash Cement Concrete Specimens (Temp: 35°C).

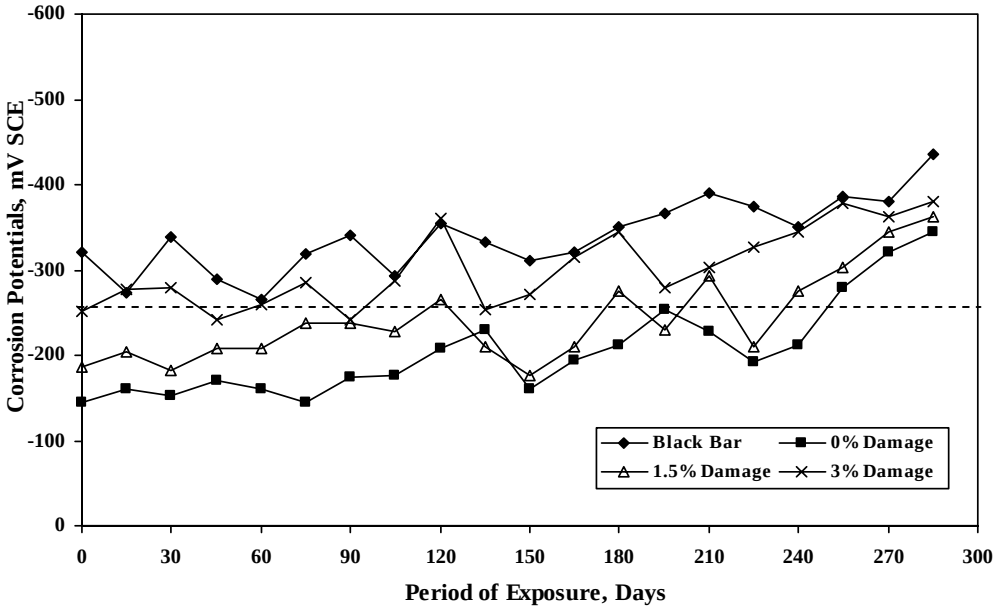

Figure 4.23: Corrosion Potentials on Uncoated and Coated Bars in Fly Ash Cement Concrete Specimens Contaminated with 1% chloride (Temp: 35°C).

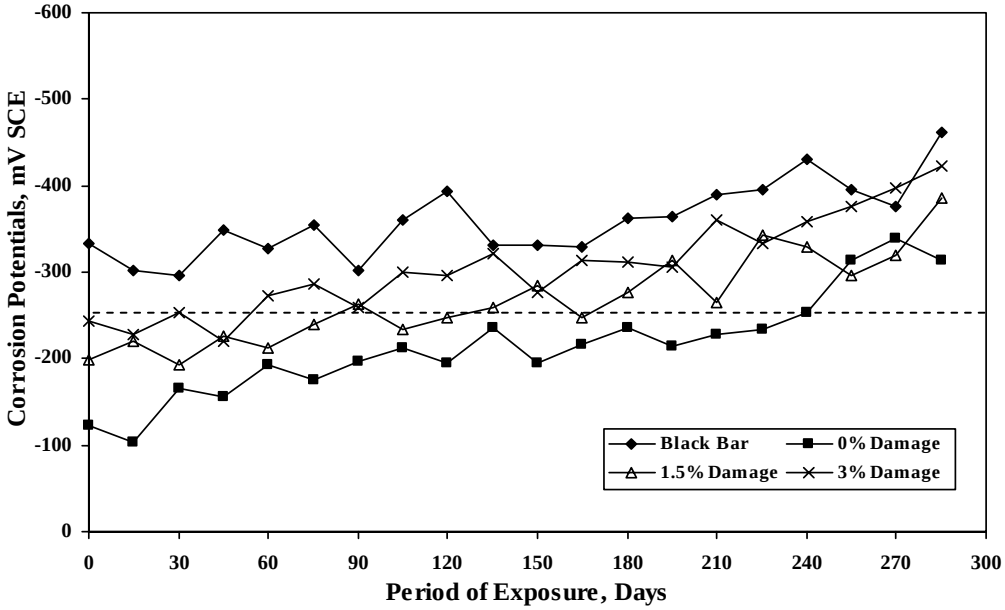

Figure 4.24: Corrosion Potentials on Uncoated and Coated Bars in Fly Ash Cement Concrete Specimens Contaminated with 2% chloride (Temp: 35°C).

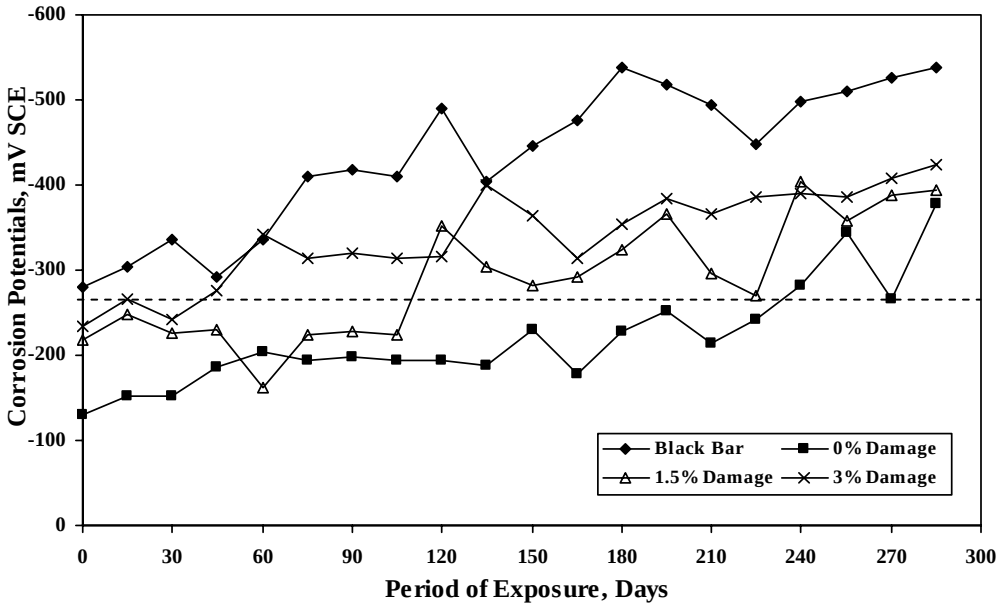

Figure 4.25: Corrosion Potentials on Uncoated and Coated Bars in Uncontaminated Plain Cement Concrete Specimens (Temp: 48°C).

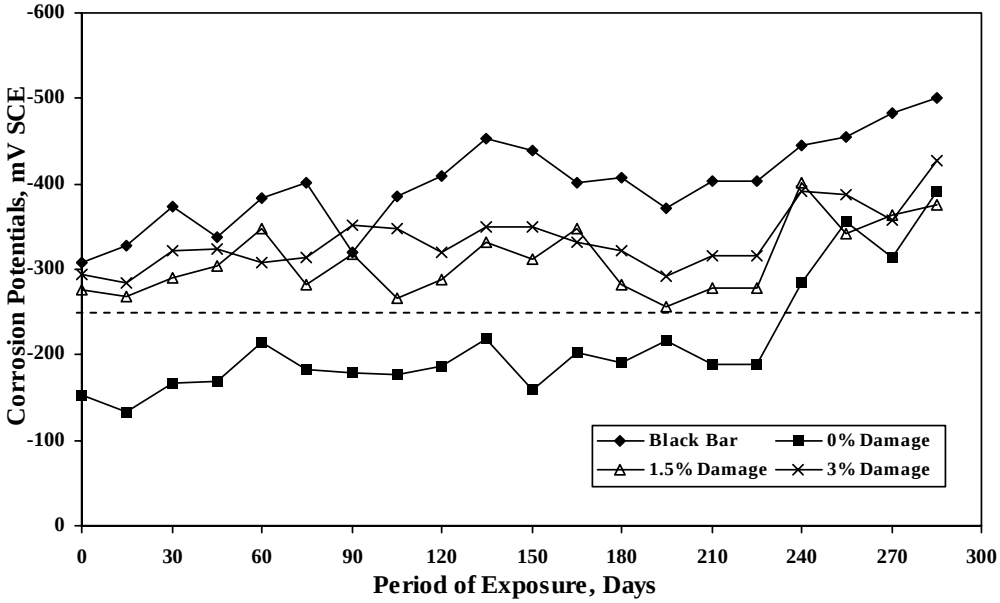

Figure 4.26: Corrosion Potentials on Uncoated and Coated Bars in Plain Cement Concrete Specimens Contaminated with 1% chloride (Temp: 48°C).

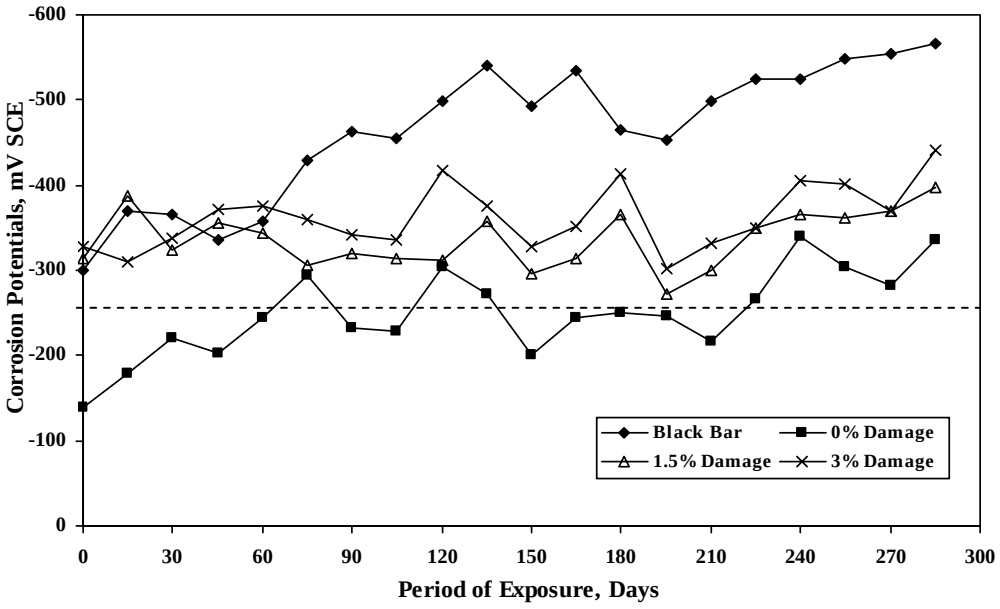

Figure 4.27: Corrosion Potentials on Uncoated and Coated Bars in Plain Cement Concrete Specimens Contaminated with 2% chloride (Temp: 48°C).

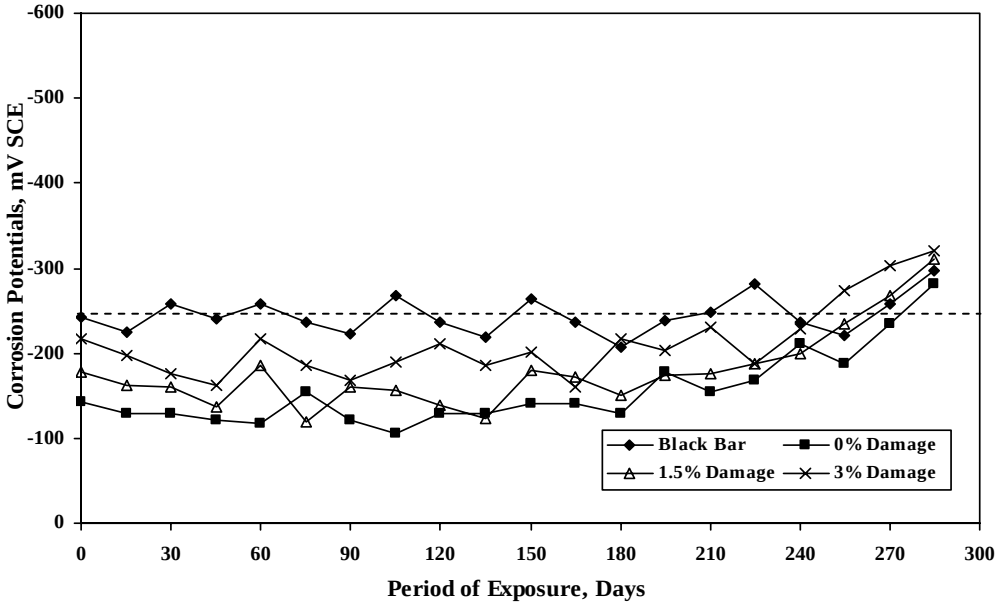

Figure 4.28: Corrosion Potentials on Uncoated and Coated Bars in Uncontaminated Silica Fume Cement Concrete Specimens (Temp: 48°C).

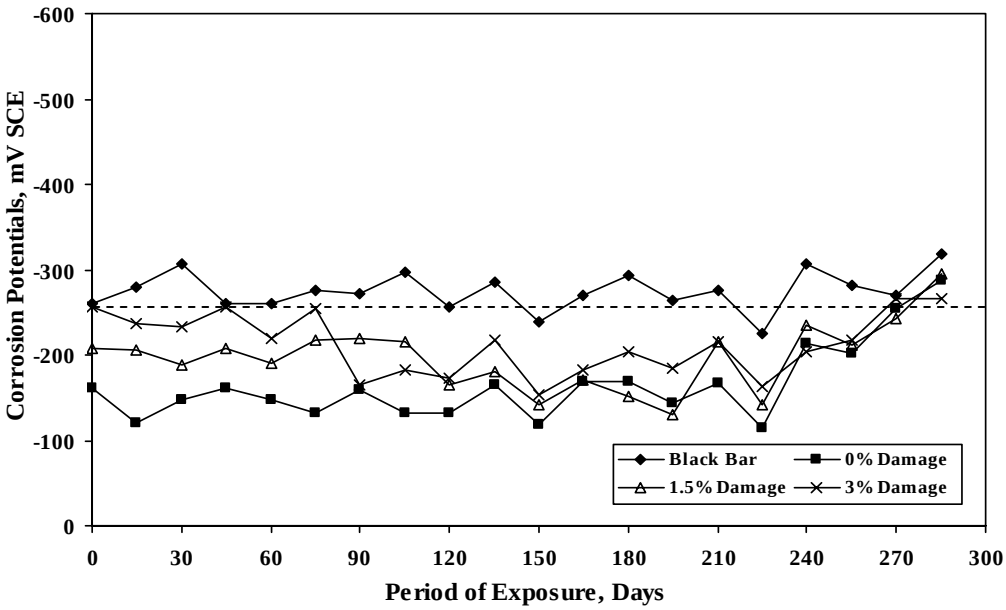

Figure 4.29: Corrosion Potentials on Uncoated and Coated Bars in Silica Fume Cement Concrete Specimens Contaminated with 1% chloride (Temp: 48°C).

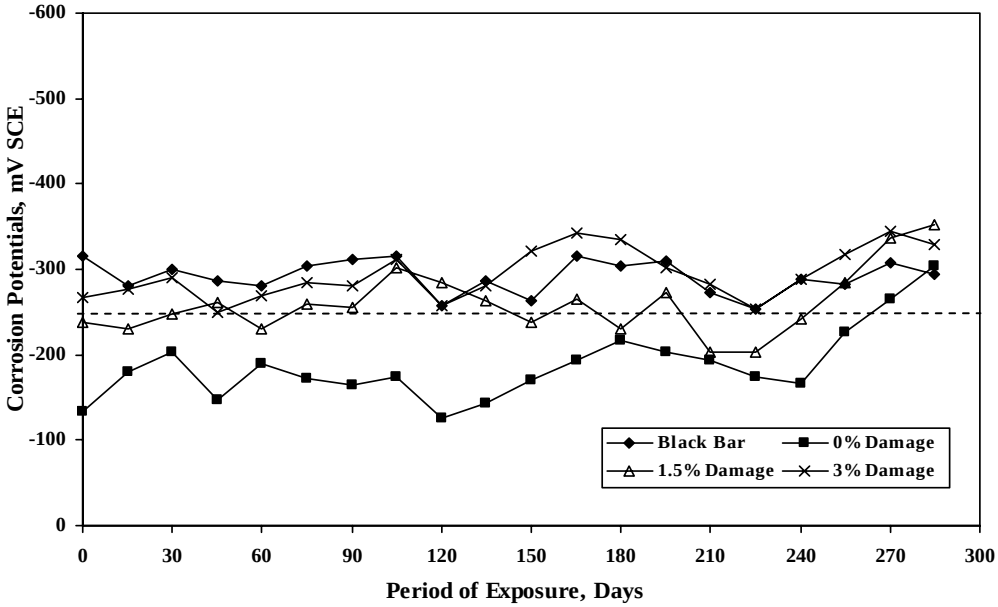

Figure 4.30: Corrosion Potentials on Uncoated and Coated Bars in Silica Fume Cement Concrete Specimens Contaminated with 2% chloride (Temp: 48°C).

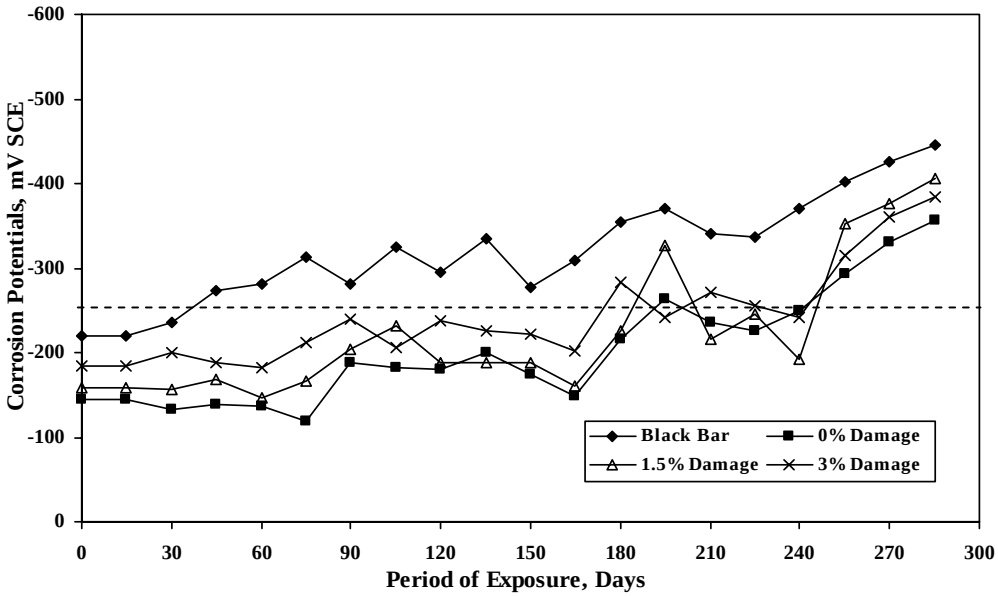

Figure 4.31: Corrosion Potentials on Uncoated and Coated Bars in Uncontaminated Blast Furnace Slag Cement Concrete Specimens (Temp: 48°C).

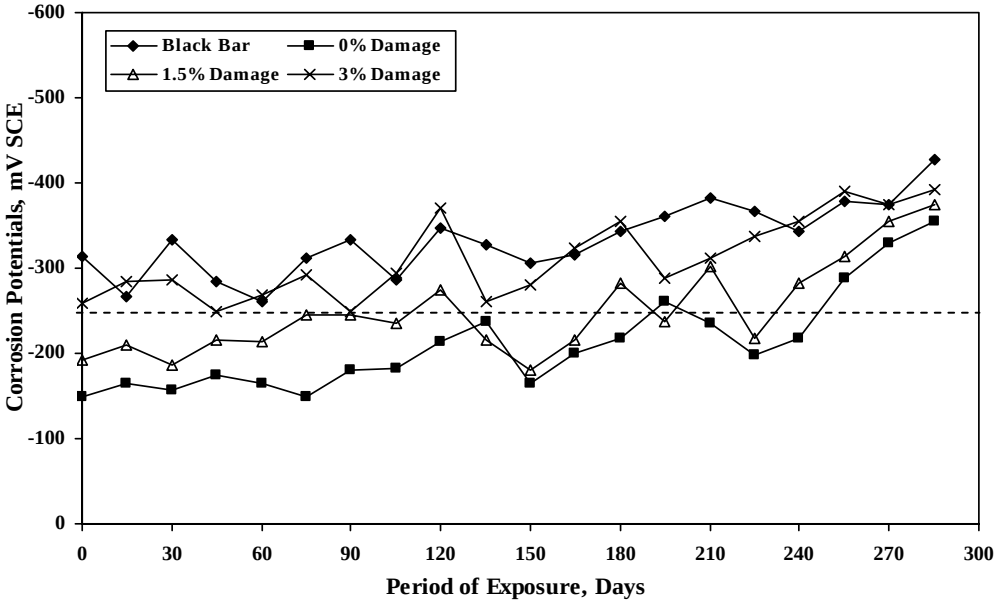

Figure 4.32: Corrosion Potentials on Uncoated and Coated Bars in Blast Furnace Slag Cement Concrete Specimens Contaminated with 1% chloride (Temp: 48°C).

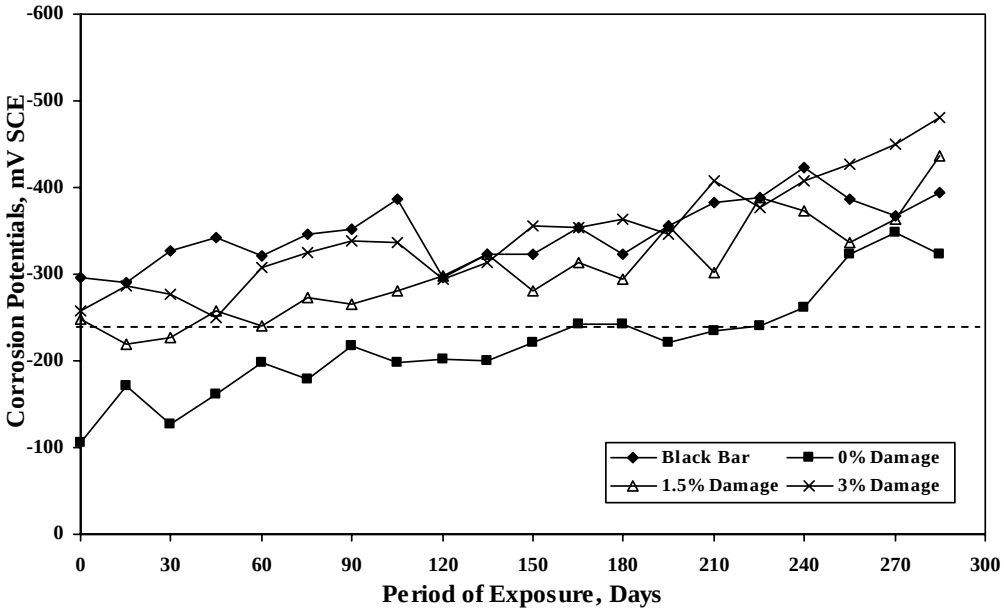

Figure 4.33: Corrosion Potentials on Uncoated and Coated Bars in Blast Furnace Slag Cement Concrete Specimens Contaminated with 2% chloride (Temp: 48°C).

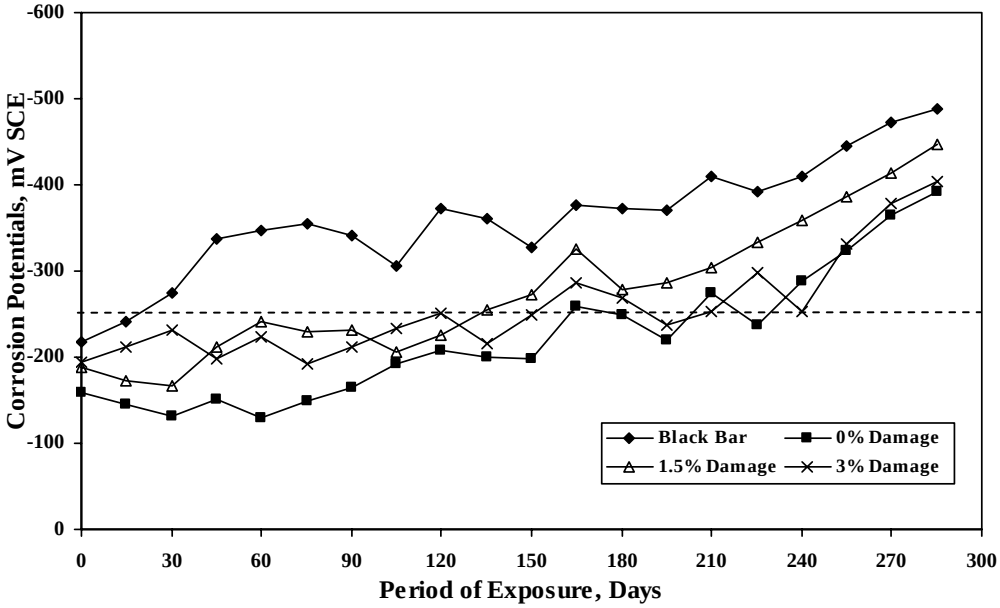

Figure 4.34: Corrosion Potentials on Uncoated and Coated Bars in Uncontaminated Fly Ash Cement Concrete Specimens (Temp: 48°C).

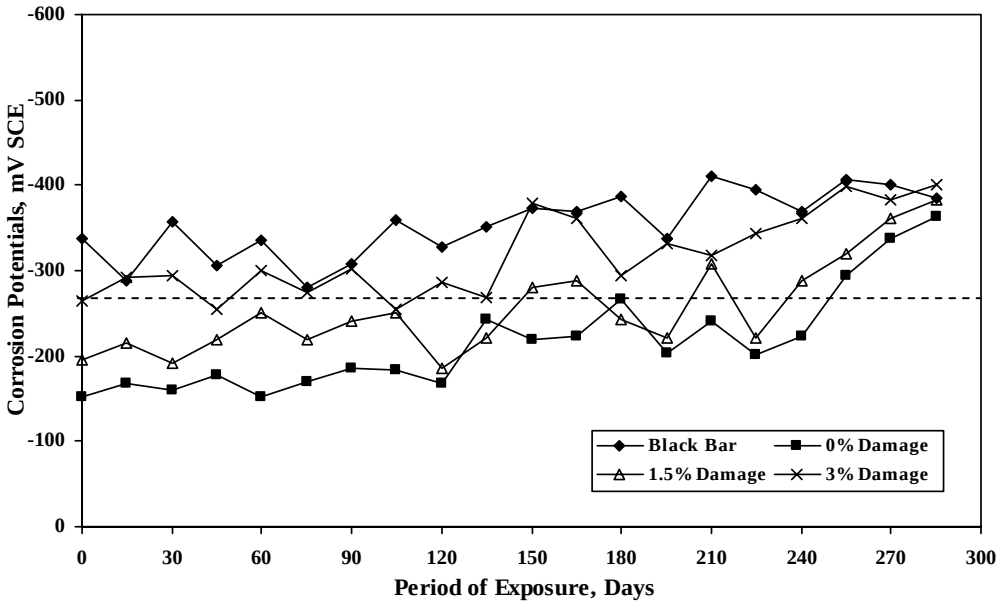

Figure 4.35: Corrosion Potentials on Uncoated and Coated Bars in Fly Ash Cement Concrete Specimens Contaminated with 1% chloride (Temp: 48°C).

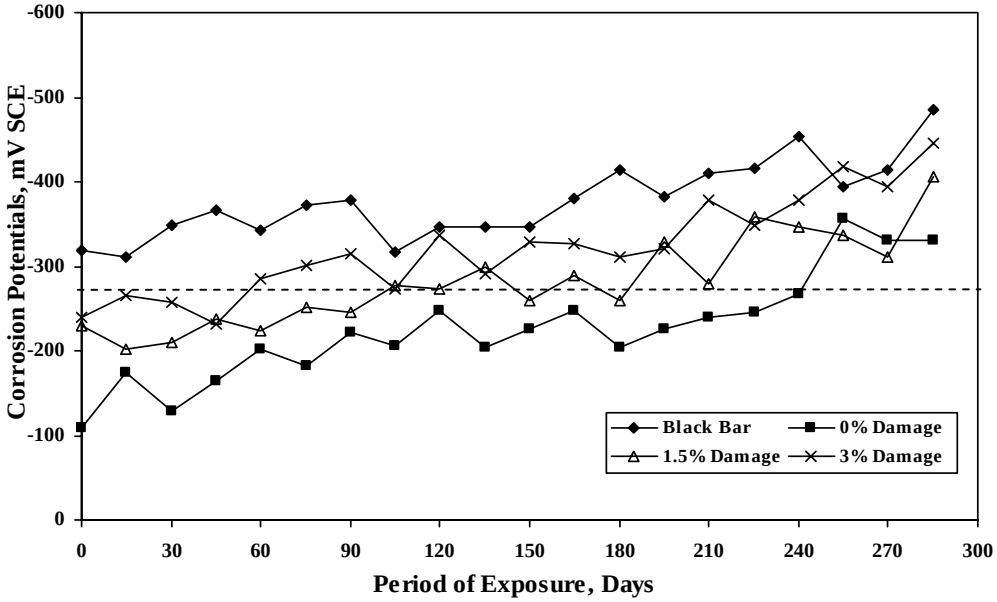

Figure 4.36: Corrosion Potentials on Uncoated and Coated Bars in Fly Ash Cement Concrete Specimens Contaminated with 2% chloride (Temp: 48°C).

Figures 4.1 through 4.3 show the corrosion potentials on steel in the plain uncoated cement concrete specimens exposed to a temperature of 23°C. The data in these figures indicate that the corrosion potentials decrease i.e., become more negative, with time. The potentials were generally the least negative in the concrete specimens with the uncoated bars.

Figures 4.4 through 4.6 show the corrosion potentials on steel the in the silica fume cement concrete specimens exposed to a temperature of 23°C. The data therein show that the corrosion potentials were maximum (more positive) on the coated bars without damage. The corrosion potentials on the FBEC bars with 1.5% and 3% damage were

marginally more positive than the uncoated steel bars. In this batch also, the corrosion potentials on the uncoated steel bars were more negative than those on the coated bars. Another important feature of the data in Figures 4.4 through 4.6 is that the potentials were more positive than -270 mV SCE, even in the specimens contaminated with 2% chlorides. This may be attributed to the denseness of silica fume cement concrete.

The corrosion potentials on the FBEC and uncoated steel bars in the blast furnace slag cement concrete specimens exposed to a temperature of 23°C are depicted in Figures 4.7 through 4.9. In this group also, the least potentials (more negative) were noted on the uncoated steel bars while they were the highest (more positive) on the FBEC bars without damage. Another point to be noted is that the potentials did not vary very much with the period of exposure. However, a significant reduction in the potentials was noted after about 200 days.

Figures 4.10 through 4.12 show the corrosion potentials on steel in the fly ash cement concrete specimens exposed to a temperature of 23°C. The potentials generally decreased with time in all the specimens. Further, the potentials were generally more negative in the uncoated bars compared to the FBEC bars. Among the FBEC bars, the potentials were more positive on the steel bars without any damage.

Figures 4.13 through 4.15 show the corrosion potentials on steel bars in plain uncoated cement concrete specimens exposed to a temperature of 35°C. They were low in the uncoated bars while they were the highest in the undamaged FBEC bars. The corrosion potentials in all the specimens decreased with the time of exposure.

The corrosion potentials in the silica fume cement concrete specimens exposed to a temperature of 35°C are shown in Figures 4.16 through 4.18. The potentials were the least in the uncoated specimens while they were more positive in the undamaged FBEC steel bars. The potentials on FBEC bars with 1.5% and 3% damage tended to be between the uncoated and undamaged FBEC bars.

Figures 4.19 through 4.21 show the corrosion potentials on the uncoated and FBEC steel bars in the blast furnace slag cement concrete specimens exposed to a temperature of 35°C. The trend of the potential data for this group of specimens was similar to that noted in the silica fume cement concrete specimens exposed to a temperature of 35°C.

The corrosion potentials on the uncoated and FBEC steel bars in the fly ash cement concrete specimens exposed to a temperature of 35°C are shown in Figures 4.22 through 4.24. The potentials decreased almost linearly with time in all the specimens. The corrosion potentials on the uncoated steel bars were generally more negative than on the FBEC bars.

Figures 4.25 through 4.27 depict the corrosion potentials on the uncoated and FBEC bars in the plain cement concrete specimens exposed to a temperature of 48°C. As expected, the corrosion potentials on the uncoated steel bars were less than those on the coated steel bars. A significant decrease in the potential values was noted on the uncoated bars both in the uncontaminated and chloride-contaminated concrete specimens. In the chloride-contaminated specimens, the corrosion potentials were less than -270 mV SCE from the beginning of exposure. The corrosion potentials on the undamaged FBEC steel

bars were more than -270 mV up to about 200 days of exposure. However, they tended to be more negative than this value later.

The corrosion potentials on the uncoated and FBEC steel bars in the silica fume cement concrete specimens exposed to a temperature of 48°C are shown in Figures 4.28 through 4.30. The corrosion potentials in all types of bars were less than the threshold value i.e. -270 mV, the corrosion potential values was well below the threshold values in coated bars in all chloride contents.

Figures 4.31 through 4.33 show the corrosion potentials on the uncoated and FBEC bars in the blast furnace slag cement concrete specimens exposed to a temperature of 48°C. The trend of these data was similar to that noted in the plain cement concrete specimens exposed to the same temperature.

The corrosion potentials on the uncoated and FBEC steel bars in the fly ash cement concrete specimens exposed to a temperature of 48°C are depicted in Figures 4.34 through 4.36. The corrosion potentials increased with the period of exposure. The potentials on the uncoated steel bars were less than the threshold value of -270 mV SCE from the initial stage of exposure in both the uncontaminated and chloride-contaminated concrete specimens. The corrosion potentials on FBEC steel bars were more than the threshold value initially, but crossed the threshold value after about 200 days of exposure.

4.1.2 Effect of Chloride Concentration on Reinforcement Corrosion

Figure 4.37 shows the corrosion current density (I_{corr}) on the uncoated steel bars in plain uncoated cement concrete specimens with varying chloride contaminations and exposed to varying temperatures. The I_{corr} increased with the increase in both chloride concentration and exposure temperature. The I_{corr} value in the uncontaminated concrete specimens exposed to temperature of 23°C and 35°C was less than 0.3 µA/cm². In the concrete specimens exposed to 48°C, the I_{corr} was more than 0.3 µA/cm² indicating corrosion activation. In the concrete specimens with both 1 and 2% chloride additions, the I_{corr} was more than 0.3 µA/cm² for all the exposure temperatures.

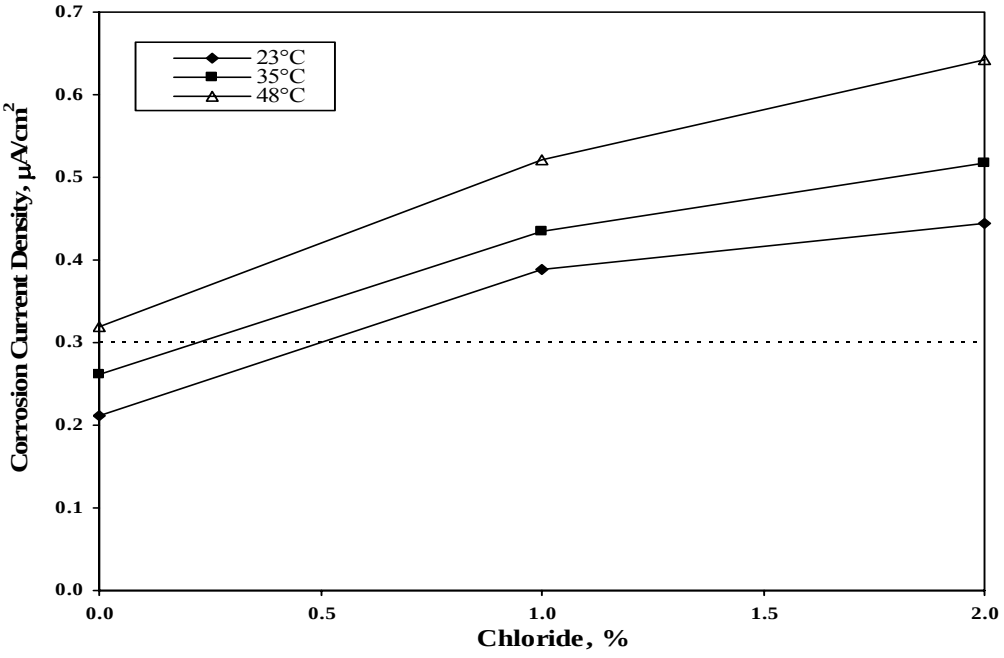

Figure 4.37: Corrosion Current Density on Uncoated Steel Bars in Plain Cement Concrete Specimens after 180 Days of Exposure.

The I_{corr} on the uncoated steel in the silica fume cement concrete specimens with varying chloride contaminations and exposed to varying exposure temperatures is depicted in Figure 4.38. The I_{corr} increased with chloride concentration and exposure temperature. However, the I_{corr} values for all the exposure temperatures and chloride contaminations were less than 0.3 μA/cm², indicating passive reinforcement conditions.

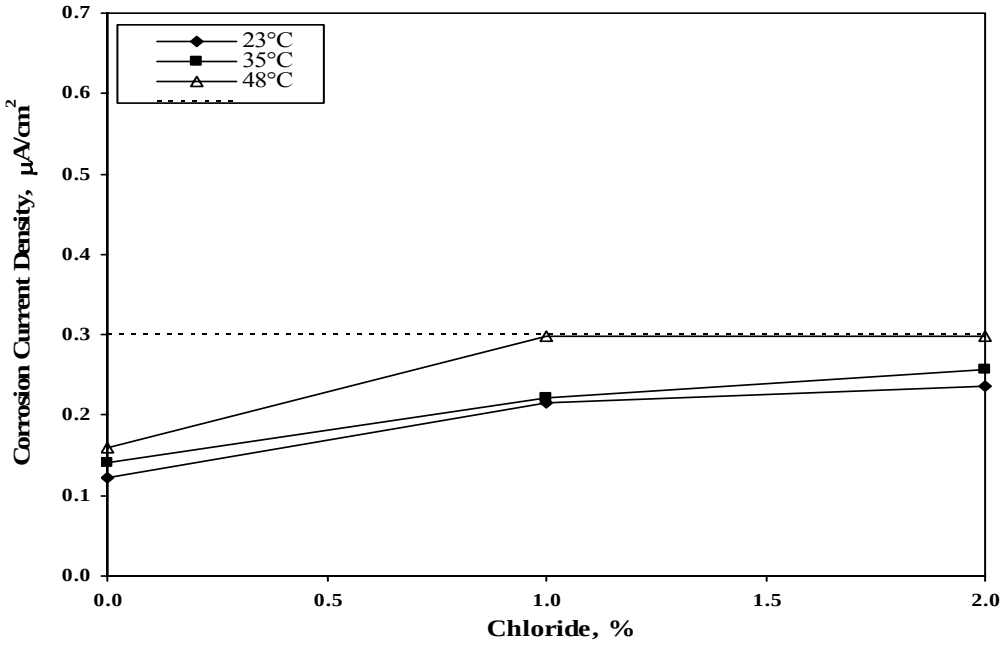

Figure 4.38: Corrosion Current Density on Uncoated Steel Bars in Silica Fume Cement Concrete Specimens after 180 Days of Exposure.

The I_{corr} on the uncoated steel bars in the blast furnace slag cement concrete specimens with varying chloride contaminations and exposed to varying temperatures is shown in Figure 4.39. The I_{corr} was less than 0.3 μA/cm² for all exposure temperatures in uncontaminated concrete specimens and in the concrete specimens contaminated with 1%

and 2% chloride and exposed to 23°C. The I_{corr} was more than 0.3 μA/cm² in the concrete exposed to 35°C and 48°C.

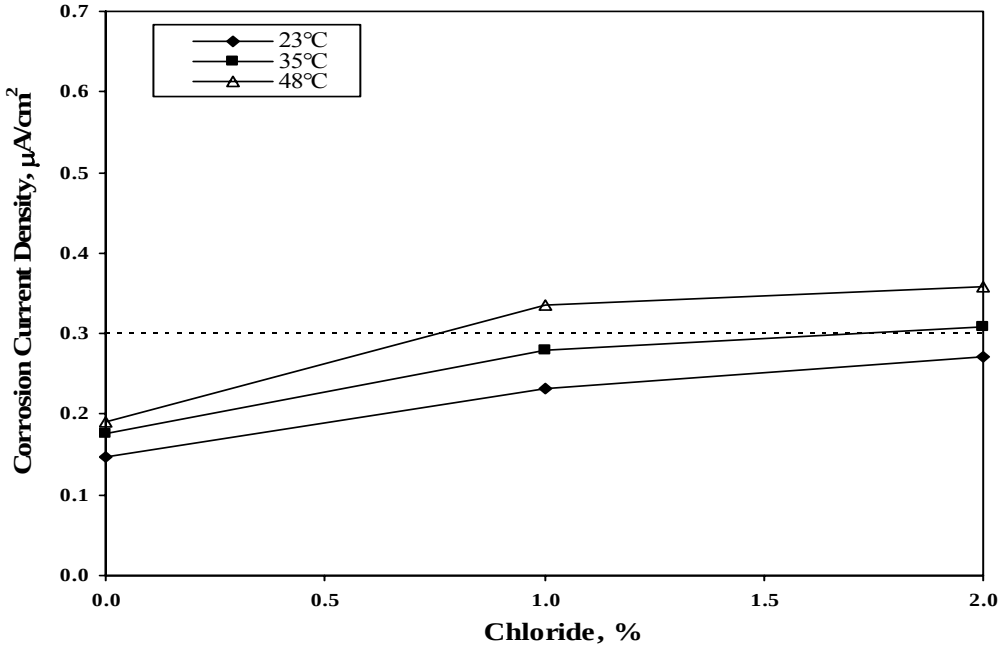

Figure 4.39: Corrosion Current Density on Uncoated Steel Bars in Blast Furnace Slag Cement Concrete Specimens after 180 Days of Exposure.

Figure 4.40 shows the I_{corr} on the uncoated steel bars in the fly ash cement concrete specimens with varying chloride contaminations and exposed to varying temperatures. The I_{corr} value was less than 0.3 μA/cm² in both the uncontaminated and chloride contaminated concrete specimens exposed to 23°C and 35°C. The I_{corr} value was more than 0.3 μA/cm² in the specimens contaminated with 1% and 2% chloride contamination and exposed to 48°C.

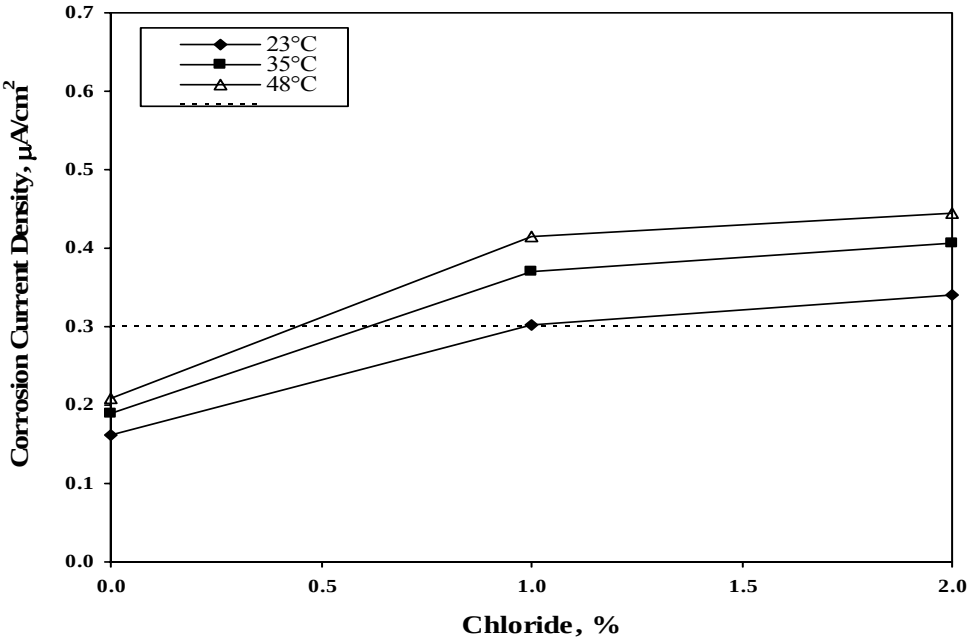

Figure 4.40: Corrosion Current Density on Uncoated Steel Bars in Fly Ash Cement Concrete Specimens after 180 Days of Exposure.

The I_{corr} on the undamaged FBEC steel bars in the plain cement concrete specimens with varying chloride contaminations and exposed to varying exposure temperatures is shown in Figure 4.41. The I_{corr} values for all the chloride contamination and exposure temperature were less than 0.1 µA/cm². Further, the I_{corr} values did not vary very significantly with the chloride contamination and exposure temperature.

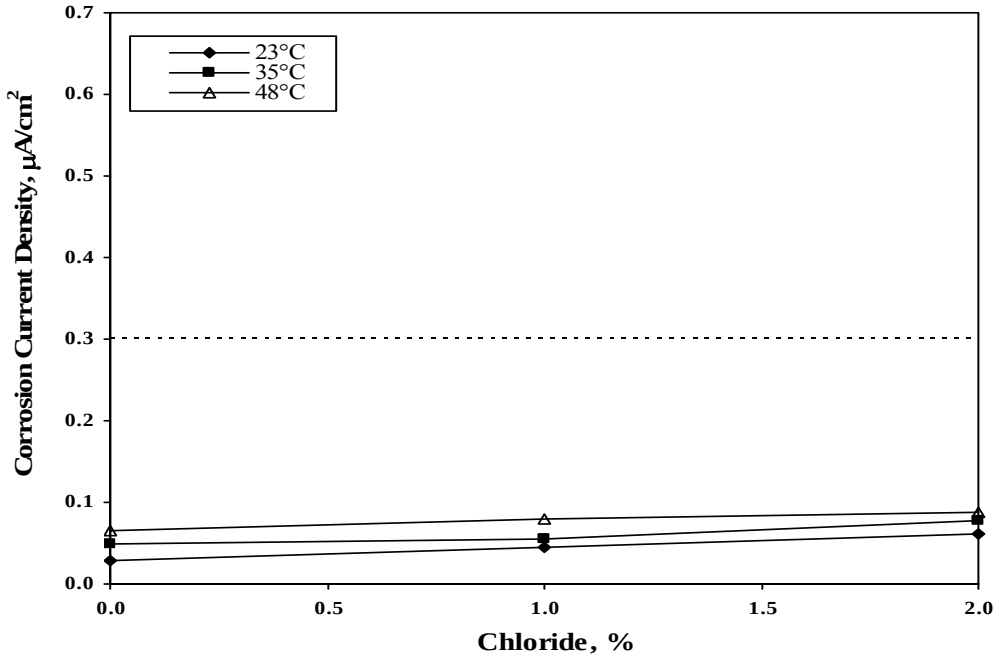

Figure 4.41: Corrosion Current Density on FBEC Steel Bars in Ordinary Plain Cement Concrete Specimens after 180 Days of Exposure.

I_{corr} on the FBEC steel bars in the silica fume cement concrete specimens with varying chloride contaminations and exposed to varying temperatures is shown in Figure 4.42. The trend of these data was similar to the plain cement concrete. The I_{corr} values in the silica fume cement concrete were less than those in the plain cement concrete specimens.

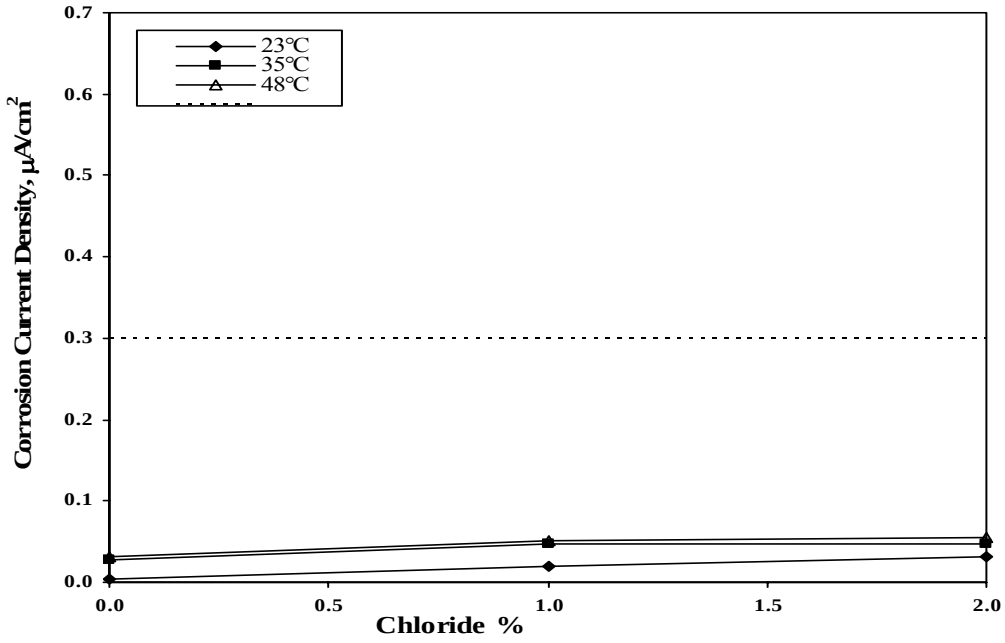

Figure 4.42: Corrosion Current Density on FBEC Steel Bars in Silica Fume Cement Concrete Specimens after 180 Days of Exposure.

The I_{corr} on FBEC steel bars in the blast furnace slag cement concrete specimens with varying chloride concentrations and exposed to varying temperatures is shown in Figure 4.43. The I_{corr} values in all the specimens were less than 0.1 µA/cm². Those values in the specimens exposed to 35 and 48°C were almost similar in both uncontaminated and contaminated concrete specimens.

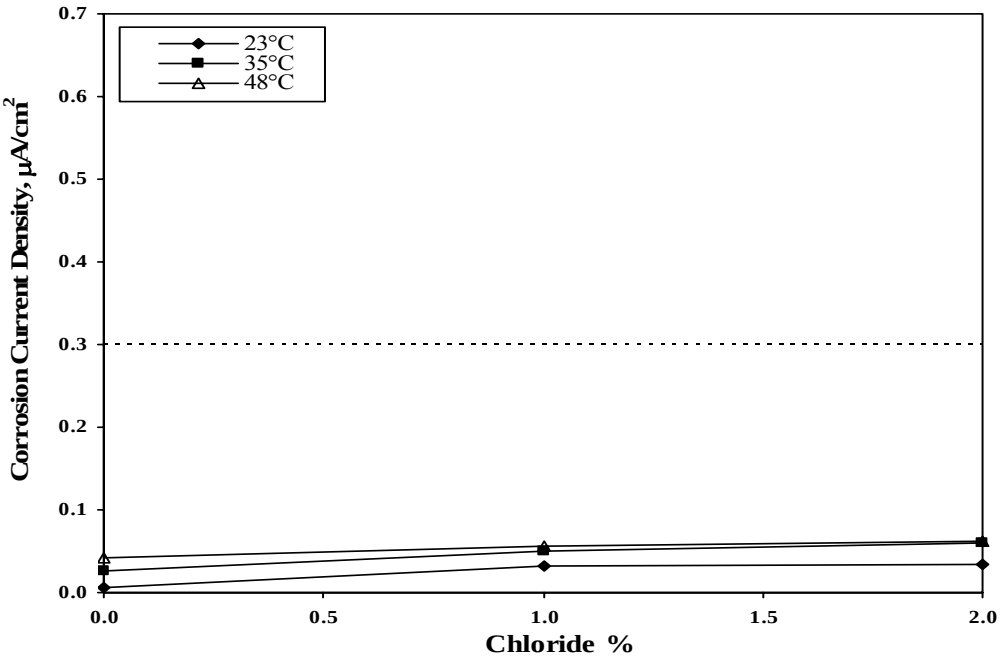

Figure 4.43: Corrosion Current Density on FBEC Steel Bars in Blast Furnace Slag Cement Concrete Specimens after 180 Days of Exposure.

The I_{corr} on the FBEC steel bars without damage in the fly ash cement concrete specimens with varying chloride contaminations and exposed to varying exposure temperatures is shown in Figure 4.44. The data show an insignificant increase in the I_{corr} value with increasing the chloride concentration and exposure temperature. Further, the I_{corr} value was less than 0.1 µA/cm².

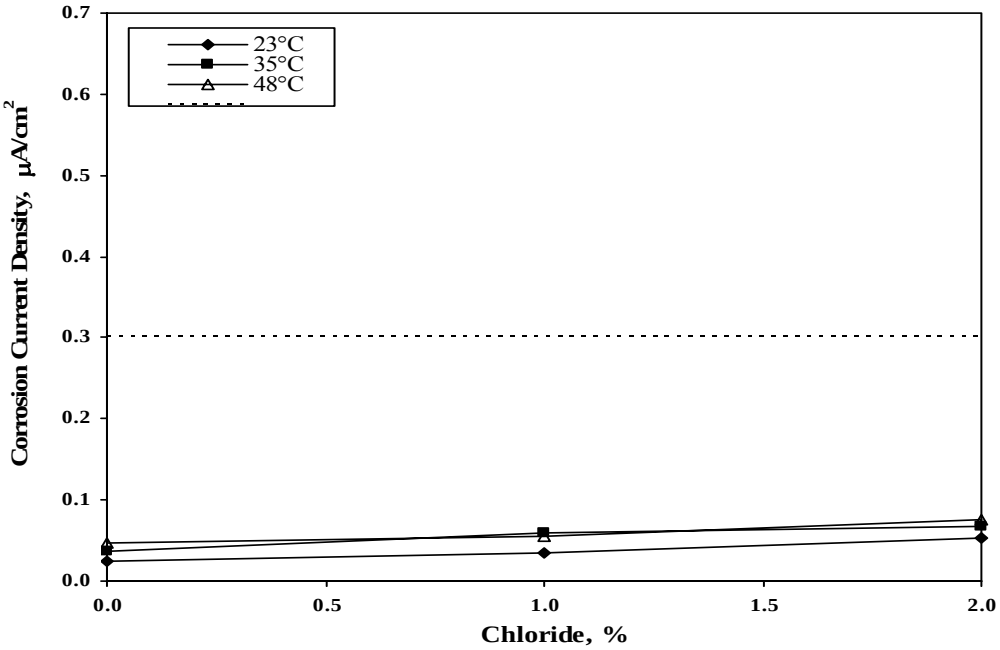

Figure 4.44: Corrosion Current Density on FBEC Steel Bars in Fly Ash Cement Concrete Specimens after 180 Days of Exposure.

I_{corr} on the FBEC bars with 1.5% surface damage in the plain cement concrete specimens with varying chloride contaminations and exposed to varying temperatures is shown in Figure 4.45. In the concrete specimens exposed to a temperature of 48°C, the I_{corr} increased with an increase in the chloride concentration, but it was less than 0.3 µA/cm². There was no significant increase in the I_{corr} with chloride concentration in the specimens exposed to 23°C and 35°C and it was less than 0.3 µA/cm².

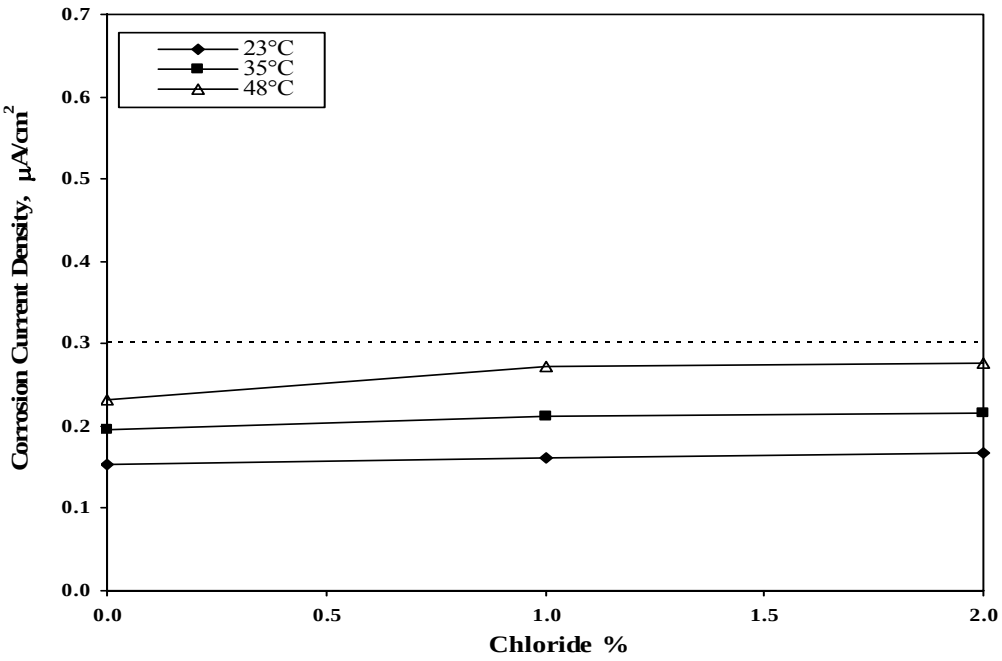

Figure 4.45: Corrosion Current Density on FBEC Steel Bars with 1.5% damage in Ordinary Plain Cement Concrete Specimens after 180 Days of Exposure.

Figure 4.46 shows the I_{corr} on the FBEC bars with 1.5% surface damage in the silica fume cement concrete specimens with varying chloride contaminations and exposed to varying temperatures. The I_{corr} values in all the specimens were less than 0.3 µA/cm² in all the concrete specimens. Further, the change in I_{corr} with chloride contamination or exposure temperature was very insignificant.

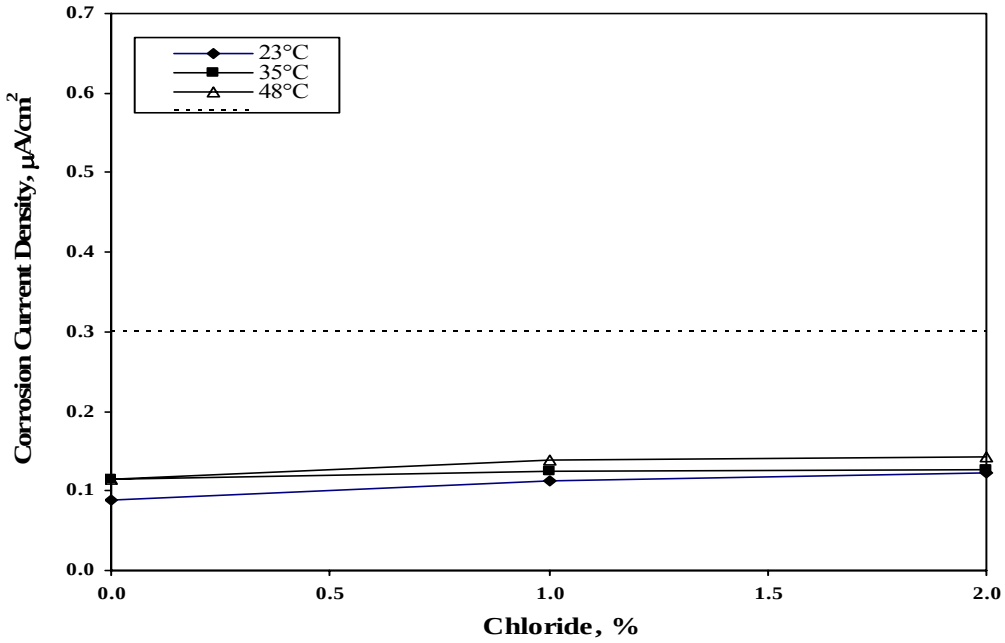

Figure 4.46: Corrosion Current Density on FBEC Steel Bars with 1.5% damage in Silica Fume Cement Concrete Specimens after 180 Days of Exposure.

The I_{corr} on the FBEC bars with 1.5% surface damage in the blast furnace slag cement concrete specimens with varying chloride contaminations exposed to varying temperatures is shown in Figure 4.47. The I_{corr} increased with the chloride contamination and exposure temperature. As expected, the I_{corr} values in the concrete specimens exposed to a temperature of 23°C were less than those exposed to temperature of 35°C and 48°C for specimens with similar contamination. However, the difference in the I_{corr} value in the concrete specimens exposed to 35°C and 48°C was not that significant.

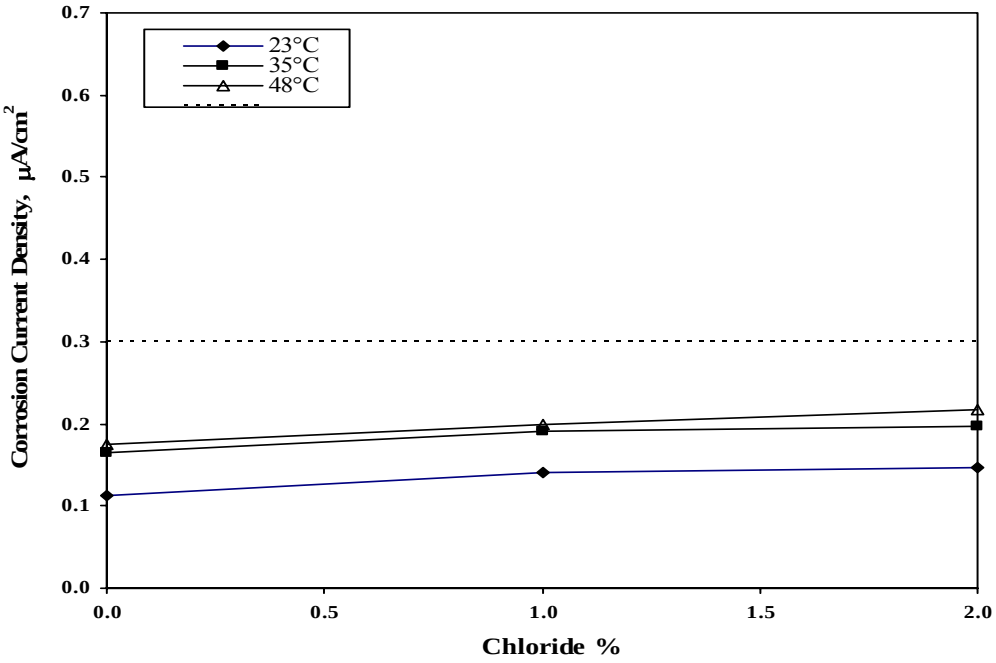

Figure 4.47: Corrosion Current Density on FBEC Steel Bars with 1.5% damage in Blast Furnace Slag Cement Concrete Specimens after 180 Days of Exposure.

The I_{corr} on the FBEC bars with 1.5% surface damage in the fly ash cement concrete specimens with varying chloride contaminations and exposed to varying exposure temperatures is shown in Figure 4.48. The data show a trend more or less similar to that noted for blast furnace slag cement concrete specimens.

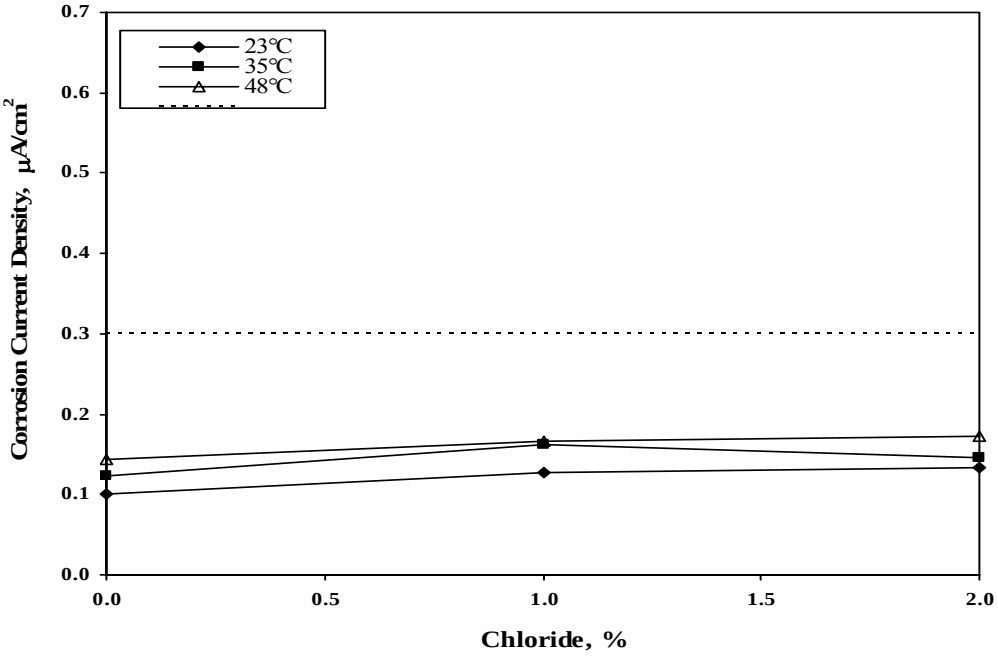

Figure 4.48: Corrosion Current Density on FBEC Steel Bars with 1.5% damage in Fly Ash Cement Concrete Specimens after 180 Days of Exposure.

Figure 4.49 shows the I_{corr} on the FBEC bars with 3% surface damage in the plain cement concrete specimens with varying chloride contaminations and exposed to varying temperatures. The I_{corr} increased with the chloride concentration and exposure temperature. The I_{corr} values in the uncontaminated and contaminated concrete specimens were less than 0.3 μA/cm².

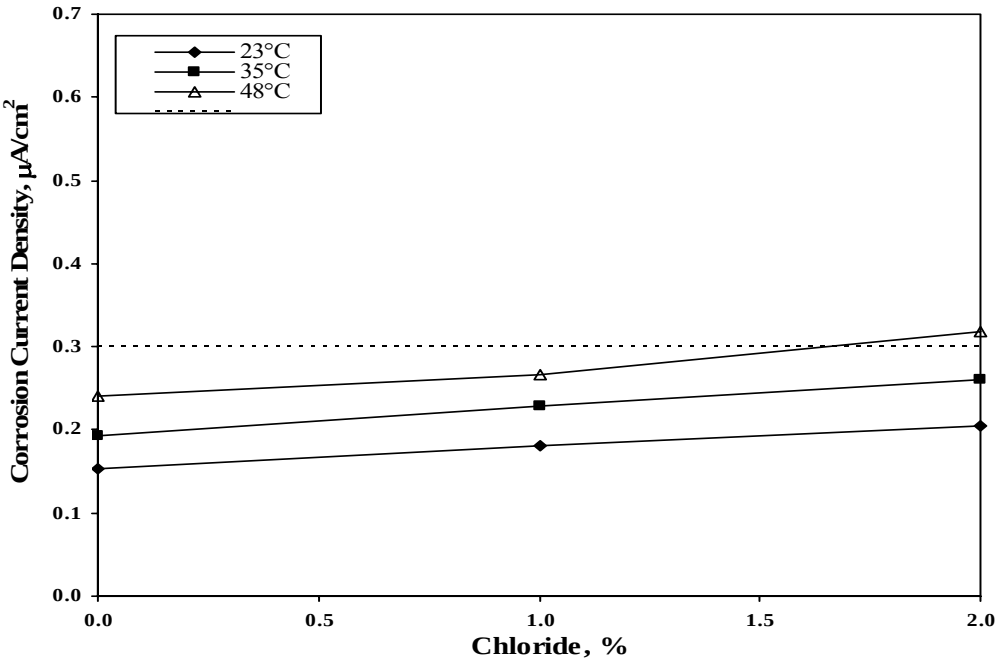

Figure 4.49: Corrosion Current Density on FBEC Steel Bars with 3% damage in Ordinary Plain Cement Concrete Specimens after 180 Days of Exposure.

The I_{corr} on the FBEC bars with 3% surface damage in the silica fume cement concrete specimens with varying chloride contaminations and exposed to varying temperatures is shown in Figure 4.50. The I_{corr} values increased with the level of chloride contamination, though this increase was not significant. Further, the I_{corr} values for a similar chloride contamination, in the concrete specimens exposed to 35 and 48°C was almost same.

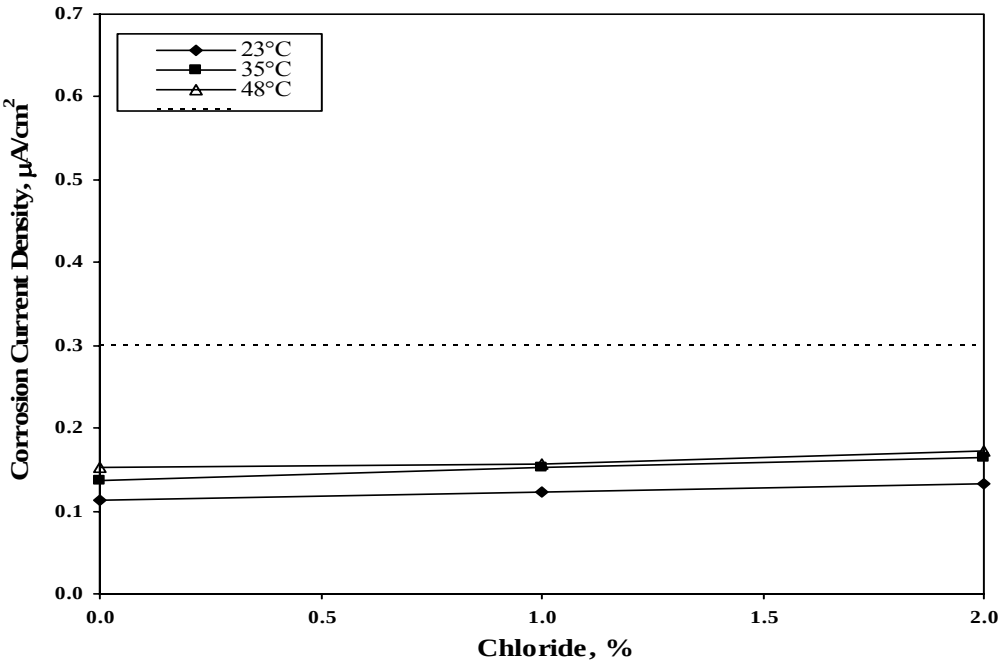

Figure 4.50: Corrosion Current Density on FBEC Steel Bars with 3% damage in Silica Fume Cement Concrete Specimens after 180 Days of Exposure.

The I_{corr} on the FBEC bar with 3% surface damage in the blast furnace slag cement concrete specimens with varying chloride contaminations and exposed to varying exposure temperatures is shown in Figure 4.51. These data also show a trend similar to that noted in the silica fume cement concrete specimens (Figure 4.50).

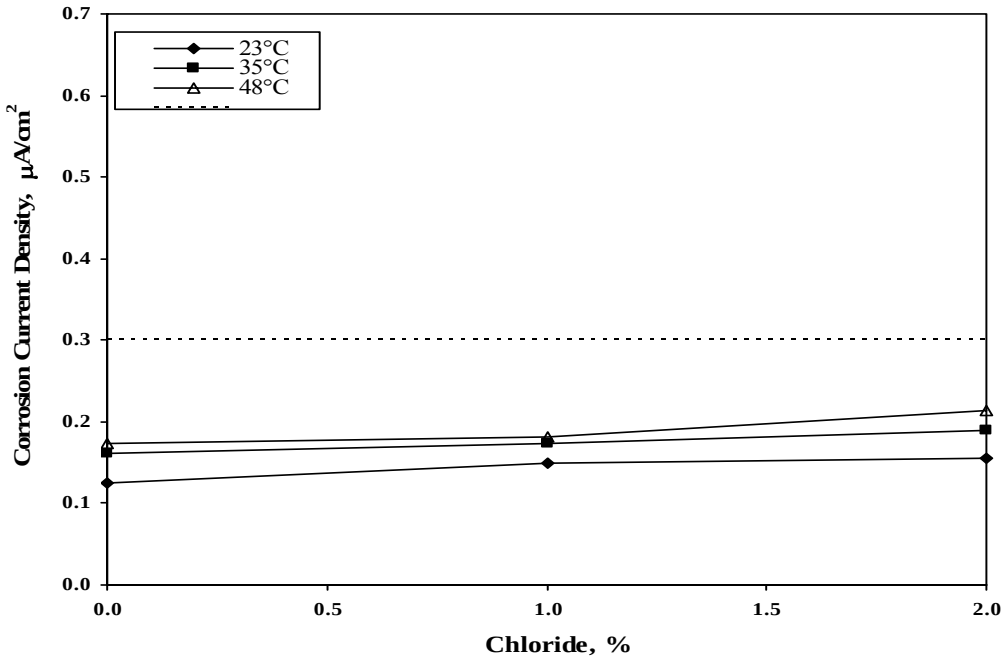

Figure 4.51: Corrosion Current Density on FBEC Steel Bars with 3% damage in Blast Furnace Slag Cement Concrete Specimens after 180 Days of Exposure.

Figure 4.52 shows I_{corr} on the FBEC steel bars with 3% surface damage in the fly ash cement concrete specimens with varying chloride contamination and exposed to varying temperature. The I_{corr} increased with the chloride contaminations and exposure temperatures. However, no significant variation in the I_{corr} was observed in the specimens exposed to temperature of 35°C and 48°C.

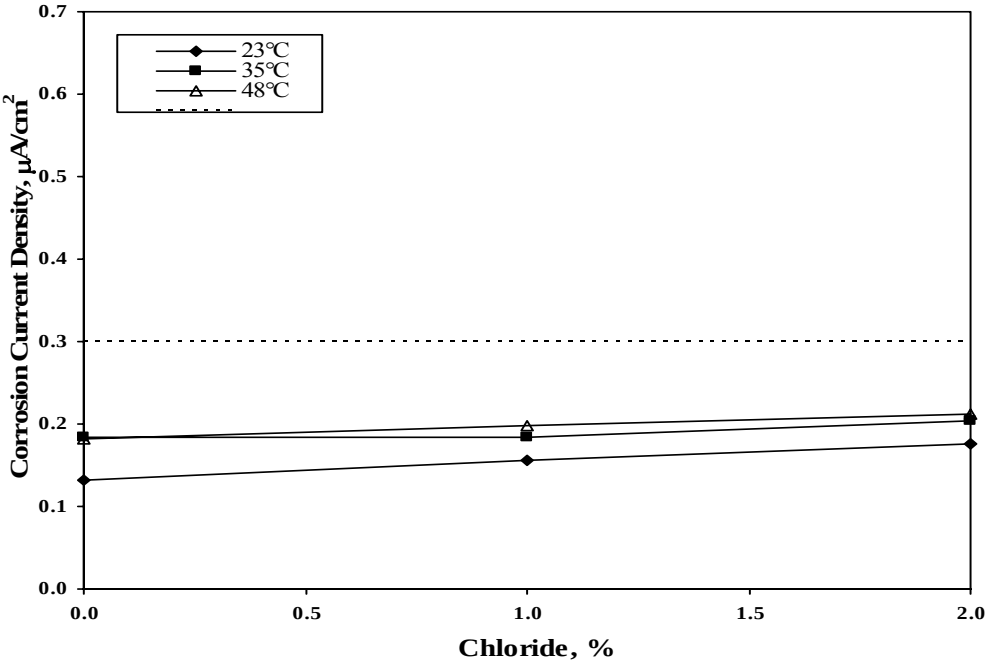

Figure 4.52**:** Corrosion Current Density on FBEC Steel Bars with 3% damage in Fly Ash Cement Concrete Specimens after 180 Days of Exposure.

4.1.3 Effect of Surface Damage on Reinforcement Corrosion

Figures 4.53 through 4.55 show the I_{corr} on steel in plain cement concrete specimens exposed to a temperature of 23°C. The data in these figures indicate that the corrosion current density increases with time. The corrosion current density was generally the least in the concrete specimens with FBEC bar with a value of less than 0.1 µA/cm² in all the chloride concentrations. The I_{corr} increased with both the chloride concentration and exposure period. However, the I_{corr} value in FBEC bars was less than 0.3 µA/cm² for all chloride concentrations. The uncoated bar shows I_{corr} value of more than 0.3 µA/cm² in

1% chloride concentration after 90 days of exposure, whereas the 2% chloride concentration bars shows I_{corr} value more than 0.3 µA/cm² from the initial period of exposure.

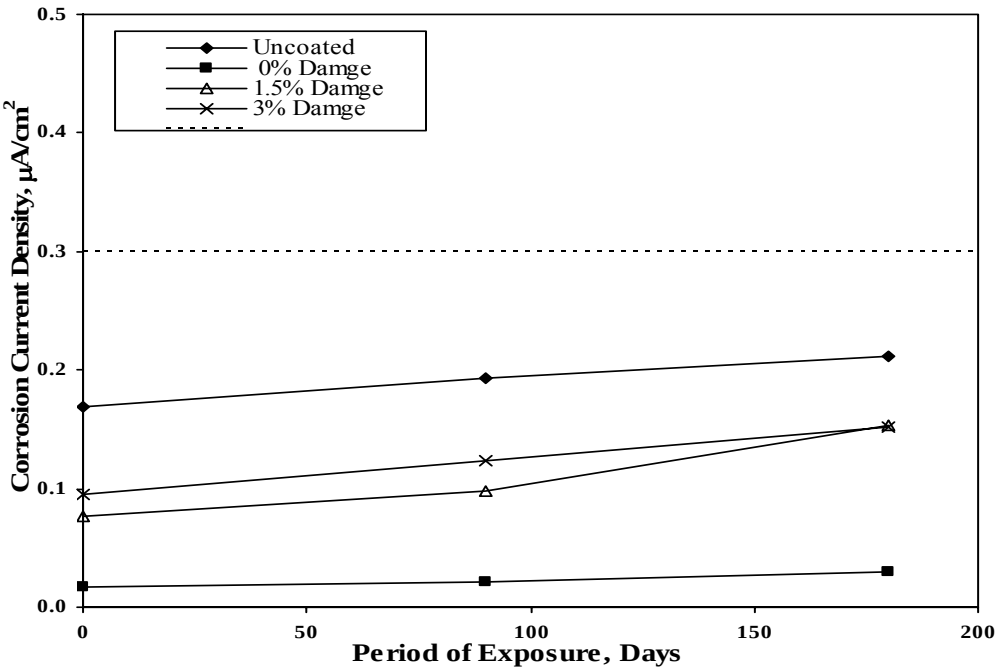

Figure 4.53: Corrosion Current Density in Uncontaminated Plain Cement Concrete Specimens on Steel Bars Exposed to 23°C.

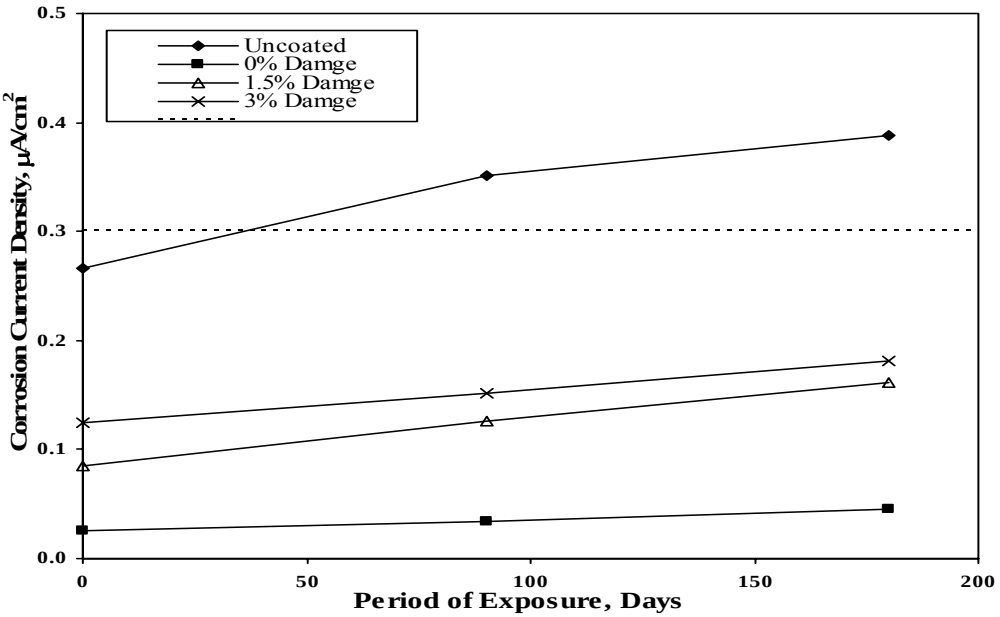

Figure 4.54: Corrosion Current Density in Plain Cement Concrete Specimens Contaminated with 1% Chloride on Steel Bars Exposed to 23°C.

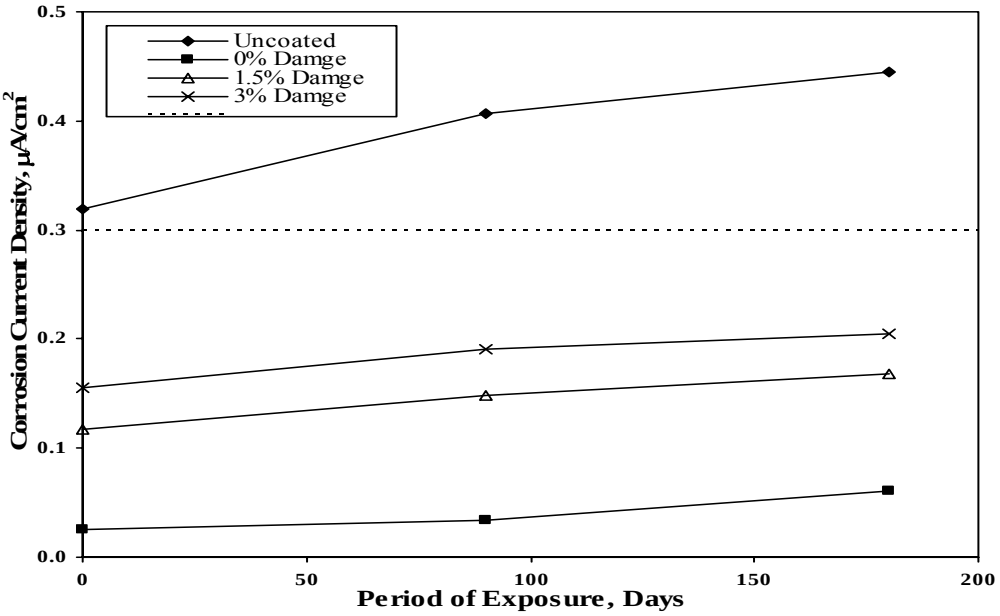

Figure 4.55: Corrosion Current Density in Plain Cement Concrete Specimens Contaminated with 2% Chloride on Steel Bars Exposed to 23°C.

The corrosion current density on steel in silica fume cement concrete specimens exposed to a temperature of 23°C are shown in Figures 4.56 through 4.58. The data therein shows very low corrosion current density in FBEC bars with all chloride concentrations. The I_{corr} on the FBEC bars with 1.5% and 3% damage was marginally more than the undamaged FBEC bars. In this batch also the corrosion current density in uncoated bars was more than those on the coated bars. Another important feature of the data in Figures 4.56 though 4.58 is that the I_{corr} was less than 0.3 μA/cm², even in the specimens contaminated with 2% chlorides. This may be attributed to the denseness of silica fume cement concrete.

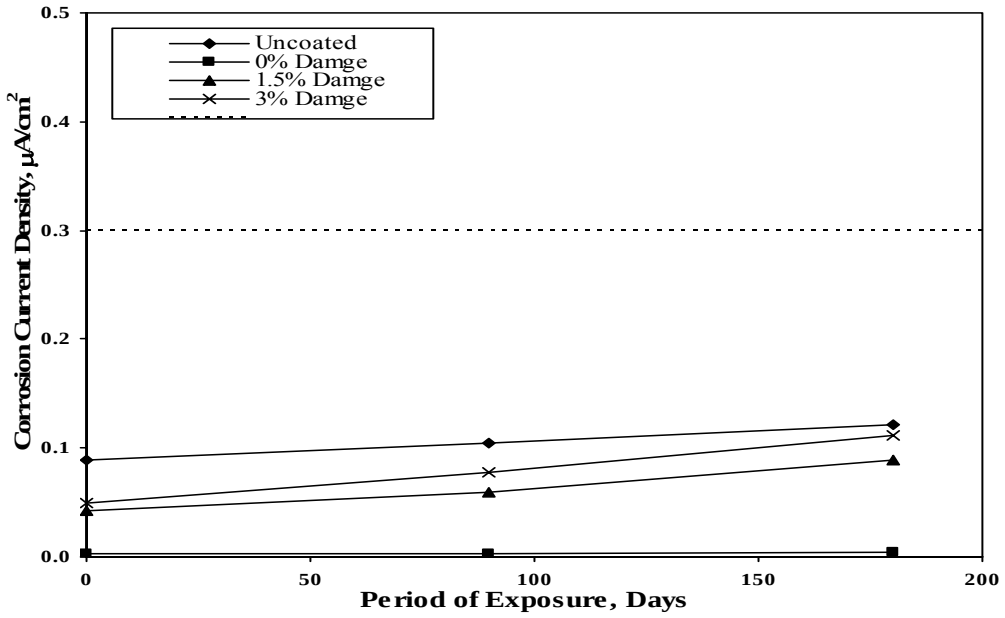

Figure 4.56: Corrosion Current Density in Uncontaminated Silica Fume-Cement Concrete Specimens on Steel Bars Exposed to 23°C.

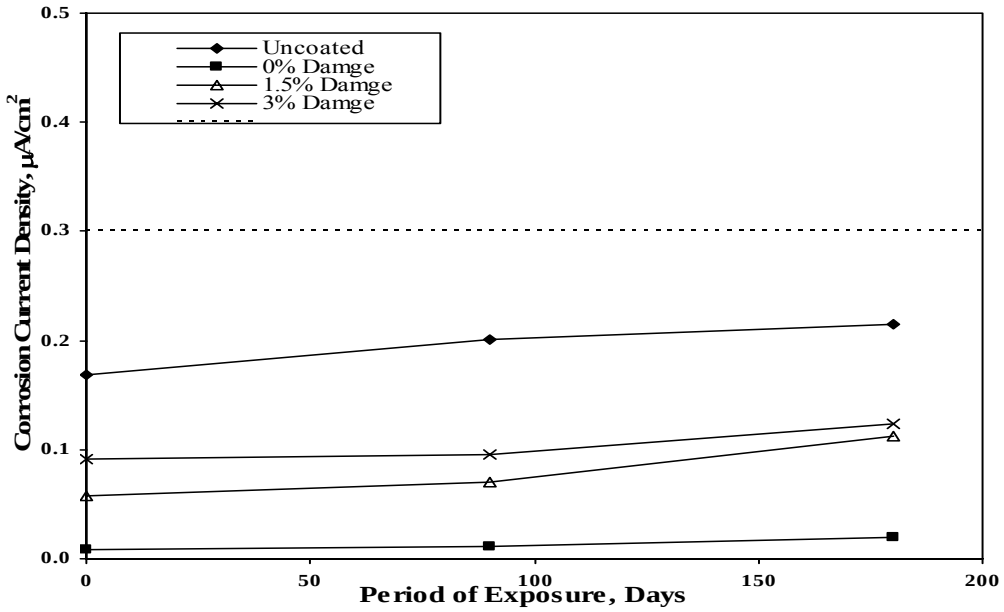

Figure 4.57: Corrosion Current Density in Silica Fume-Cement Concrete Specimens Contaminated with 1% Chloride on Steel Bars Exposed to 23°C.

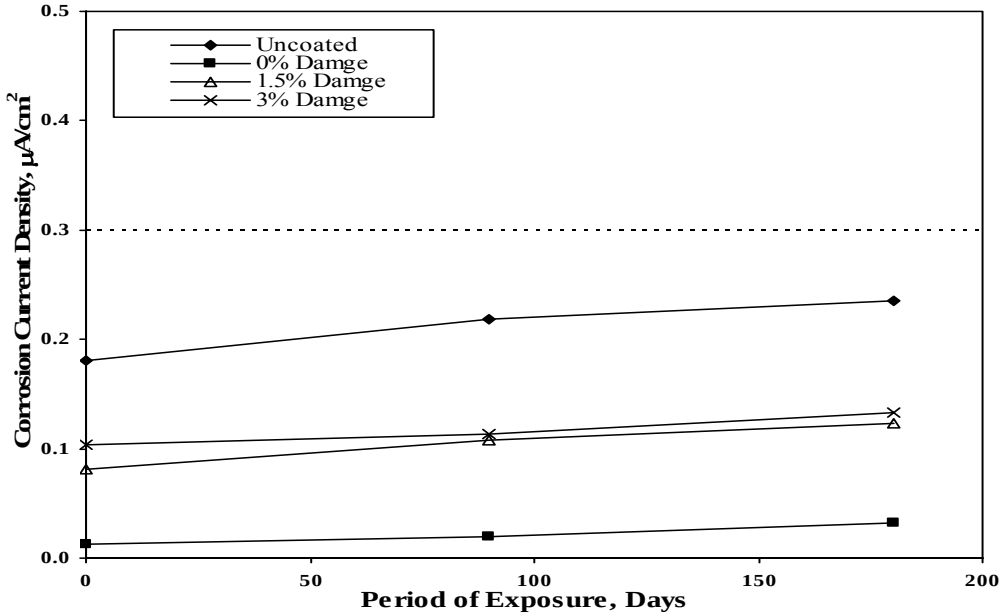

Figure 4.58: Corrosion Current Density in Silica Fume-Cement Concrete Specimens Contaminated with 2% Chloride on Steel Bars Exposed to 23°C.

Figures 4.59 through 4.61 depict the corrosion current density on steel in blast furnace slag cement concrete specimens exposed to a temperature of 23°C. In this group also, the least corrosion current density was noted on the FBEC bars without damage while I_{corr} was the highest on the uncoated bars. Another point to be noted is that the I_{corr} increased with the chloride concentration in all types of bars but remained less than 0.3 μA/cm². The corrosion current density in the FBEC bars with surface damage did not vary very much with the period of exposure.

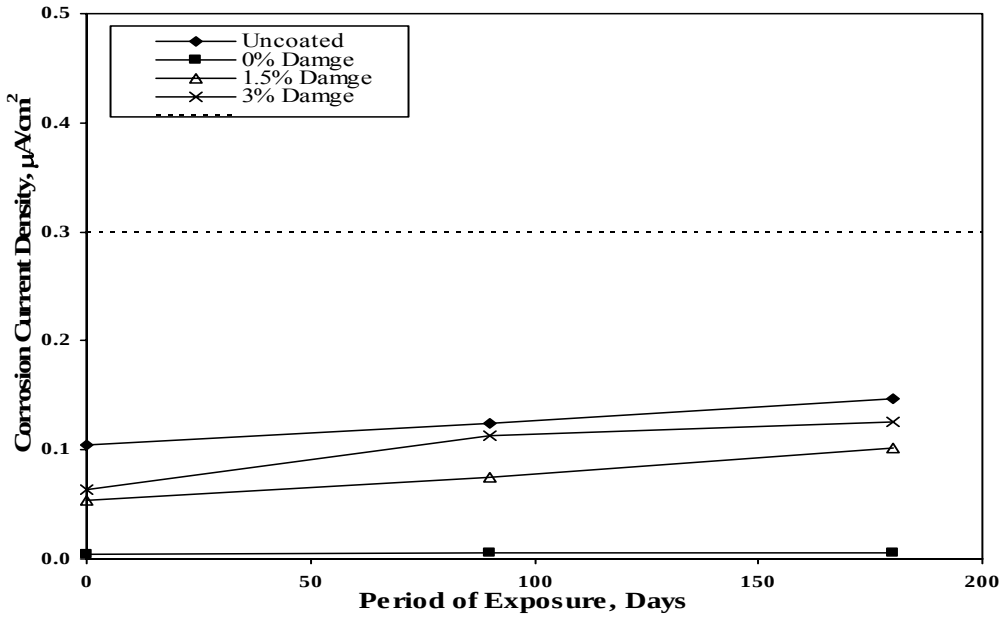

Figure 4.59: Corrosion Current Density in Uncontaminated Blast Furnace Slag-Cement Concrete Specimens on Steel Bars Exposed to 23°C.

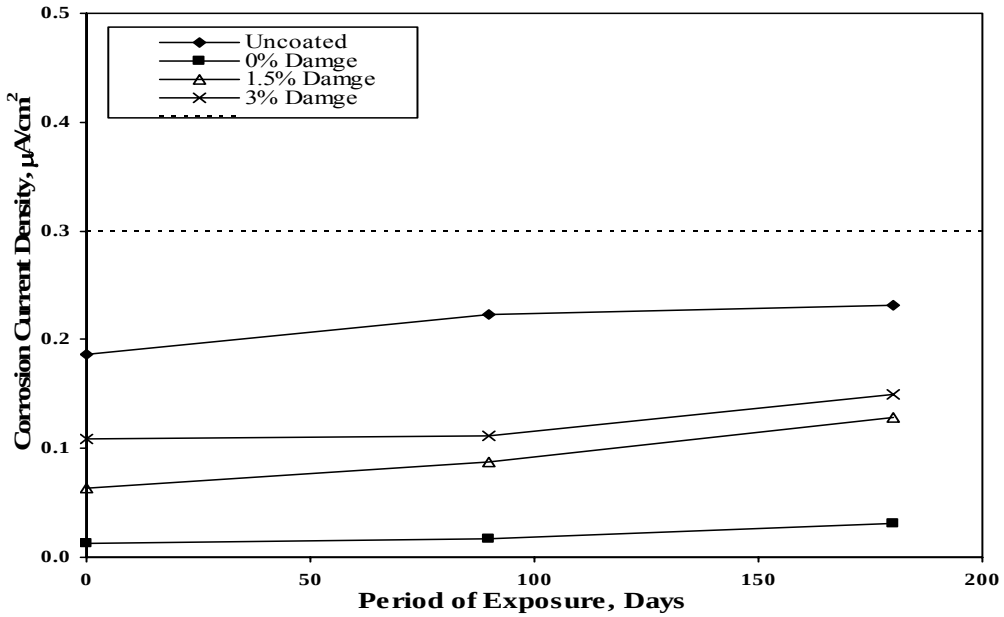

Figure 4.60: Corrosion Current Density in Blast Furnace Slag-Cement Concrete Specimens Contaminated with 1% Chloride on Steel Bars Exposed to 23°C.

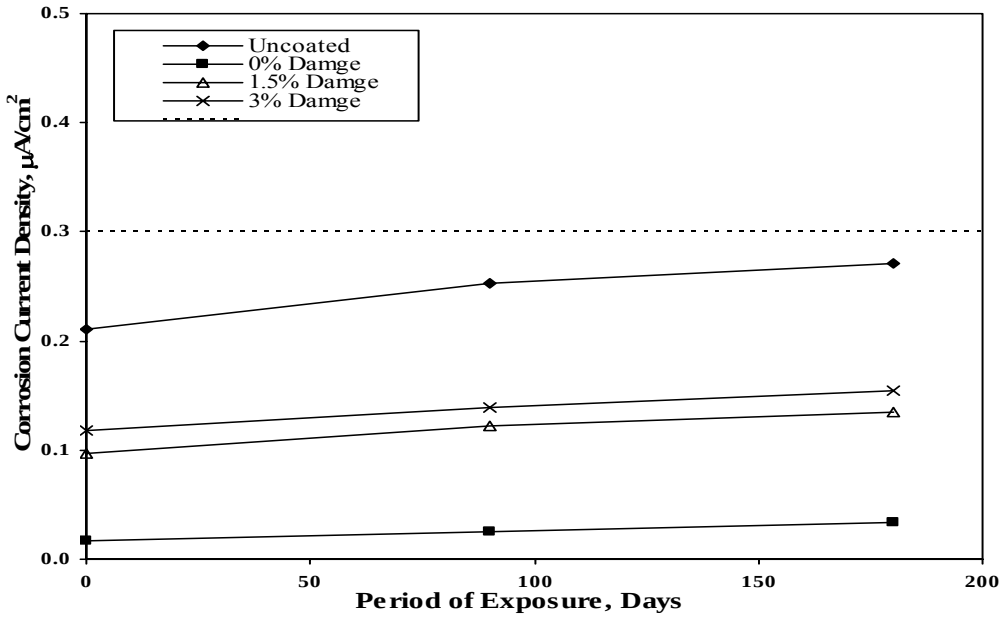

Figure 4.61: Corrosion Current Density in Blast Furnace Slag-Cement Concrete Specimens Contaminated with 2% Chloride on Steel Bars Exposed to 23°C.

The corrosion current density on steel in fly ash cement concrete specimens exposed to a temperature of 23°C are shown in Figures 4.62 through 4.64. The corrosion current density generally increased with time in all the specimens. Further, the I_{corr} values were generally low in the FBEC bars compared to the uncoated bars. Among the FBEC bars, the corrosion current density was less in the FBEC bars without damage. The I_{corr} was increasing with the chloride concentration, and it was noted that in the uncoated bars I_{corr} value was more than 0.3 µA/cm² 90 days of exposure when the specimens were contaminated with 2% chloride after.

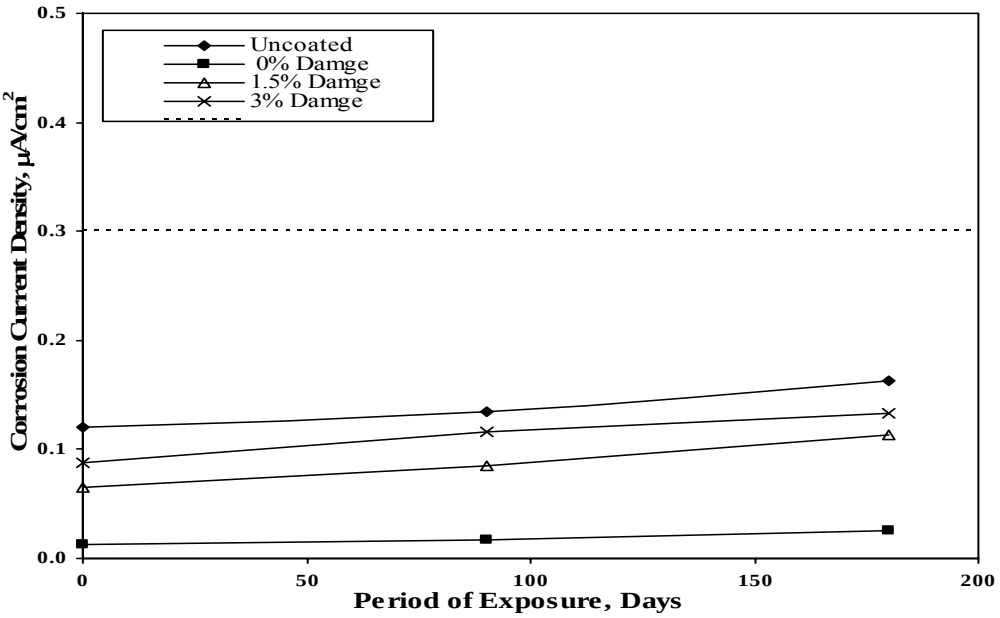

Figure 4.62: Corrosion Current Density in Uncontaminated Fly Ash-Cement Concrete Specimens on Steel Bars Exposed to 23°C.

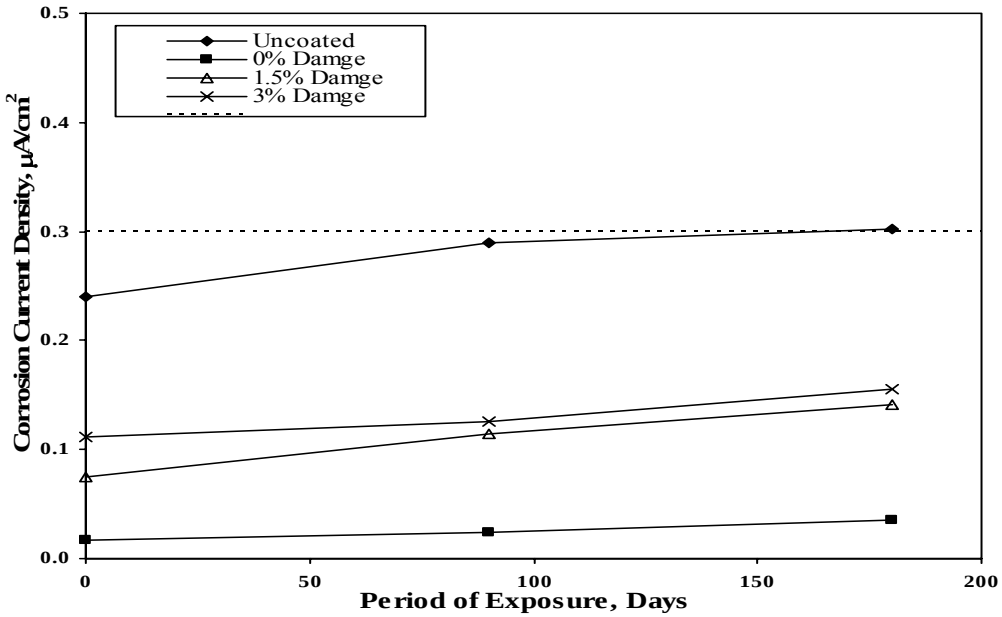

Figure 4.63: Corrosion Current Density in Fly Ash-Cement Concrete Specimen Contaminated with 1% Chloride on Steel Bars Exposed to 23°C.

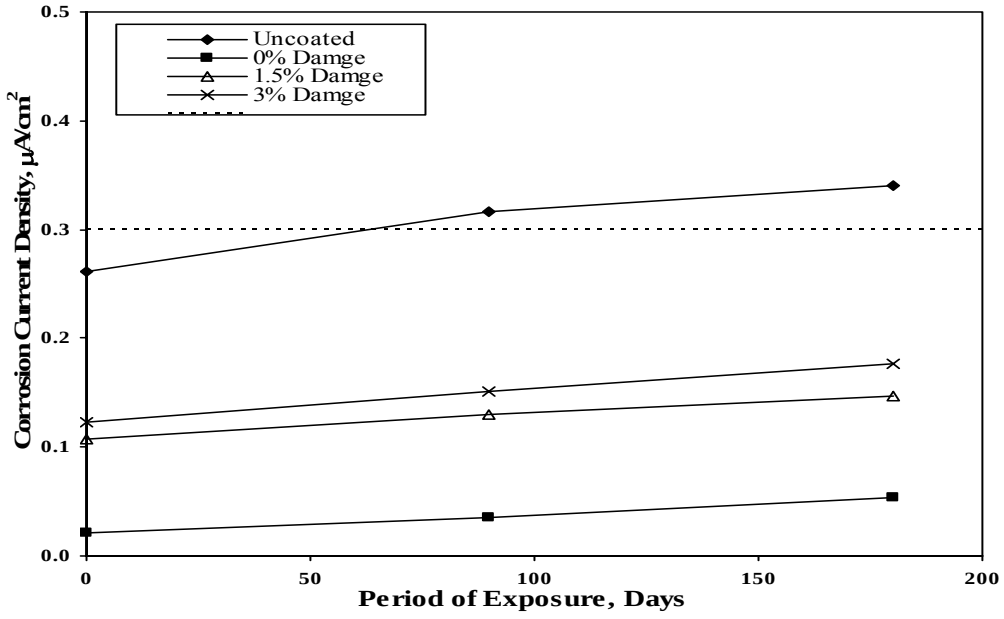

Figure 4.64: Corrosion Current Density in Fly Ash-Cement Concrete Specimens Contaminated with 2% Chloride on Steel Bars Exposed to 23°C.

Figures 4.65 through 4.67 show the corrosion current density I_{corr} on steel in plain cement concrete specimens exposed to a temperature of 35°C. The corrosion current density was generally the least in the concrete specimens with FBEC bars with a value less than 0.1 μA/cm² for all the chloride concentrations. The uncoated bar exhibited I_{corr} value more than 0.3 μA/cm² in 1% chloride concentration after 25 days of exposure, whereas the 2% chloride concentration bars shows form the initial period of exposure. The corrosion current density in all the specimens increased with the time of exposure.

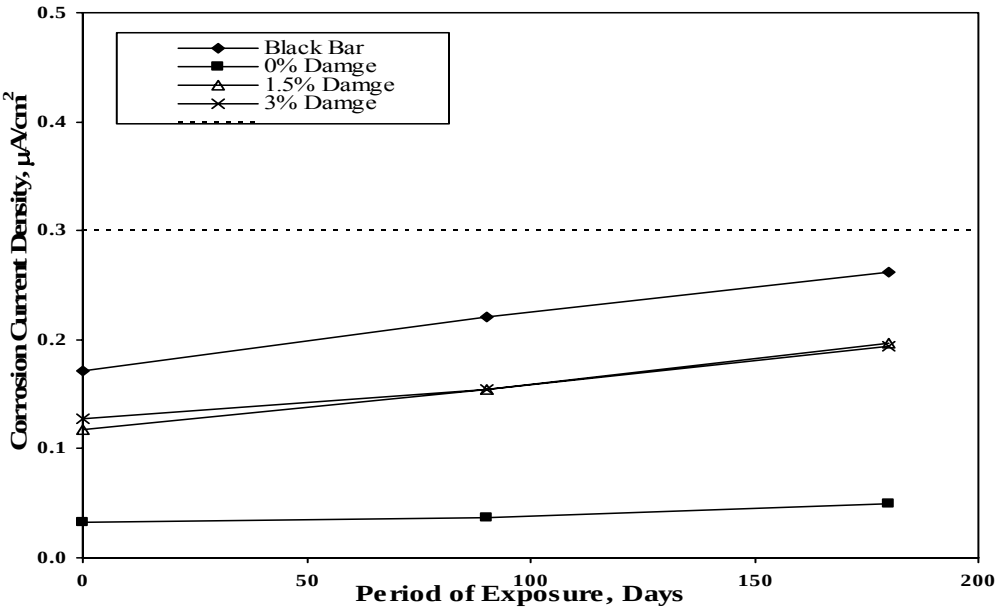

Figure 4.65: Corrosion Current Density in Uncontaminated Plain Cement Concrete Specimens on Steel Bars Exposed to 35°C.

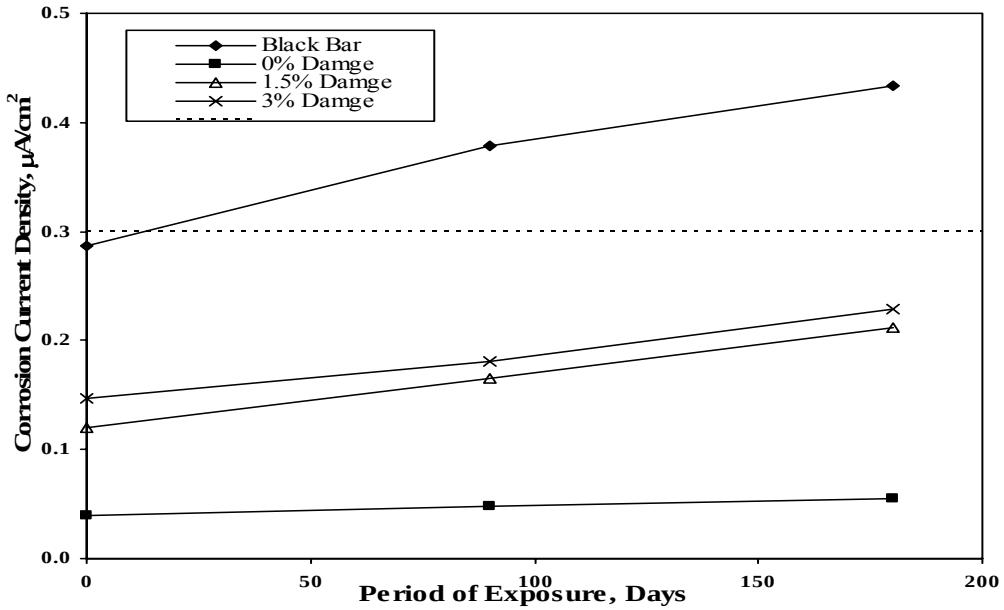

Figure 4.66: Corrosion Current Density in Plain Cement Concrete Specimens Contaminated with 1% Chloride on Steel Bars Exposed to 35°C.

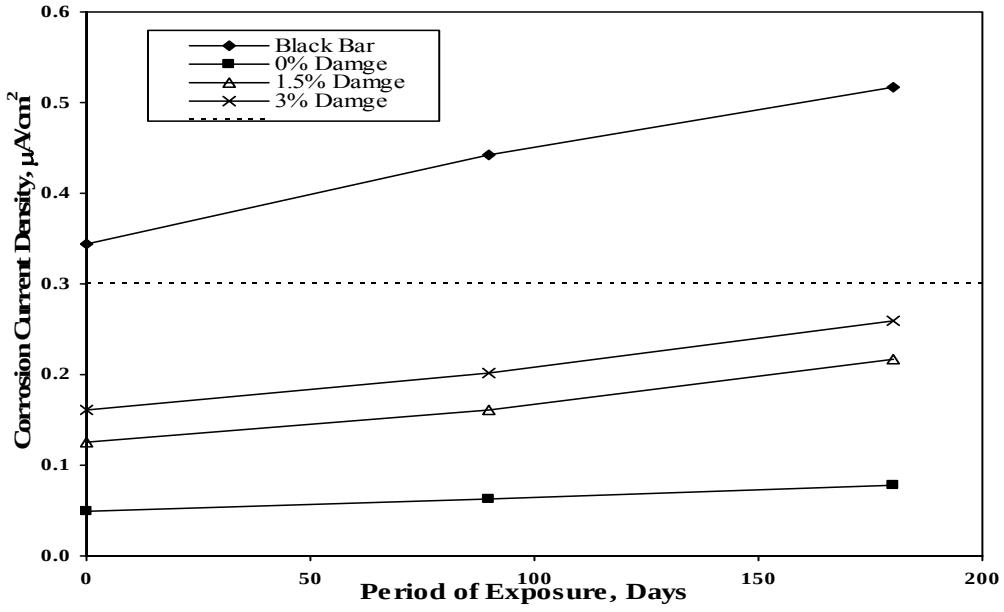

Figure 4.67: Corrosion Current Density in Plain Cement Concrete Specimens Contaminated with 2% Chloride on Steel Bars Exposed to 35°C.

The corrosion current density on steel in silica fume cement concrete specimens exposed to a temperature of 35°C is shown in Figures 4.68 through 4.70. The corrosion current density was the least in FBEC steel bars while corrosion current density was more in the uncoated specimens. The I_{corr} in FBEC bars with 1.5% and 3% damage tended to be between that of the uncoated and FBEC bars. In all the specimens, the I_{corr} value remained less than 0.3 μA/cm² indicating better resistance to corrosion, the I_{corr} increased with the chloride concentration.

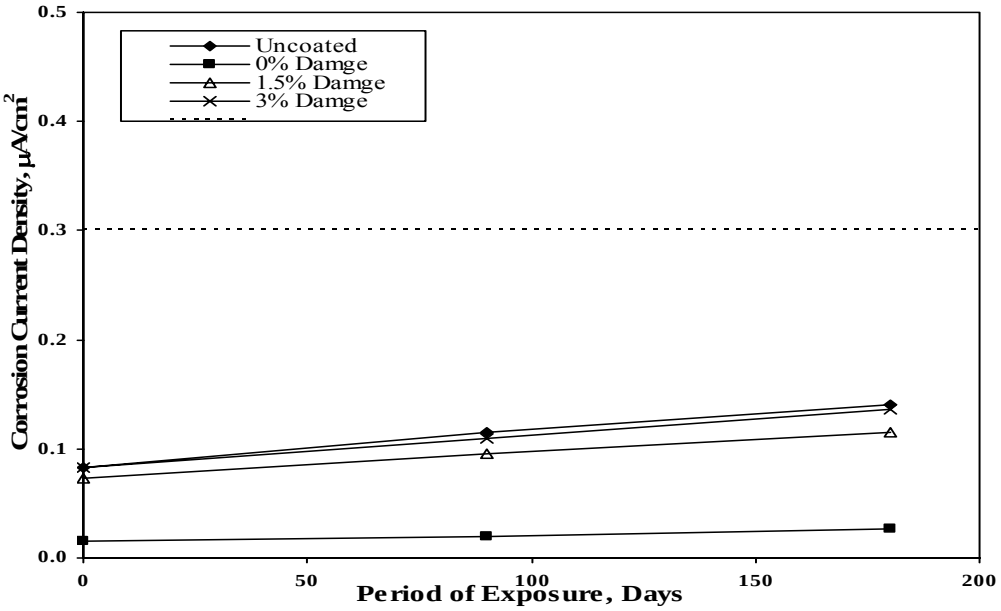

Figure 4.68: Corrosion Current Density in Uncontaminated Silica Fume-Cement Concrete Specimens on Steel Bars Exposed to 35°C.

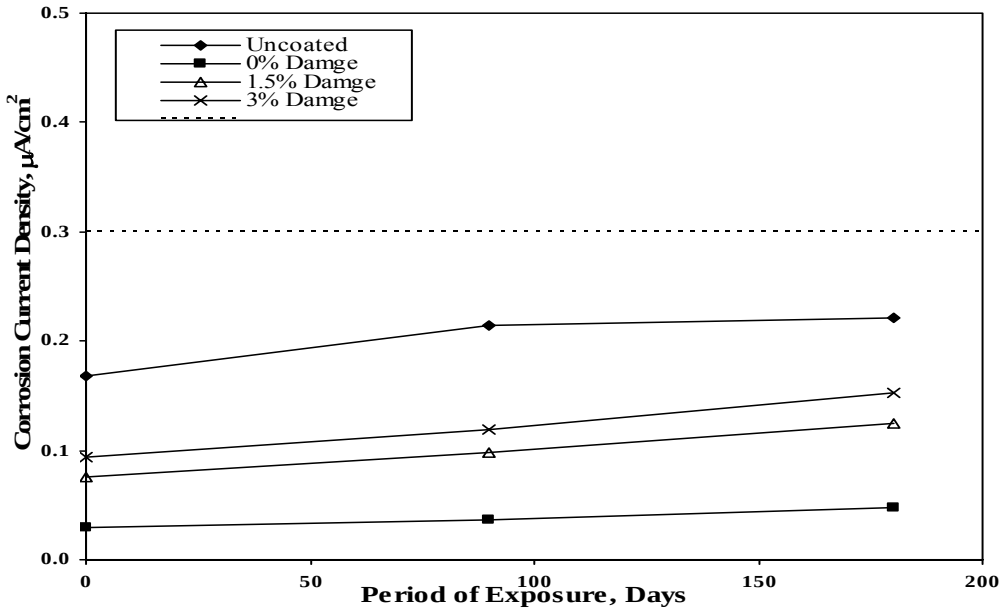

Figure 4.69: Corrosion Current Density in Silica Fume-Cement Concrete Specimens Contaminated with 1% Chloride on Steel Bars Exposed to 35°C.

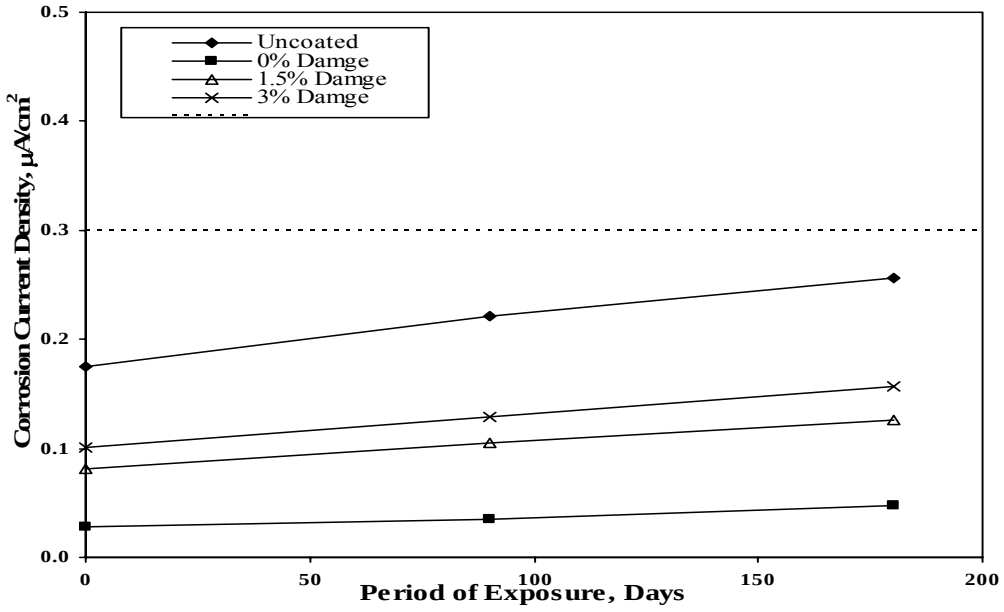

Figure 4.70: Corrosion Current Density in Silica Fume-Cement Concrete Specimens Contaminated with 2% Chloride on Steel Bars Exposed to 35°C.

Figures 4.71 through 4.73 show the corrosion current density on steel in blast furnace slag cement concrete specimens exposed to a temperature of 35°C. The data of the corrosion current density for this group of specimens was similar to that noted in the silica fume cement concrete specimens exposed to the same temperature with only one change, i.e. the I_{corr} value reached more than 0.3 μA/cm² in the uncoated bars contaminated with 2% chloride after 160 days of exposure.

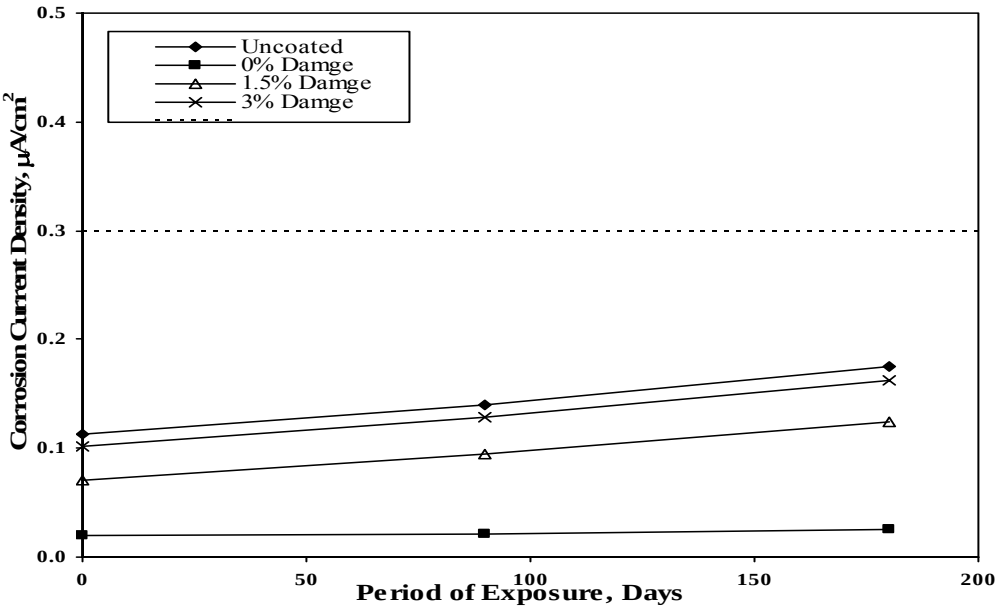

Figure 4.71: Corrosion Current Density in Uncontaminated Blast Furnace Slag-Cement Concrete Specimens on Steel Bars Exposed to 35°C.

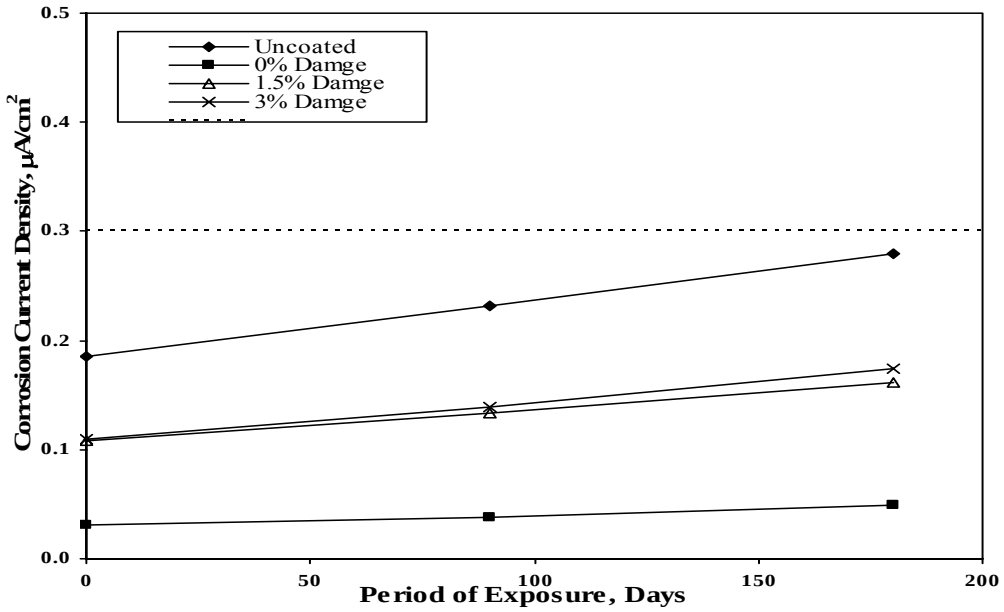

Figure 4.72: Corrosion Current Density in Blast Furnace Slag-Cement Concrete Specimens Contaminated with 1% Chloride on Steel Bars Exposed to 35°C.

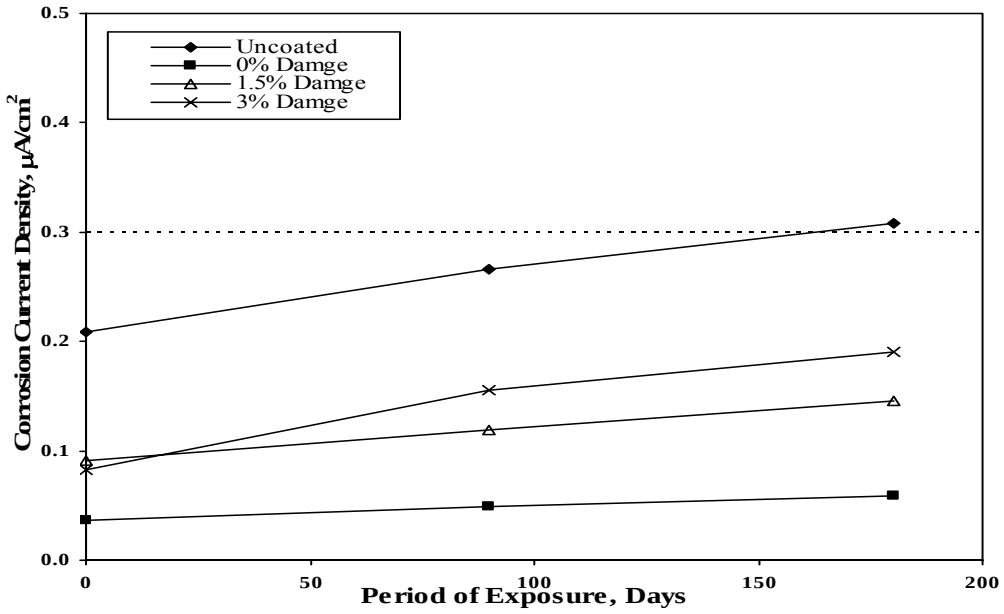

Figure 4.73: Corrosion Current Density in Blast Furnace Slag-Cement Concrete Specimens Contaminated with 2% Chloride on Steel Bars Exposed to 35°C.

The corrosion current density on steel in fly ash cement concrete specimens exposed to a temperature of 23°C was depicted in Figures 4.74 through 4.76. The corrosion current density increased with time in all the specimens. The I_{corr} in the uncoated steel bars was generally more than that on the FBEC bars. The I_{corr} reached more than 0.3 μA/cm² in the uncoated specimens contaminated with 1% chloride after 90 days of exposure, whereas here as in the specimens contaminated with 2% chloride after 45 days of exposure.

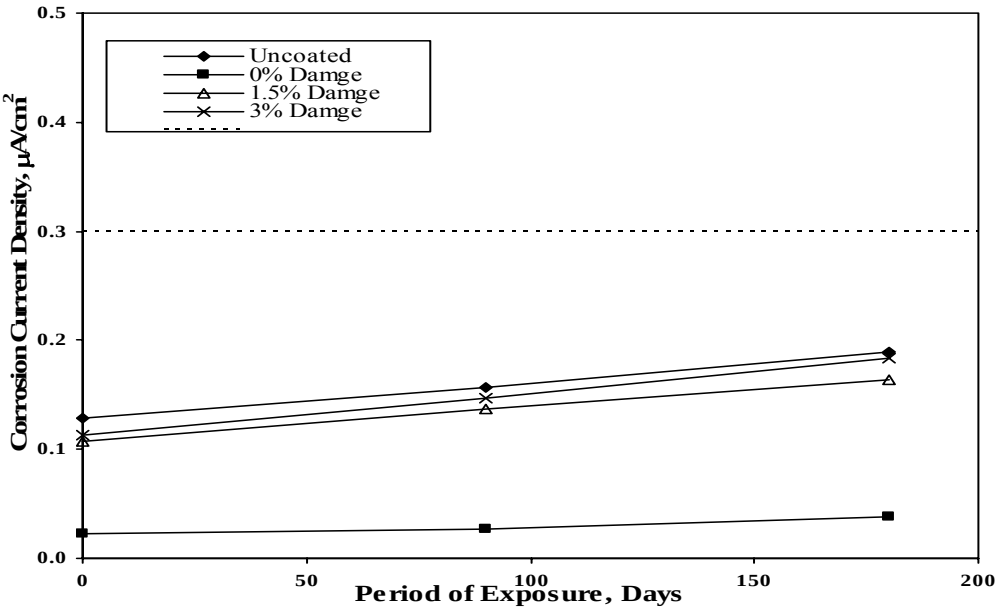

Figure 4.74: Corrosion Current Density in Uncontaminated Fly Ash-Cement Concrete Specimens on Steel Bars Exposed to 35°C.

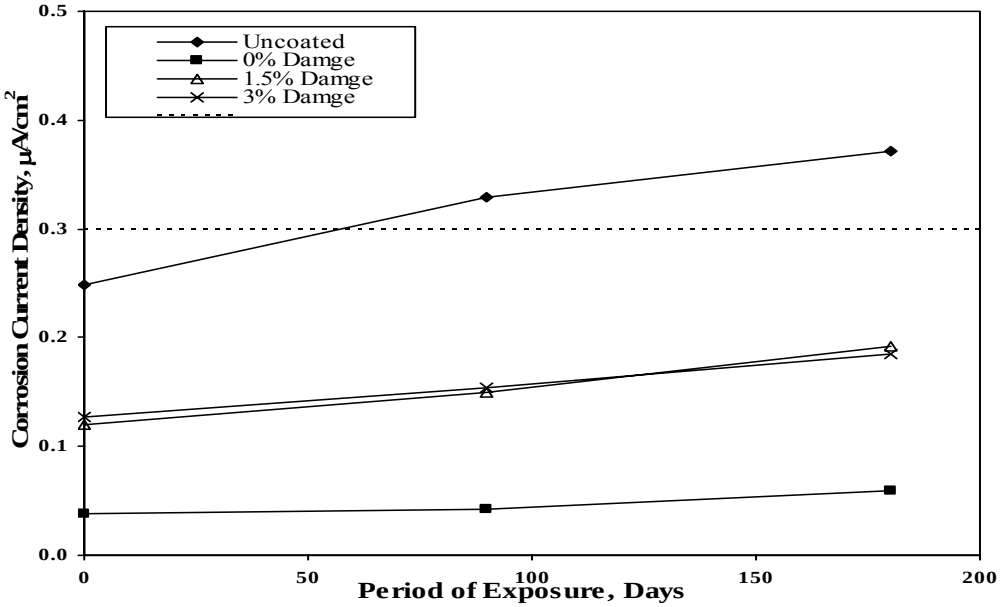

Figure 4.75: Corrosion Current Density in Fly Ash-Cement Concrete Specimens Contaminated with 1% Chloride on Steel Bars Exposed to 35°C.

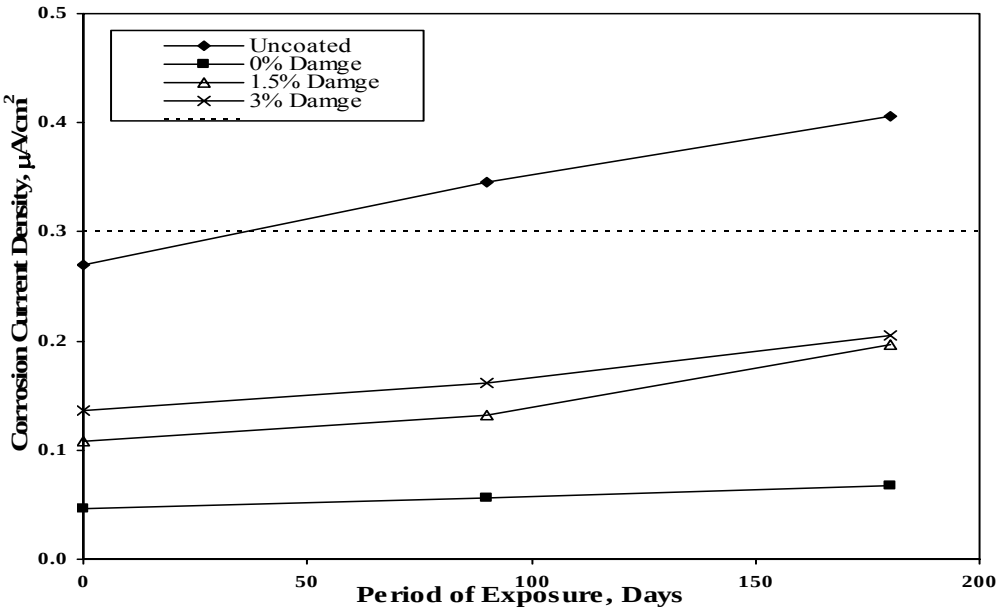

Figure 4.76: Corrosion Current Density in Fly Ash-Cement Concrete Specimens Contaminated with 2% Chloride on Steel Bars Exposed to 35°C.

Figures 4.77 through 4.79 show the I_{corr} on steel in plain cement concrete specimens exposed to a temperature of 48°C. As expected, the I_{corr} in the uncoated steel bars was more than those in the coated steel bars. A significant increase in the I_{corr} values was noted in the uncoated bars both in uncontaminated and chloride-contaminated concrete specimens. In the 1% and 2% chloride-contaminated specimens, the corrosion current density was more than 0.3 μA/cm² from initiation of exposure. The corrosion current density in the undamaged FBEC steel bars were less than 0.3 μA/cm². However, I_{corr} increased with time.

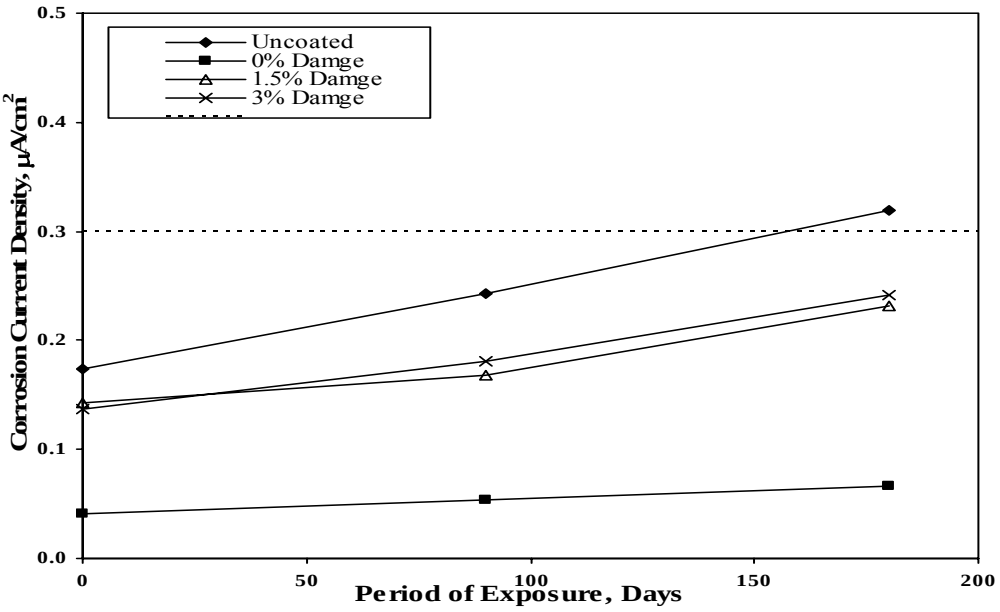

Figure 4.77: Corrosion Current Density in Uncontaminated Plain Cement Concrete Specimens on Steel Bars Exposed to 48°C.

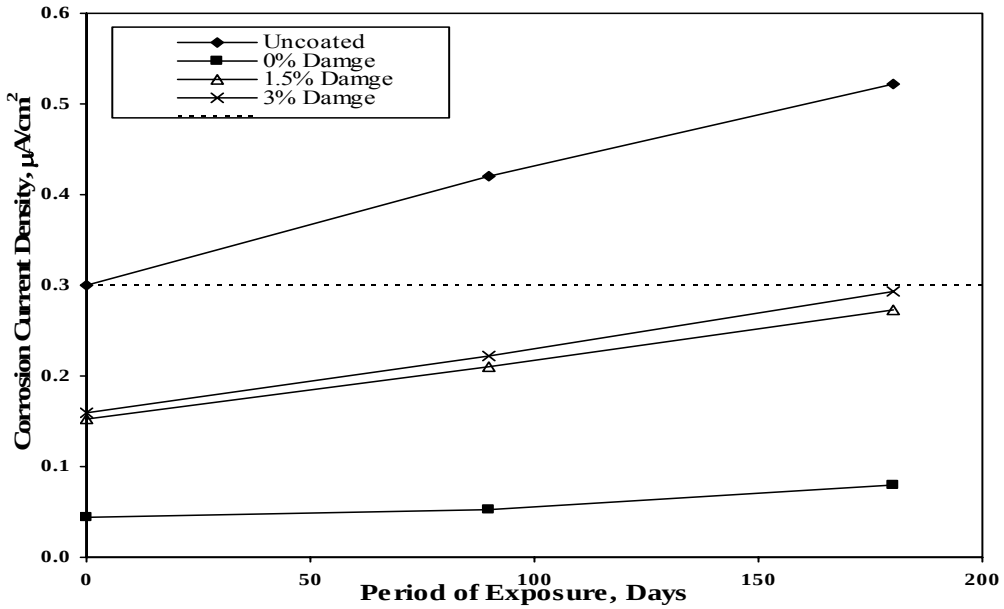

Figure 4.78: Corrosion Current Density in Plain Cement Concrete Specimens Contaminated with 1% Chloride on Steel Bars Exposed to 48°C.

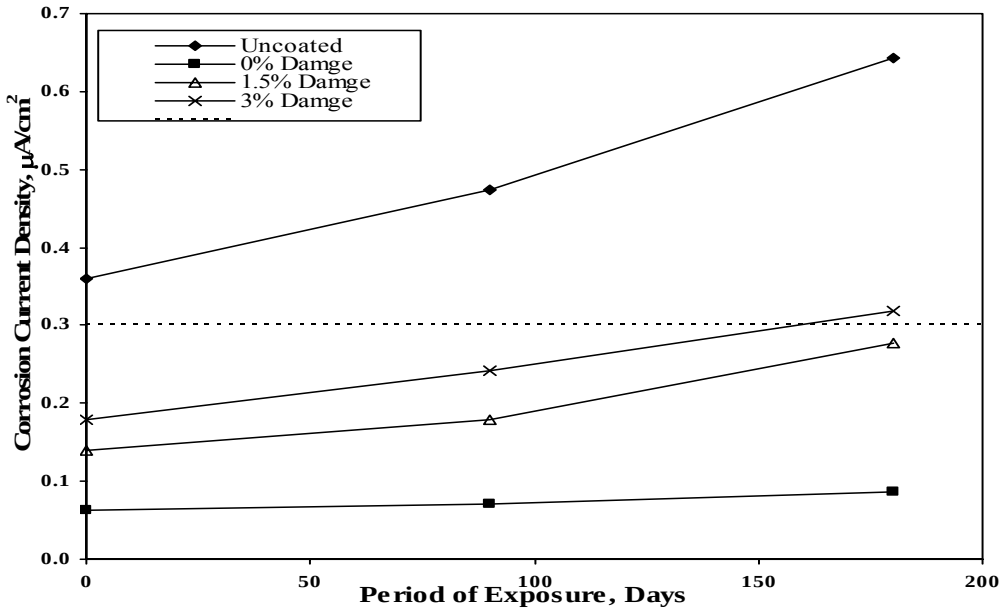

Figure 4.79: Corrosion Current Density in Plain Cement Concrete Specimens Contaminated with 2% Chloride on Steel Bars Exposed to 48°C.

The corrosion current density on steel in silica fume cement concrete specimens exposed to a temperature of 48°C is shown in Figures 4.80 through 4.82. The data of the corrosion current density for this group of specimens were similar but more than that of the data noted in the silica fume cement concrete specimens exposed to a temperature of 35°C.

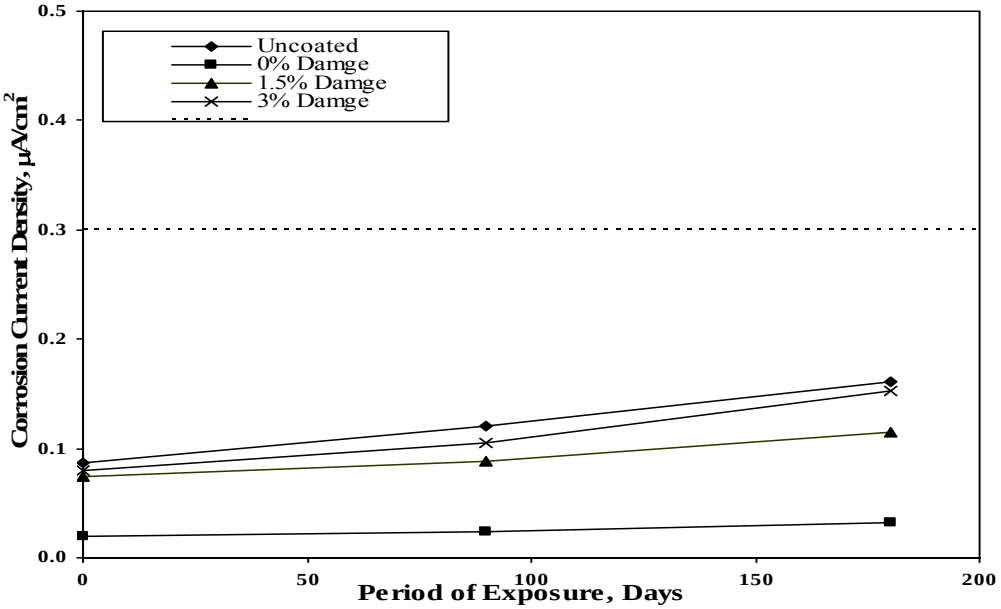

Figure 4.80: Corrosion Current Density in Uncontaminated Silica Fume-Cement Concrete Specimens on Steel Bars Exposed to 48°C.

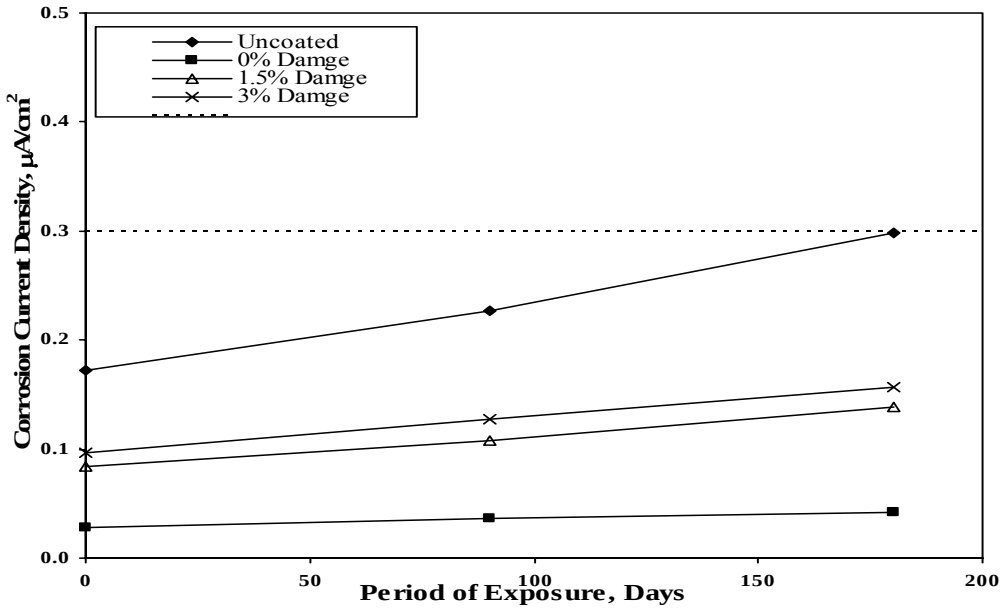

Figure 4.81: Corrosion Current Density in Silica Fume-Cement Concrete Specimens Contaminated with 1% Chloride on Steel Bars Exposed to 48°C.

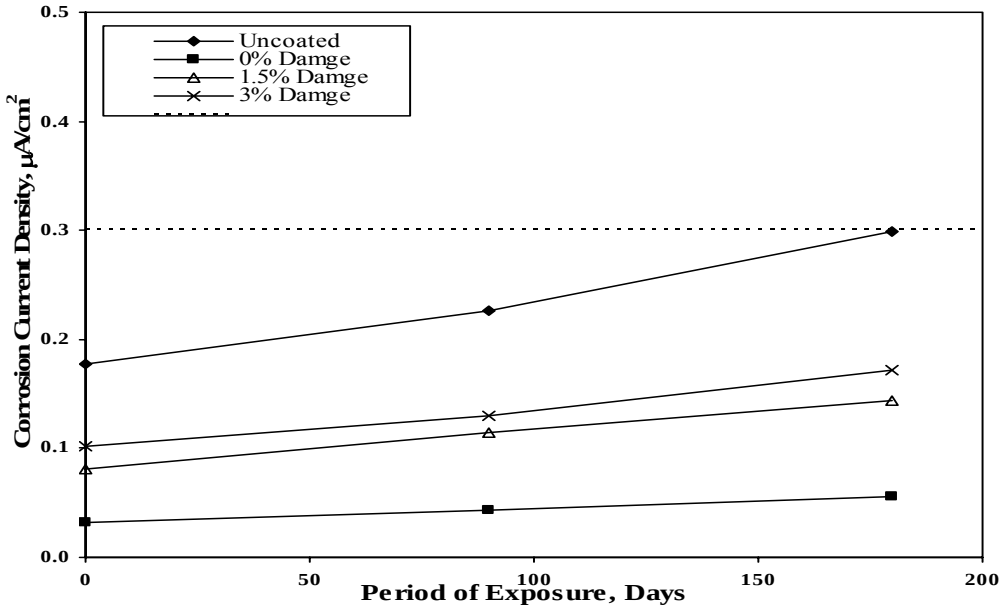

Figure 4.82: Corrosion Current Density in Silica Fume-Cement Concrete Specimens Contaminated with 2% Chloride on Steel Bars Exposed to 48°C.

Figures 4.83 through 4.85 show the corrosion current density on steel in blast furnace slag cement concrete specimens exposed to a temperature of 48°C. The corrosion current density increased with time in all specimens. I_{corr} on the uncoated steel bars was generally more than that on FBEC steel bars. In all the specimens, I_{corr} value remains less than 0.3 μA/cm².

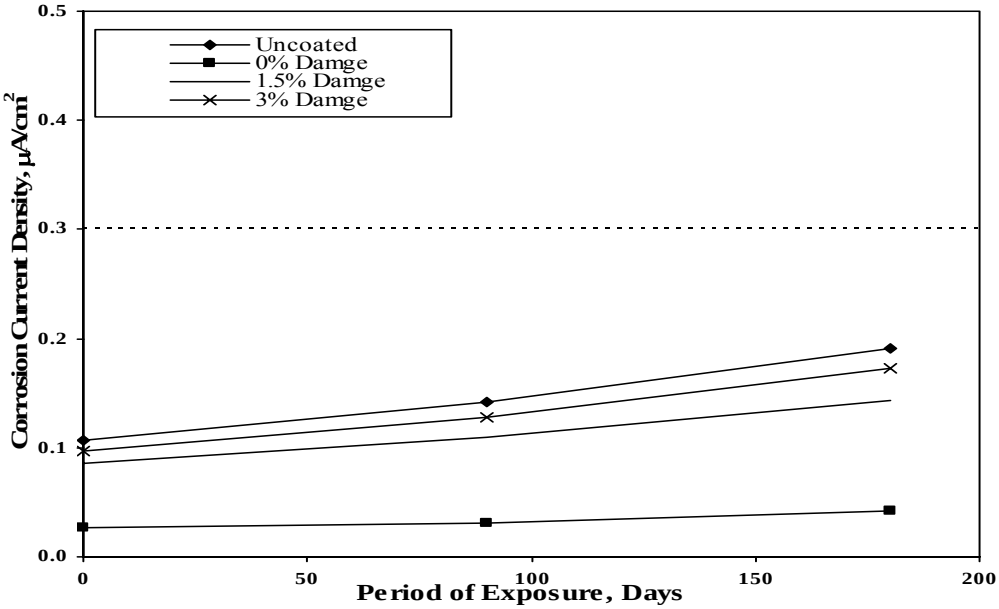

Figure 4.83: Corrosion Current Density in Uncontaminated Blast Furnace Slag-Cement Concrete Specimens on Steel Bars Exposed to 48°C.

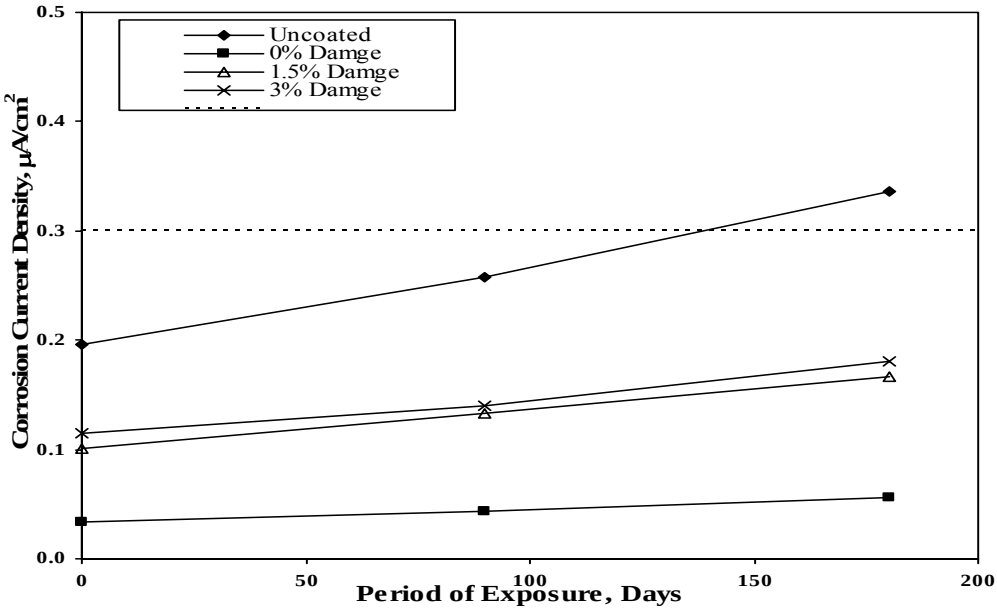

Figure 4.84: Corrosion Current Density in Blast Furnace Slag-Cement Concrete Specimens Contaminated with 1% Chloride on Steel Bars Exposed to 48°C.

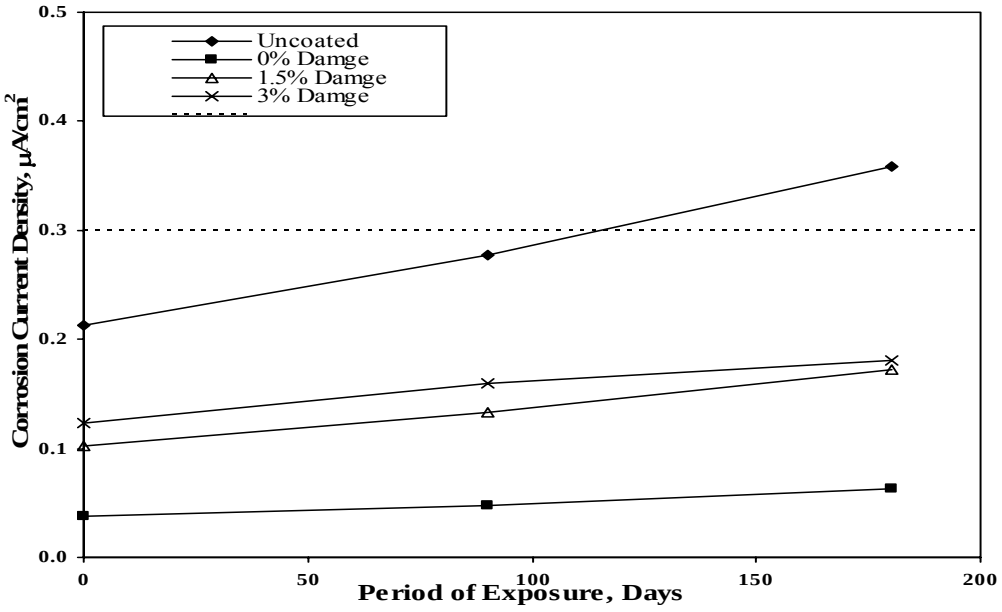

Figure 4.85: Corrosion Current Density in Blast Furnace Slag-Cement Concrete Specimens Contaminated with 2% Chloride on Steel Bars Exposed to 48°C.

The corrosion current density on steel in fly ash cement concrete specimens exposed to a temperature of 48°C is shown in Figures 4.86 through 4.88. The corrosion current density increased with the period of exposure. The I_{corr} value in the uncoated steel bars was more than that on FBEC steel bars. The uncoated bar exhibited I_{corr} value more than 0.3µA/cm² in 1% chloride concentration after 80 days of exposure, whereas the 2% chloride concentration bars exhibited after 35 days of exposure.

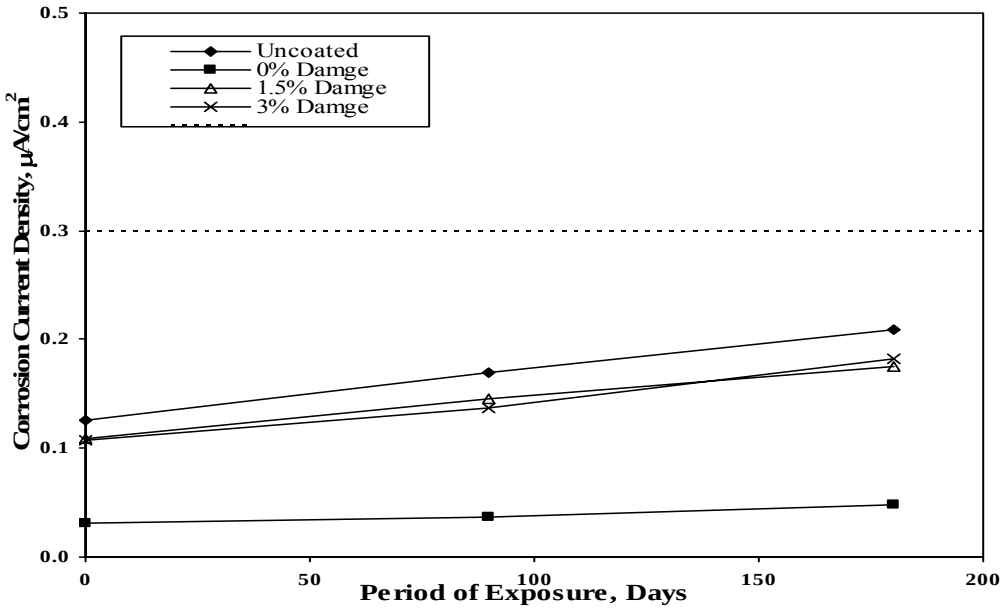

Figure 4.86: Corrosion Current Density in Uncontaminated Fly Ash-Cement Concrete Specimens on Steel Bars Exposed to 48°C.

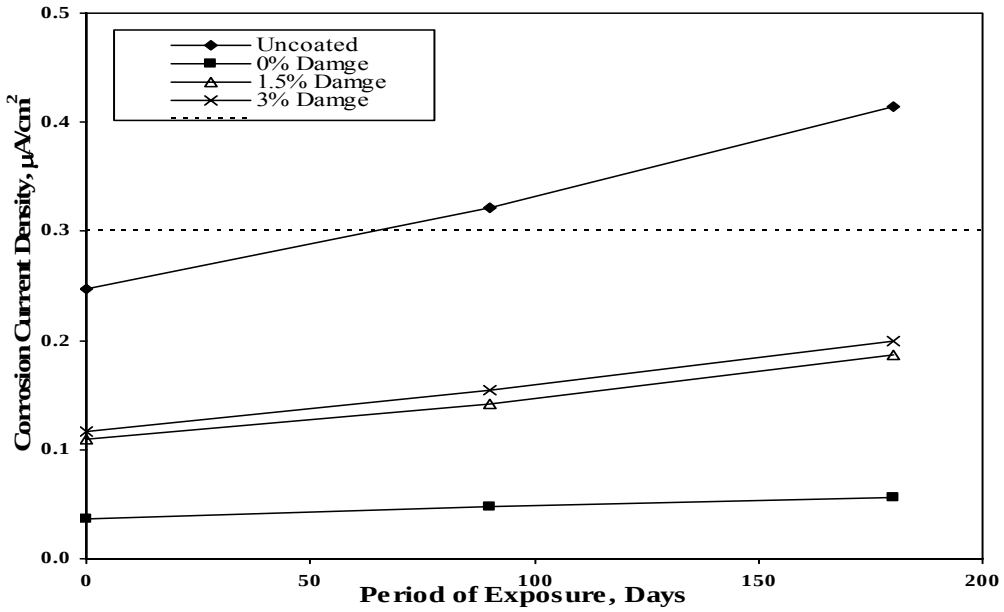

Figure 4.87: Corrosion Current Density in Fly Ash-Cement Concrete Specimens Contaminated with 1% Chloride on Steel Bars Exposed to 48°C.

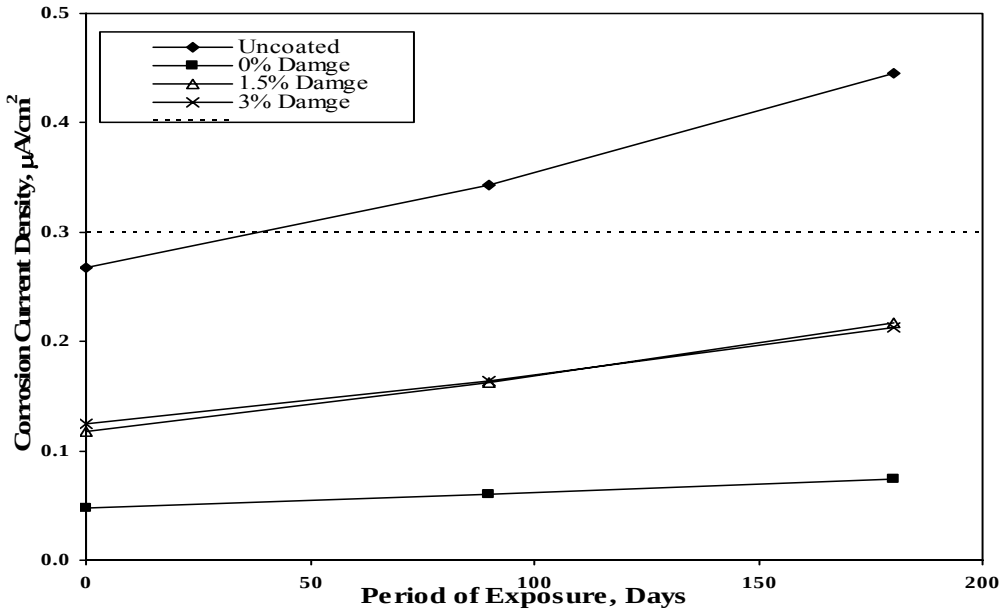

Figure 4.88: Corrosion Current Density in Fly Ash-Cement Concrete Specimens Contaminated with 2% Chloride on Steel Bars Exposed to 48°C.

4.2 DISCUSSION OF RESULTS

4.2.1 Time to Initiation of Reinforcement Corrosion

The corrosion potential curves in Figures. 4.1 through 4.36 were utilized to assess the time to initiation of reinforcement corrosion according to ASTM C 876 criterion. The time to initiation of reinforcement corrosion of the uncoated and FBEC bars in plain and blended cement concrete specimens with varying chloride contamination and exposed to 5% NaCl Solution at 23°C is summarized in Table 4.1. Corrosion initiation was not noted in the FBEC bars without damage. This trend was noted in both plain and blended cements and for all chloride contaminations.

The time to initiation of reinforcement corrosion in the plain and blended cement concrete specimens with varying chloride contamination and exposed at 35°C is shown in Table 4.2. These data exhibit a trend similar to that noted in the concrete specimens exposed to 23°C. The time to initiation of reinforcement corrosion in the plain and blended cement concrete specimens exposed to 48°C is summarized in Table 4.3. Corrosion initiation was noted much earlier in the uncoated steel bars compared to the coated steel bars. Among the coated steel bars, reinforcement corrosion was noted earlier in the bars with 3% damage to FBE coating followed by bars with 1.5% and 0% damage.

The data in Tables 4.1 through 4.3 exhibit the following trends:

Table 4.1: Time to corrosion initiation in concrete specimens exposed to 23°C.

Cement	Cl%	Rebar	Time to Initiation of corrosion, days	Cement	Cl%	Rebar	Time to Initiation of corrosion, days
OPC	0%	0% Damage	*	BFS	0%	0% Damage	*
		1.5% Damage	110			1.5% Damage	250
		3% Damage	90			3% Damage	280
		Uncoated bar	30			Uncoated bar	100
	1%	0% Damage	*		1%	0% Damage	*
		1.5% Damage	110			1.5% Damage	240
		3% Damage	55			3% Damage	220
		Uncoated bar	25			Uncoated bar	60
	2%	0% Damage	*		2%	0% Damage	250
		1.5% Damage	120			1.5% Damage	120
		3% Damage	60			3% Damage	80
		Uncoated bar	270			Uncoated bar	30
SF	0%	0% Damage	*	FA	0%	0% Damage	*
		1.5% Damage	260			1.5% Damage	210
		3% Damage	270			3% Damage	150
		Uncoated bar	240			Uncoated bar	80
	1%	0% Damage	*		1%	0% Damage	280
		1.5% Damage	270			1.5% Damage	160
		3% Damage	280			3% Damage	130
		Uncoated bar	160			Uncoated bar	40
	2%	0% Damage	*		2%	0% Damage	*
		1.5% Damage	250			1.5% Damage	120
		3% Damage	190			3% Damage	110
		Uncoated bar	140			Uncoated bar	50

*No corrosion has been noted within the duration of measurement.

Table 4.2: Time to corrosion initiation in concrete specimens exposed to 35°C.

Cement	Cl%	Rebar	Time to Initiation of corrosion, days	Cement	Cl%	Rebar	Time to Initiation of corrosion, days
OPC	0%	0% Damage	250	BFS	0%	0% Damage	250
		1.5% Damage	110			1.5% Damage	180
		3% Damage	70			3% Damage	130
		Uncoated	15			Black Bar	90
	1%	0% Damage	240		1%	0% Damage	250
		1.5% Damage	100			1.5% Damage	180
		3% Damage	45			3% Damage	130
		Uncoated	15			Black Bar	30
	2%	0% Damage	150		2%	0% Damage	250
		1.5% Damage	15			1.5% Damage	120
		3% Damage	15			3% Damage	50
		Uncoated	*			Black Bar	40
SF	0%	0% Damage	*	FA	0%	0% Damage	210
		1.5% Damage	*			1.5% Damage	150
		3% Damage	*			3% Damage	120
		Black Bar	120			Uncoated bar	50
	1%	0% Damage	*		1%	0% Damage	250
		1.5% Damage	*			1.5% Damage	180
		3% Damage	240			3% Damage	100
		Uncoated bar	110			Uncoated bar	15
	2%	0% Damage	*		2%	0% Damage	240
		1.5% Damage	*			1.5% Damage	140
		3% Damage	140			3% Damage	70
		Uncoated bar	50			Uncoated bar	30

*No corrosion has been noted within the duration of measurement

Table 4.3: Time to corrosion initiation in concrete specimens exposed to 48°C.

Cement	Cl%	Rebar	Time to Initiation of corrosion, days	Cement	Cl%	Rebar	Time to Initiation of corrosion, days
OPC	0%	0% Damage	200	BFS	0%	0% Damage	220
		1.5% Damage	100			1.5% Damage	160
		3% Damage	60			3% Damage	130
		Uncoated bar	15			Black Bar	90
	1%	0% Damage	220		1%	0% Damage	230
		1.5% Damage	30			1.5% Damage	170
		3% Damage	20			3% Damage	120
		Uncoated bar	15			Black Bar	30
	2%	0% Damage	130		2%	0% Damage	225
		1.5% Damage	15			1.5% Damage	110
		3% Damage	10			3% Damage	50
		Uncoated bar	*			Black Bar	40
SF	0%	0% Damage	*	FA	0%	0% Damage	200
		1.5% Damage	*			1.5% Damage	150
		3% Damage	*			3% Damage	150
		Uncoated bar	100			Uncoated bar	50
	1%	0% Damage	*		1%	0% Damage	230
		1.5% Damage	*			1.5% Damage	160
		3% Damage	220			3% Damage	100
		Uncoated bar	110			Uncoated bar	15
	2%	0% Damage	220		2%	0% Damage	220
		1.5% Damage	*			1.5% Damage	130
		3% Damage	110			3% Damage	65
		Uncoated bar	40			Uncoated bar	25

*No corrosion has been noted within the duration of measurement

(i) The time to corrosion initiation in the uncoated steel bars was less than that in the FBEC steel bars. This trend was noted in both plain and blended cement concrete specimens and exposed to all the temperatures. The time to initiation of corrosion in the uncoated steel bars generally decreased with an increase in the chloride contamination in the concrete specimens.

(ii) Corrosion initiation was not noted in the concrete specimens with undamaged FBEC steel bars exposed to 23^0C with all chloride contaminations. However, corrosion initiation was noted on the FBEC steel bars, even without damage, in the concrete specimens exposed to 35°C and 48°C due the hot environment.

(iii) The time to initiation generally decreased with the decrease in the level of chloride contamination and exposure temperature. The increase in the exposure temperature influenced the time to corrosion initiation more than the chloride contamination.

(iv) In the concrete specimens with similar FBEC bars and chloride contamination, corrosion initiation was noted later in the blended cement concretes, particularly those made with silica fume cements, than the plain cement concrete.

4.2.2 Corrosion Current Density

As noted earlier, corrosion of both the uncoated and FBEC steel bars was affected by the level of chloride contamination, exposure temperature and the type of cement. Among the FBEC steel bars, the extent of damage was also a governing factor. The experimental data developed in this study were therefore discussed below to cover all these parameters.

Figure 4.89 shows the I_{corr} on the uncoated steel bars in the plain and blended cement concrete specimens exposed to the 5% NaCl solution at 23°C for 180 days. The I_{corr} in the plain cement concrete specimens was more than that in the blended cement concrete specimens. Among the blended cements, the least I_{corr} was noted in the silica fume cement concrete specimens. This trend was noted in both the uncontaminated and chloride-contaminated concrete specimens. Further, the I_{corr} in the uncontaminated concrete, made with both plain and blended cements, was less than 0.3 $\mu A/cm^2$, taken as threshold for corrosion initiation. However, the I_{corr} in the plain and fly ash cement concrete specimens contaminated with 1% and 2% chlorides was more than the threshold value of 0.3 $\mu A/cm^2$.

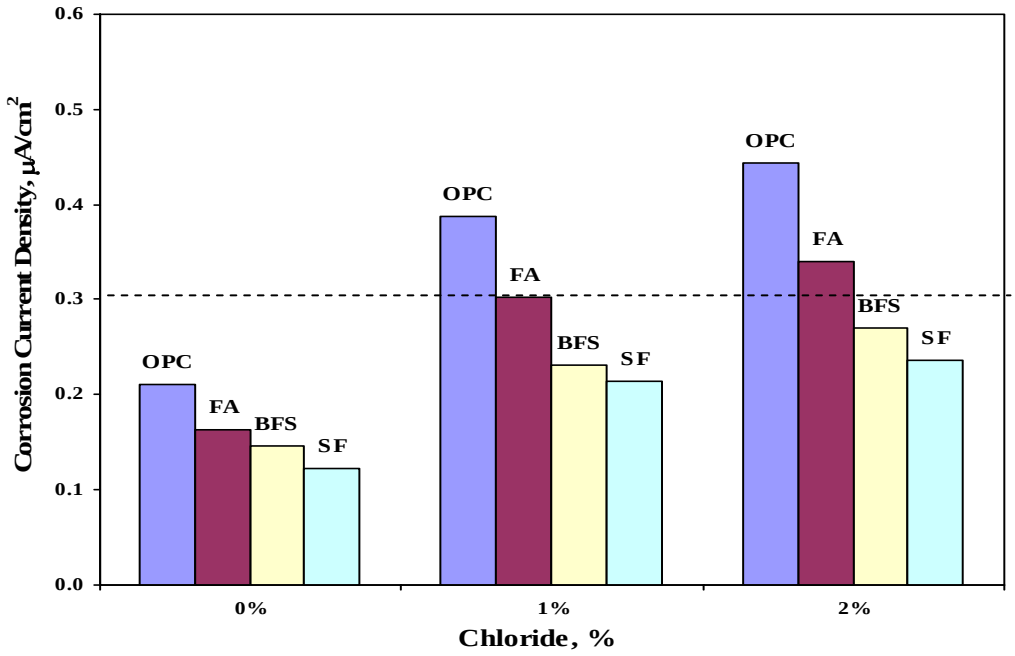

Figure 4.89: Corrosion Current Density on Uncoated steel bars in Plain and Blended Cement Concrete Specimens after 180 Days of Exposure (Temp: 23°C).

The I_{corr} on FBEC steel bars without damage in the plain and blended cement concrete specimens exposed to 23°C is compared in Figure 4.90. The I_{corr} values were less than 0.3 µA/cm^2 in both the contaminated and uncontaminated concrete specimens. In the uncontaminated blast furnace slag and silica fume cement concrete specimens, the I_{corr} values were less than 0.01 µA/cm^2. This very low value of I_{corr} indicates the possibility of maintenance free service life of reinforced concrete.

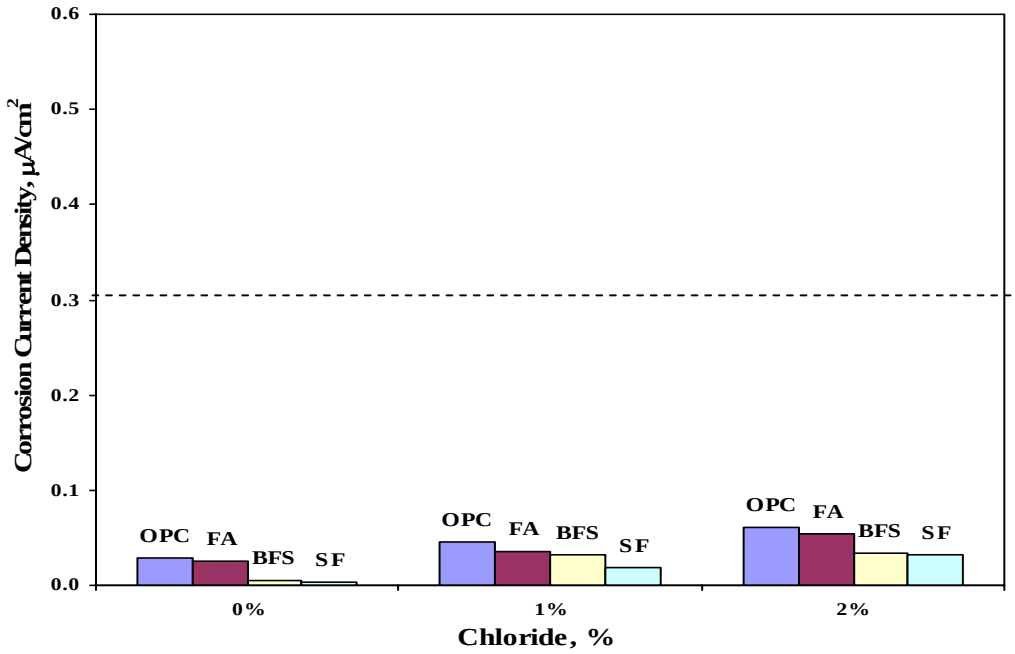

Figure 4.90: Corrosion Current Density on Coated Steel bars in Plain and Blended Cement Concrete Specimens after 180 Days of Exposure (Temp: 23°C).

Figure 4.91 depicts the I_{corr} data on 1.5% damage plain and blended cement concrete specimens exposed to 23°C. The Icorr after 180 days of exposure was less than 0.3 $\mu A/cm^2$ in all the concrete specimens. The I_{corr} on steel bars in the plain cement concrete specimens was more than that on the steel bars in the blended cement concrete specimens. Though the I_{corr} values tended to increase with the chloride contamination, this increase was not very significant. This indicates that under normal exposure conditions, i.e. 23°C, chloride contamination of up to 2% should not be of concern for steel bars with up to 1.5% damage.

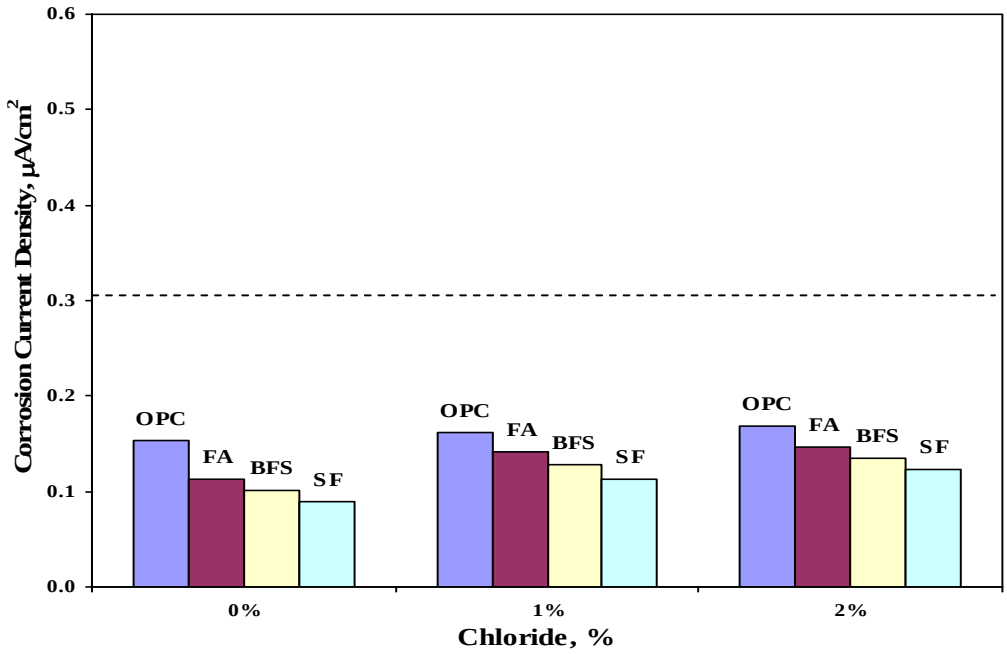

Figure 4.91: Corrosion Current Density on 1.5% damage bars in Plain and Blended Cement Concrete Specimens after 180 Days of Exposure (Temp: 23°C).

The I_{corr} on FBEC steel bars with 3% damage in plain and blended cement concrete specimens exposed to 35°C for 180 days is plotted in Figure 4.92. In these concrete specimens also, the I_{corr} was less than 0.3 µA/cm^2, in both plain and blended cement concrete specimens. The I_{corr} generally tended to increase with an increase in the chloride contamination, though this increase was not significant.

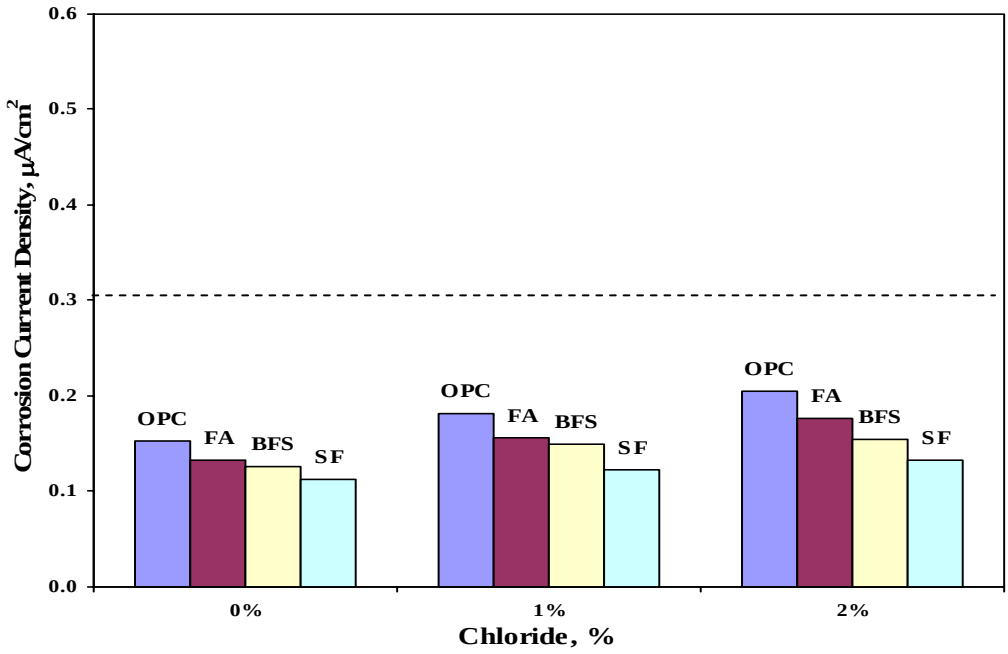

Figure 4.92: Corrosion Current Density on 3% damage bars in Plain and Blended Cement Concrete Specimens after 180 Days of Exposure (Temp: 23°C).

The I_{corr} on uncoated steel bars in the plain and blended cement concrete specimens exposed for 180 days at 35°C is depicted in Figure 4.93. The I_{corr} was less than 0.3 $\mu A/cm^2$ in the uncontaminated plain and blended cement concrete specimens. In the plain and fly ash cement concrete specimens contaminated with 1% and 2% chloride, the I_{corr} was more than 0.3 $\mu A/cm^2$. In the fly ash cement concrete specimens with 2% chloride it was slightly more than the threshold value.

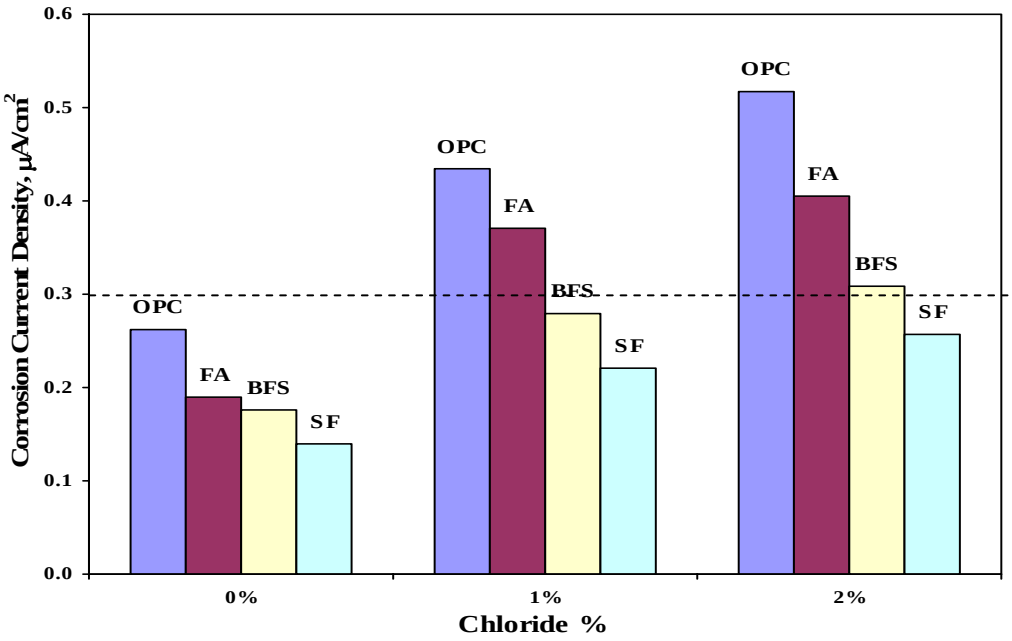

Figure 4.93: Corrosion Current Density on Uncoated Steel bars in Plain and Blended Cement Concrete Specimens after 180 Days of Exposure (Temp: 35°C).

Figure 4.94 depicts the I_{corr} on undamaged FBEC steel bars in the plain and blended cement concrete specimens exposed for 180 days at 35°C. The I_{corr} values were less than 0.3 µA/cm^2. The I_{corr} on steel bars in the plain cement concrete specimens was less than that on the steel bars in the blended cement concrete specimens. The increase in the I_{corr} values with increasing chloride contamination was not significant. This trend was noted in both the plain and blended cement concrete specimens.

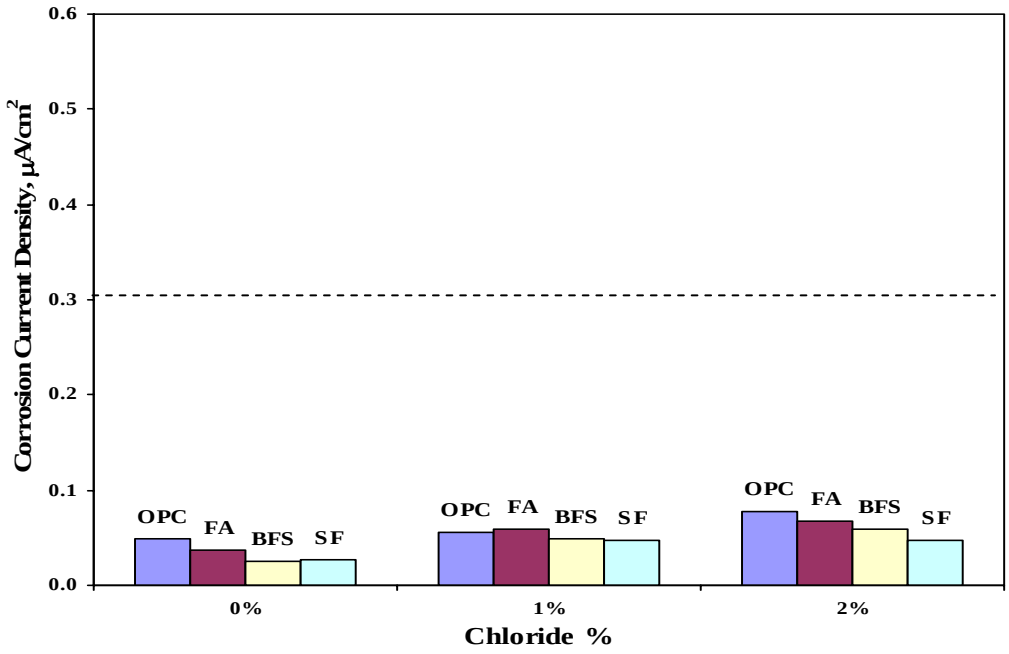

Figure 4.94: Corrosion Current Density on Undamaged Coated Steel bars in Plain and Blended Cement Concrete Specimens after 180 Days of Exposure (Temp: 35°C).

The I_{corr} on FBEC steel bars with 1.5% surface damage is plotted in Figure 4.95. The Icorr values in all the concrete specimens were less than 0.3 µA/cm^2. The I_{corr} on steel bars in the blended cement concrete specimens was generally less than that in the plain cement concrete specimens, the least being in the silica fume cement concrete specimens.

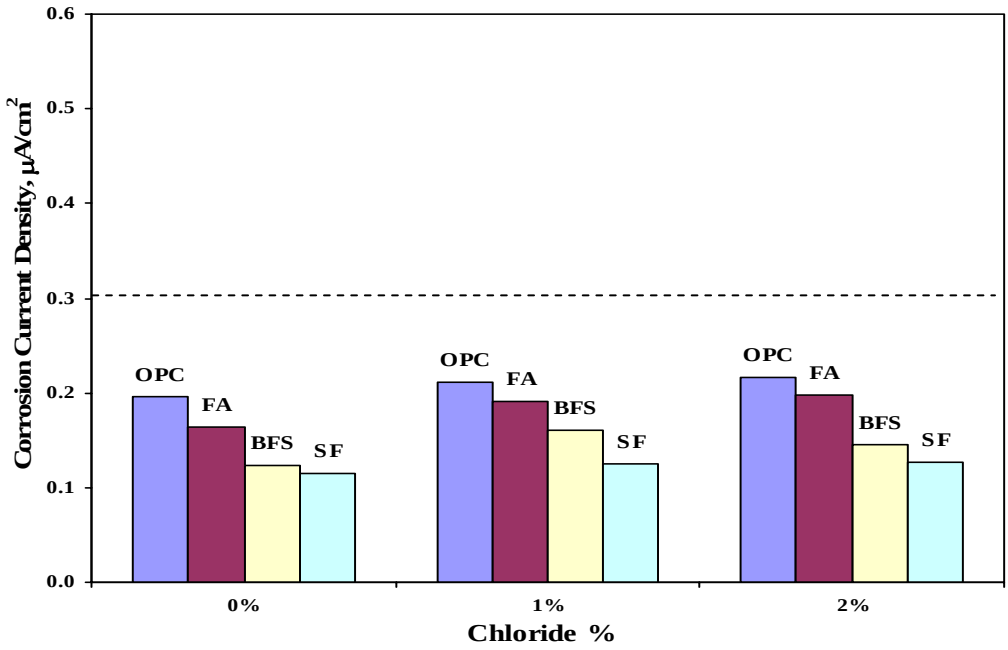

Figure 4.95: Corrosion Current Density on 1.5% damage bars in Plain and Blended Cement Concrete Specimens after 180 Days of Exposure (Temp: 35°C).

The I_{corr} on FBEC steel bars with 3% surface damage embedded in plain and blended cement concrete specimens exposed for 180 days at 35°C is plotted in Figure 4.96. The I_{corr} values in all the specimens were smaller than the threshold value of 0.3 $\mu A/cm^2$. The I_{corr} values in both the plain and blended cement concrete specimens increased with the level of chloride contamination, though the increase was not that significant. As in the other batches, the I_{corr} in the blended cement concrete specimens was less than that in the plain cement concrete specimens.

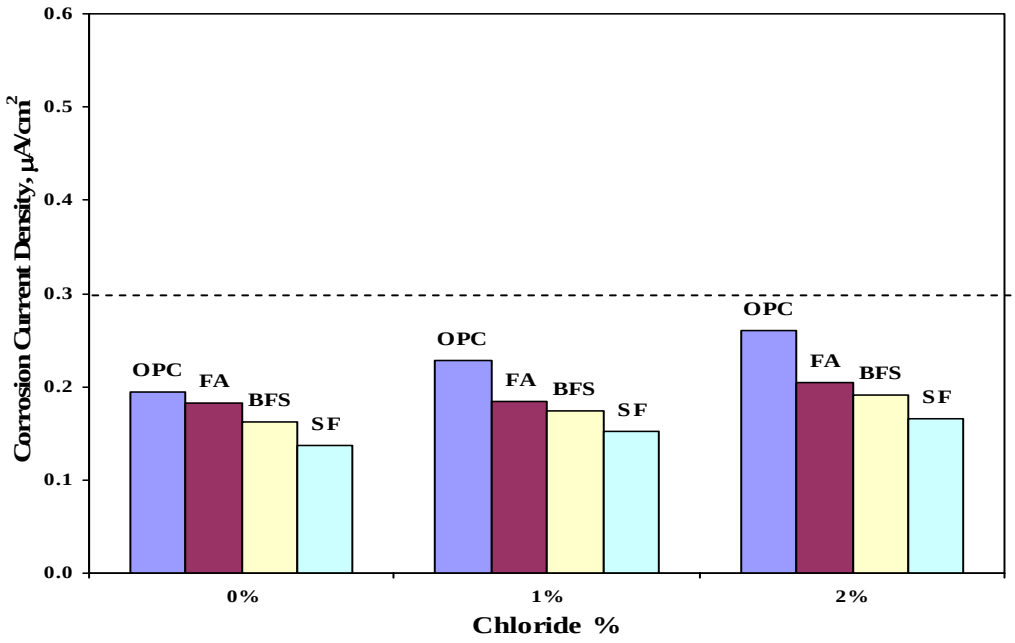

Figure 4.96: Corrosion Current Density on 3% damage bars in Plain and Blended Cement Concrete Specimens after 180 Days of Exposure (Temp: 35°C).

Figure 4.97 shows the I_{corr} on uncoated steel bars in plain and blended cement concrete specimens exposed for 180 days at 48°C. The I_{corr} on steel bars in the plain cement concrete specimens was more than 0.3 µA/cm^2 both in the uncontaminated and contaminated concrete specimens. In the uncontaminated blended cement concrete specimens, the I_{corr} was more than 0.3 µA/cm^2. However, in the blended cement concrete specimens with 1% and 2% chloride contamination, the I_{corr} was more than 0.5 µA/cm^2. This trend was noted in the silica fume cement concrete specimens.

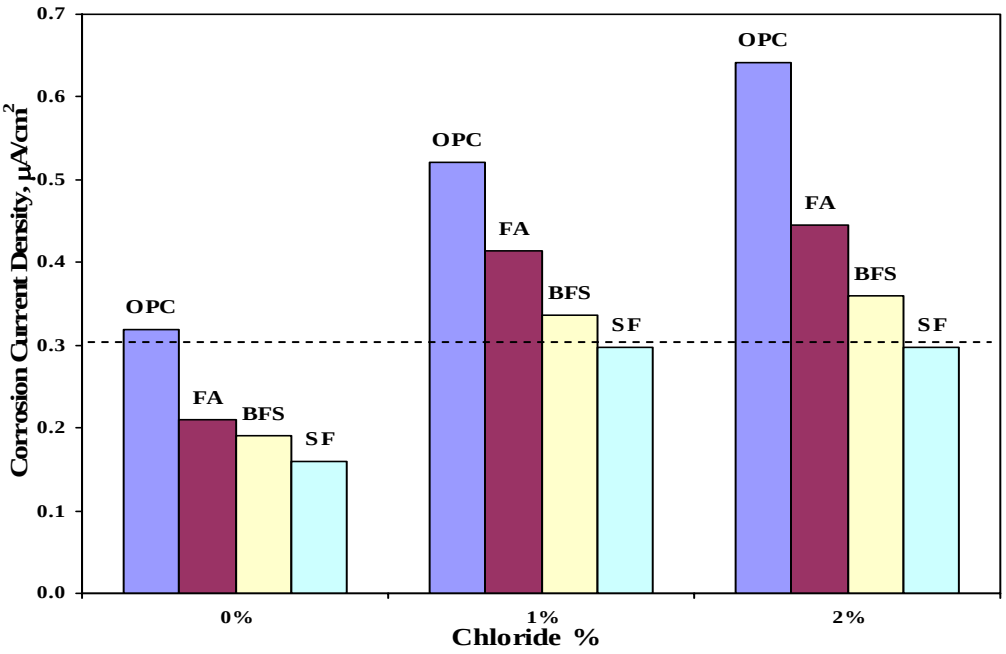

Figure 4.97: Corrosion Current Density on Uncoated Steel bars in Plain and Blended Cement Concrete Specimens after 180 Days of Exposure (Temp: 48°C).

Figures 4.98 shows the I_{corr} values on FBEC steel bars without surface damage in plain and blended cement concrete specimens exposed for 180 days at 48°C. The I_{corr} on FBEC steel bars with 1.5% surface damage are plotted in Figure 4.99. The I_{corr} values in both the groups of specimens were less than 0.3 µA/cm^2. As expected, the I_{corr} values on the steel bars with 1.5% surface damage were more than that on the steel bars without any damage.

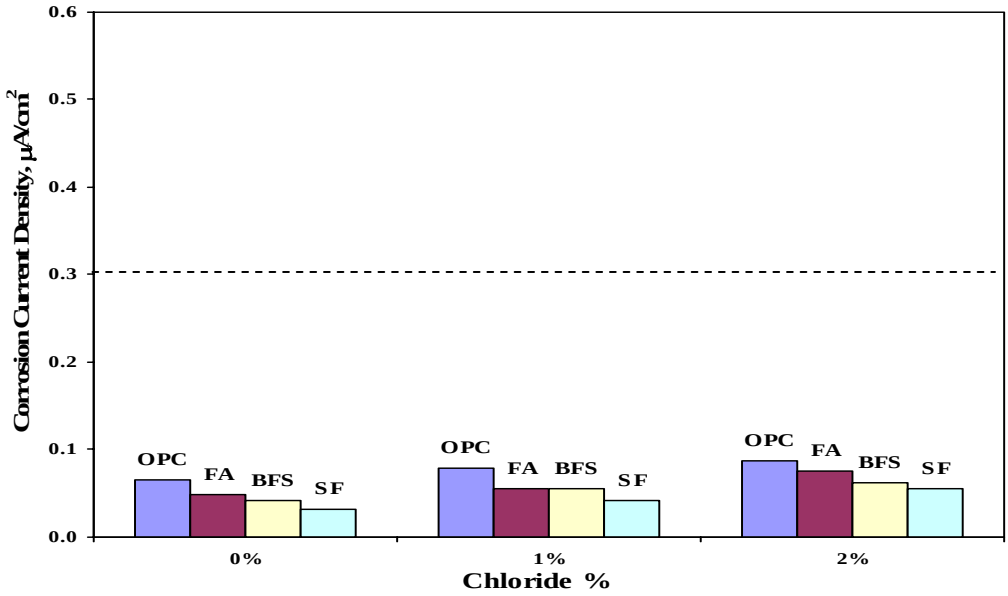

Figure 4.98: Corrosion Current Density on Coated steel bars in Plain and Blended Cement Concrete Specimens after 180 Days of Exposure (Temp: 48°C).

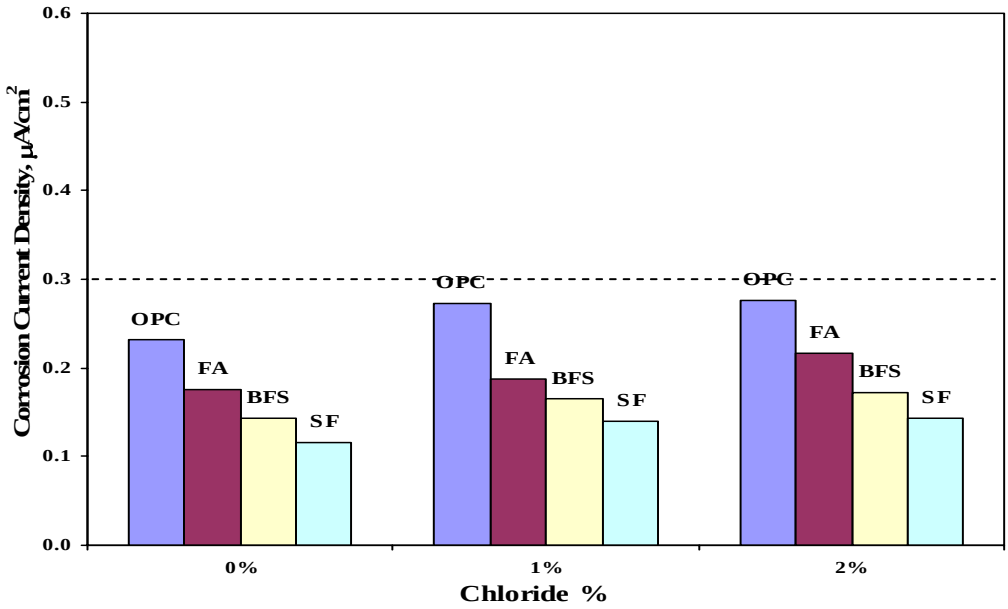

Figure 4.99: Corrosion Current Density on 1.5% damage bars in Plain and Blended Cement Concrete Specimens after 180 Days of Exposure (Temp: 48°C).

The I_{corr} on FBEC steel bars with 3% surface damage in the plain and blended cement concrete specimens exposed for 180 days at 48°C is shown in Figure 4.100. The I_{corr} was more than 0.3 $\mu A/cm^2$ in the plain cement concrete specimens contaminated with 2% chloride. In all the other concrete specimens the I_{corr} was less than 0.3 $\mu A/cm^2$.

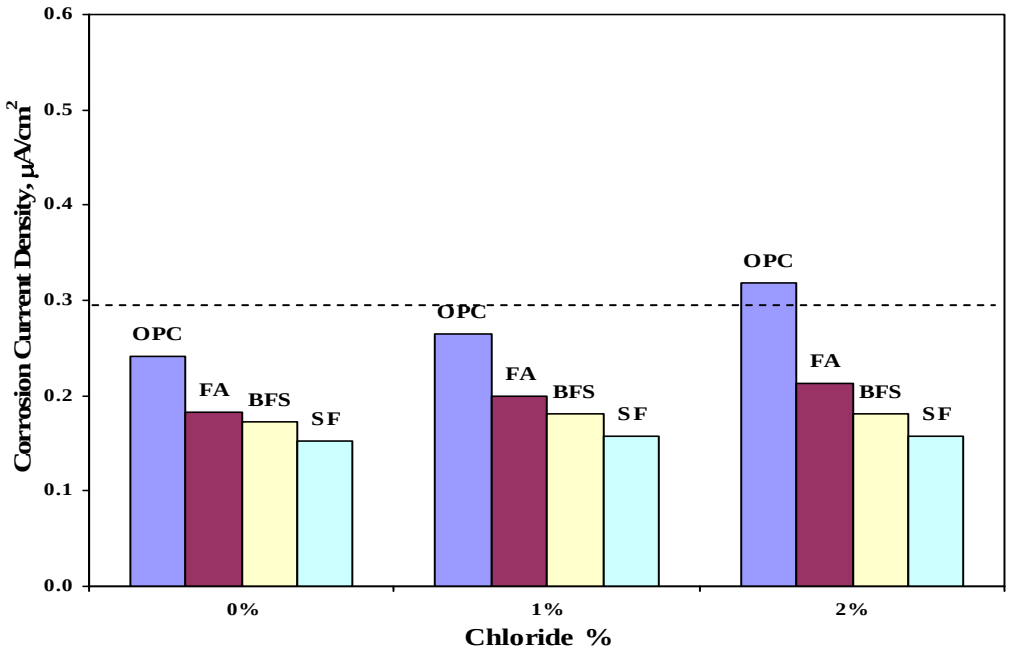

Figure 4.100: Corrosion Current Density on 3% damage bars in Plain and Blended Cement Concrete Specimens after 180 Days of Exposure (Temp: 48°C).

4.2.3 Projected Time to Cracking of Concrete

The projected time to cracking of concrete was calculated assuming an I_{corr} value of 1 μA/cm². The projected time to cracking of concrete with the uncoated and FBEC bars with varying chloride-contamination and exposed at 23°C is summarized in Table 4.4. As can be expected, the time to cracking was the least in the concrete specimens with the uncoated steel bars. The highest time to cracking was noted in the FBEC bars without any damage. However, it decreased with the extent of surface damage. For similar bar type, the time to cracking decreased with the extent of chloride contamination. The data in Table 4.4 also show that the time to cracking in the silica fume cement concrete was more than that in the plain and other blended cement concretes.

The projected time to cracking of plain and blended cement concrete specimens with varying chloride contamination and exposed at 35°C is summarized in Table 4.5. The data therein show a trend similar to that noted in the concrete specimens exposed to 23°C. The projected time to cracking of plain and blended cement concrete specimens exposed to 48°C is summarized in Table 4.6. The projected time to cracking of concrete with the FBEC bars without damage is 14,051 days from table 4.4 which is almost four to five times the time to cracking of concrete with uncoated bars. This shows the better performance of FBEC bars. The time to cracking of FBEC bars with 1.5% and 3% damage was three and four times, respectively that in the uncoated bars. Among blended cements, silica fume cement exhibited better resistance to corrosion and its projected time

to cracking was 1.5 times that in the plain cement concrete. Similarly, silica fume cement concrete performed better than the blast furnace slag and fly ash cement concretes.

Table 4.4: Projected time for I_{corr} of 1µA/cm² in plain and blended cement concrete specimens exposed to 23°C.

Cement Type	Chloride %	Rebar Type	Projected Time for I_{corr} of 1µA/cm², Days	Cement Type	Chloride %	Rebar Type	Projected Time for I_{corr} of 1µA/cm², Days
OPC	0%	0% Damage	14,051	BFS	0%	0% Damage	9,446
		1.5% Damage	4,153			1.5% Damage	3,159
		3% Damage	3,017			3% Damage	3,100
		Uncoated bar	2,918			Uncoated bar	4,482
	1%	0% Damage	9,754		1%	0% Damage	9,893
		1.5% Damage	2,322			1.5% Damage	4,482
		3% Damage	2,285			3% Damage	2,698
		Uncoated bar	1,036			Uncoated bar	2,348
	2%	0% Damage	4,887		2%	0% Damage	10,921
		1.5% Damage	2,936			1.5% Damage	4,507
		3% Damage	2,807			3% Damage	4,406
		Uncoated bar	961			Uncoated bar	2,618
SF	0%	0% Damage	16,082	FA	0%	0% Damage	9,911
		1.5% Damage	3,200			1.5% Damage	3,121
		3% Damage	3,172			3% Damage	3,036
		Uncoated bar	4,558			Uncoated bar	4,407
	1%	0% Damage	14,543		1%	0% Damage	9,838
		1.5% Damage	4,564			1.5% Damage	4,454
		3% Damage	3,158			3% Damage	2,307
		Uncoated bar	2,762			Uncoated bar	2,512
	2%	0% Damage	9,877		2%	0% Damage	6,897
		1.5% Damage	4,586			1.5% Damage	4,461
		3% Damage	4,492			3% Damage	2,923
		Uncoated bar	2,718			Uncoated bar	1,834

Table 4.5: Projected time for I_{corr} of 1µA/cm² in plain and blended cement concrete specimens exposed to 35°C.

Cement Type	Chloride %	Rebar Type	Projected Time for I_{corr} of 1µA/cm², Days	Cement Type	Chloride %	Rebar Type	Projected Time for I_{corr} of 1µA/cm², Days
OPC	0%	0% Damage	10,764	BFS	0%	0% Damage	9,867
		1.5% Damage	2,208			1.5% Damage	3,102
		3% Damage	2,187			3% Damage	2,999
		Uncoated bar	1,653			Uncoated bar	2,223
	1%	0% Damage	8,666		1%	0% Damage	9,702
		1.5% Damage	1,760			1.5% Damage	2,973
		3% Damage	1,711			3% Damage	2,228
		Uncoated bar	884			Uncoated bar	1,631
	2%	0% Damage	4,754		2%	0% Damage	9,632
		1.5% Damage	1,755			1.5% Damage	3,028
		3% Damage	1,404			3% Damage	1,519
		Uncoated bar	653			Uncoated bar	1,315
SF	0%	0% Damage	14,073	FA	0%	0% Damage	12,225
		1.5% Damage	4,633			1.5% Damage	2,976
		3% Damage	3,057			3% Damage	2,218
		Uncoated bar	3,051			Uncoated bar	2,906
	1%	0% Damage	9,713		1%	0% Damage	9,641
		1.5% Damage	3,081			1.5% Damage	2,910
		3% Damage	3,026			3% Damage	2,207
		Uncoated bar	2,749			Uncoated bar	1,064
	2%	0% Damage	9,723		2%	0% Damage	9,539
		1.5% Damage	3,063			1.5% Damage	2,167
		3% Damage	2,995			3% Damage	1,796
		Uncoated bar	1,648			Uncoated bar	909

Table 4.6: Projected time for I_{corr} of 1µA/cm² in plain and blended cement concrete specimens exposed to 48°C.

Cement Type	Chloride %	Rebar Type	Projected Time for I_{corr} of 1µA/cm², Days	Cement	Cl%	Rebar Type	Projected Time for I_{corr} of 1µA/cm², Days
OPC	0%	0% Damage	9,587	BFS	0%	0% Damage	10,831
		1.5% Damage	1,728			1.5% Damage	3,051
		3% Damage	1,728			3% Damage	2,264
		Uncoated bar	1,034			Uncoated bar	1,790
	1%	0% Damage	4,797		1%	0% Damage	9,674
		1.5% Damage	1,210			1.5% Damage	2,249
		3% Damage	1,203			3% Damage	2,218
		Uncoated bar	580			Uncoated bar	1,009
	2%	0% Damage	1,354		2%	0% Damage	9,628
		1.5% Damage	1,087			1.5% Damage	2,247
		3% Damage	1,028			3% Damage	2,913
		Uncoated bar	406			Uncoated bar	988
SF	0%	0% Damage	12,014	FA	0%	0% Damage	10,770
		1.5% Damage	4,641			1.5% Damage	2,224
		3% Damage	2,309			3% Damage	2,238
		Uncoated bar	2,284			Uncoated bar	1,746
	1%	0% Damage	10,139		1%	0% Damage	9,633
		1.5% Damage	3,057			1.5% Damage	2,231
		3% Damage	3,009			3% Damage	1,770
		Uncoated bar	1,187			Uncoated bar	839
	2%	0% Damage	9,679		2%	0% Damage	4,764
		1.5% Damage	3,060			1.5% Damage	1,473
		3% Damage	2,252			3% Damage	1,753
		Uncoated bar	1,180			Uncoated bar	737

4.2.4 Chloride Profile

Chloride ions from selected concrete specimens were extracted and analyzed to determine the water-soluble chloride content at various depths. Plain and blended cements concrete specimens were immersed in 5% sodium chloride solution for six months with varying temperatures. At the end of the exposure period, the chloride concentration at various depths was determined and the chloride profile was plotted.

The variation of chloride concentration with depth is numerically summarized in Table 4.7 and schematically plotted in Figures 4.101 through 4.103. The chloride ion concentration decreased with depth in all concrete specimens. It was the highest, at all depths, in the plain cement concrete specimens while it was the least in the silica fume concrete specimens. This indicates that the diffusion of chloride ion was more in the plain cement concrete than in a blended cement concretes. The chloride ion concentration also increased with the exposure temperature. This trend confirms the well known trend that proves the hypothesis that the diffusion of ions increases with the temperature.

Table 4. 7: Chloride Concentration in Plain and blended Cements Concrete Specimens at various depths.

Mix Type	Temperature(°C)	Chloride Concentration (% wt. of Concrete) at Depths of			
		5 mm	10 mm	15 mm	20 mm
OPC	25	0.62	0.54	0.49	0.42
OPC+SF 7.5%	25	0.26	0.23	0.21	0.18
OPC+BFS 70%	25	0.42	0.37	0.34	0.29
OPC+FA 30%	25	0.5	0.43	0.4	0.34
OPC	35	0.63	0.54	0.51	0.43
OPC+SF 7.5%	35	0.28	0.24	0.22	0.19
OPC+BFS 70%	35	0.44	0.38	0.35	0.3
OPC+FA 30%	35	0.55	0.48	0.44	0.37
OPC	48	0.7	0.61	0.56	0.48
OPC+SF 7.5%	48	0.4	0.35	0.32	0.27
OPC+BFS 70%	48	0.47	0.41	0.38	0.32
OPC+FA 30%	48	0.61	0.52	0.47	0.42

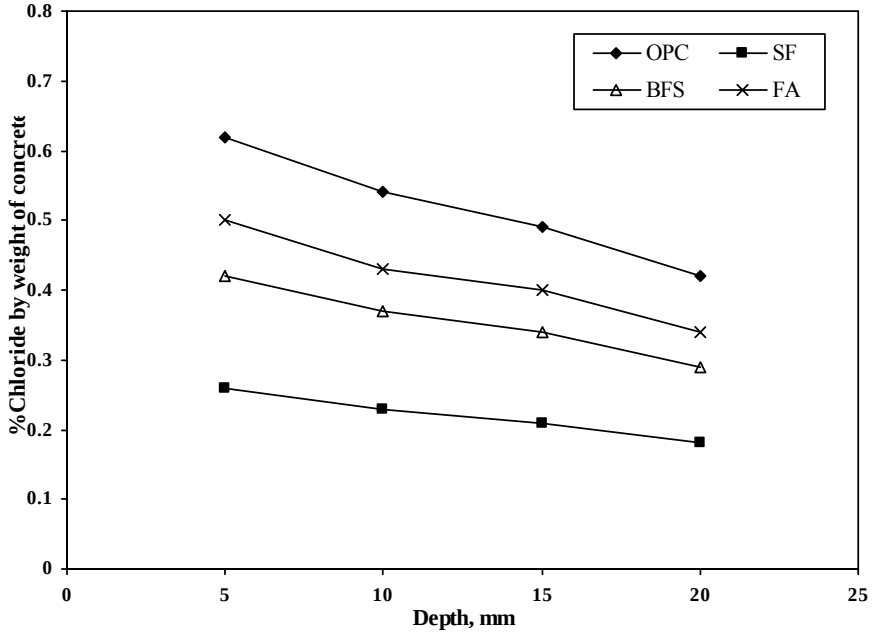

Figure 4.101: Variation of Chloride Content in ordinary and blended cements concrete specimens with depth with depth after 180 days of exposure at room temperature.

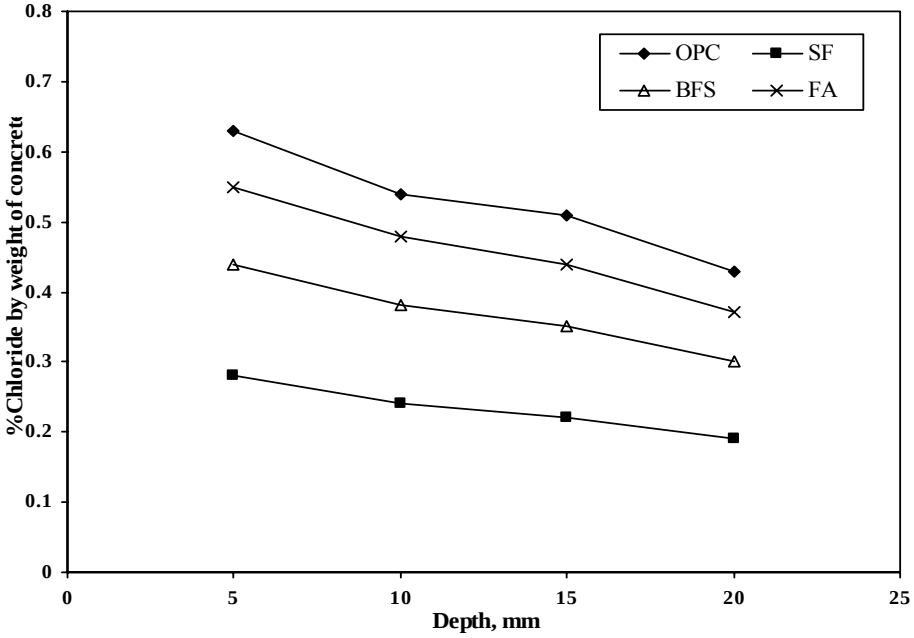

Figure 4.102: Variation of Chloride Content in ordinary and blended cements concrete specimens with depth with depth after 180 days of exposure at 35°C.

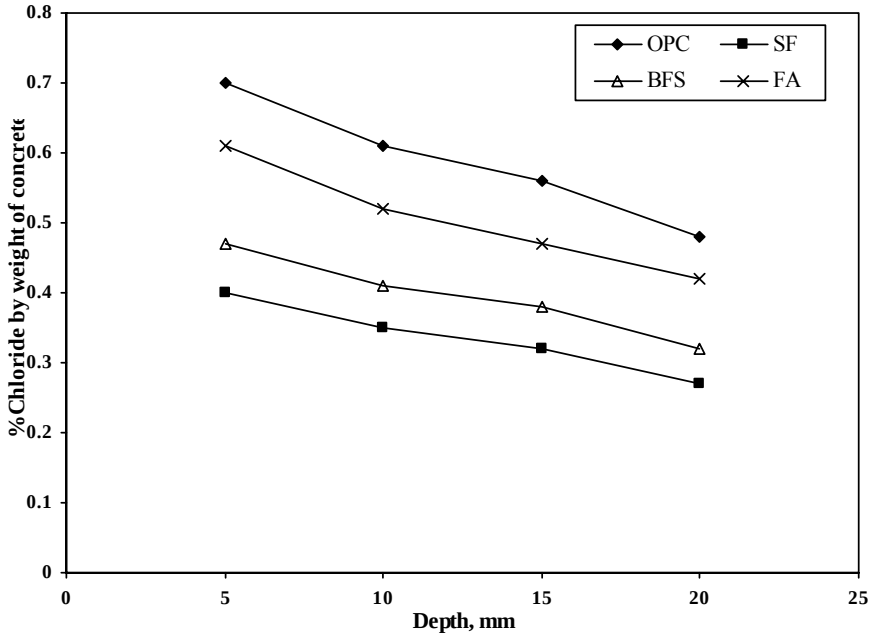

Figure 4.103: Variation of Chloride Content in ordinary and blended cements concrete specimens with depth with depth after 180 days of exposure at 48°C.

4.2.5 Visual Examination

The plain and blended cement concrete specimens prepared with uncoated and FBEC steel bars with varying surface damages and chloride contaminations and exposed to varying temperatures were broken to retrieve the steel bars. The bars were then examined visually for the degree of corrosion. Figures 4.104 through 4.115 show the reinforcing steel bars retrieved from the concrete specimens while Tables 4.8 through 4.10 summarize the corrosion ratings.

Corrosion was not noted on the uncoated steel bars in the plain cement concrete specimens contaminated with 1% chloride and exposed to 23°C within the exposure period of 180 days. Minor corrosion was noted on the uncoated steel bars in the plain cement concrete specimens with 2% chloride concentration and exposed to 35°C. Minor to moderate corrosion was noted on the uncoated and FBEC steel bars with 3% damage in the plain cement concrete specimens with 2% chloride exposed to 48°C.

Corrosion was not noted on the uncoated and FBEC steel bars in all the silica fume cement concrete specimens with the various chloride concentrations and exposed to the three selected temperatures.

Corrosion was not noted on the uncoated and FBEC steel bars in the fly ash and blast furnace slag cement concrete specimens with 2% chloride concentrations and exposed to 23°C. However Minor corrosion was noted on the uncoated steel bars in the fly ash and blast furnace slag cement concrete specimens with 2% chloride and exposed to both 35°C and 48°C.

Corrosion of reinforcing steel was not noted on the FBEC steel bars without damage in both plain and blended cement concrete specimens with all the chloride concentration and exposure temperature. Corrosion was noted on the FBEC steel bars with 1.5% damage in both plain and blended cements with 2% chloride concentration and exposed to room temperature.

Minor to moderate corrosion was noted on the FBEC steel bars with 3% damage in plain and fly ash cement concrete specimens with 2% chloride contamination exposed to 35°C and 48°C.

Minor corrosion was noted on the FBEC steel bars with 1.5% and 3% damage in blast furnace slag cement concrete specimens with 2% chloride concentrations exposed to 35°C.

Figure 4.104: Steel Bar Retrieved from Plain Cement Concrete Specimen with 2% Chloride Concentration and Exposed to 48°C.

Figure 4.105: Epoxy Coated Bar with 3% Damage Retrieved from Plain Cement Concrete Specimen with 2% Chloride Concentration Exposed to 35°C.

Figure 4.106: Epoxy Coated Bar with 1.5% Damage Retrieved from Plain Cement Concrete Specimen with 1% Chloride Concentration Exposed to 35°C.

Figure 4.107: Uncoated Bars retrieved from Plain Cement Concrete Specimen with 2% Chloride Concentration Exposed to 35°C.

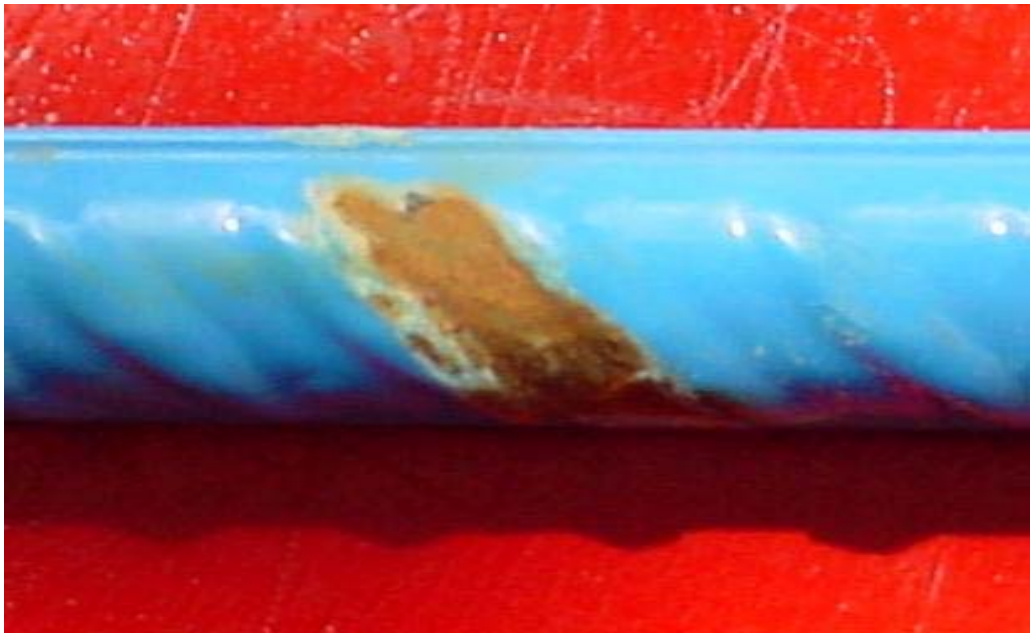

Figure 4.108: Epoxy Coated Bar with 3% Damage Retrieved from Plain Cement Concrete Specimen with 2% Chloride Concentration Exposed to 48°C.

Figure 4.109: Uncoated Steel Bar retrieved from Fly Ash Cement Concrete Specimen with 2% Chloride Concentration Exposed to 48°C.

Figure 4.110: Epoxy Coated Bar with 1.5% Damage Retrieved from Blast Furnace Slag Cement Concrete Specimen with 1% Chloride Concentration Exposed to 23°C.

Figure 4.111: Epoxy Coated Bar retrieved from Silica Fume Cement Concrete Specimen with 2% Chloride Concentration Exposed to 48°C.

Figure 4.112: Epoxy Coated Bar with 3% Damage Retrieved from Plain Cement Concrete Specimen with 1% Chloride Concentration Exposed to 48°C.

Figure 4.113: Epoxy Coated Bar with 3% Damage Retrieved from Plain Cement Concrete Specimen with 1% Chloride Concentration Exposed to Room Temperature.

Figure 4.114: Uncoated Steel Bar Retrieved from Silica Fume Cement Concrete Specimen with 2% Chloride Concentration Exposed to 48°C.

Figure 4.115: Epoxy Coated Bar with 3% Damage Retrieved from Silica Fume Cement Concrete Specimen with 1% Chloride Concentration Exposed to 23°C.

Table 4.8: Corrosion Rating for Steel Bars in the Concrete Specimens Exposed to varying Chloride Concentrations (Temp: 23ºC).

Type of Cement	Cl, %	Rebar Coating	Corrosion Rating*	Type of Cement	Cl, %	Rebar Coating	Corrosion Rating*
OPC		Uncoated bar	0	BFS		Uncoated bar	0
	0	0% Damage	0		0	0% Damage	0
		1.5% Damage	0			1.5% Damage	0
		3% Damage	0			3% Damage	0
		Uncoated bar	1			Uncoated bar	0
	1	0% Damage	0		1	0% Damage	0
		1.5% Damage	0			1.5% Damage	0
		3% Damage	0			3% Damage	1
		Uncoated bar	1			Uncoated bar	1
	2	0% Damage	0		2	0% Damage	0
		1.5% Damage	1			1.5% Damage	0
		3% Damage	1			3% Damage	1
SF		Uncoated bar	0	FA		Uncoated bar	0
	0	0% Damage	0		0	0% Damage	0
		1.5% Damage	0			1.5% Damage	0
		3% Damage	0			3% Damage	0
		Uncoated bar	0			Uncoated bar	0
	1	0% Damage	0		1	0% Damage	0
		1.5% Damage	0			1.5% Damage	0
		3% Damage	0			3% Damage	0
		Uncoated bar	0			Uncoated bar	1
	2	0% Damage	0		2	0% Damage	0
		1.5% Damage	0			1.5% Damage	0
		3% Damage	0			3% Damage	1

*Corrosion rating: 0: No corrosion; 1: Minor corrosion; 2: Minor to moderate corrosion; 3: Moderate corrosion

Table 4.9: Corrosion Rating for Steel Bars in the Concrete Specimens Exposed to varying Chloride Concentrations (Temp: 35ºC).

Type of Cement	Cl, %	Rebar	Corrosion Rating*	Type of Cement	Cl, %	Rebar Type	Corrosion Rating*
OPC		Uncoated bar	1	BFS		Uncoated bar	0
	0	0% Damage	0		0	0% Damage	0
		1.5% Damage	0			1.5% Damage	0
		3% Damage	1			3% Damage	0
		Uncoated bar	0			Uncoated bar	1
	1	0% Damage	0		1	0% Damage	0
		1.5% Damage	0			1.5% Damage	0
		3% Damage	0			3% Damage	1
		Uncoated bar	1			Black Bar	1
	2	0% Damage	0		2	0% Damage	0
		1.5% Damage	1			1.5% Damage	0
		3% Damage	1			3% Damage	1
SF		Uncoated bar	0	FA		Uncoated bar	0
	0	0% Damage	0		0	0% Damage	0
		1.5% Damage	0			1.5% Damage	0
		3% Damage	0			3% Damage	0
		Black Bar	0		1	Uncoated bar	1
	1	0% Damage	0			0% Damage	0
		1.5% Damage	0			1.5% Damage	0
		3% Damage	0			3% Damage	1
		Uncoated bar	0			Uncoated bar	1
	2	0% Damage	0		2	0% Damage	0
		1.5% Damage	0			1.5% Damage	0
		3% Damage	0			3% Damage	1

*Corrosion rating: 0: No corrosion; 1: Minor corrosion; 2: Minor to moderate corrosion; 3: Moderate corrosion

Table 4.10: Corrosion Rating for Steel Bars in the Concrete Specimens exposed to varying Chloride Concentrations (Temp: 48ºC).

Type of cement	Cl, %	Rebar	Corrosion Rating*	Type of cement	Cl, %	Rebar	Corrosion Rating*
OPC	0	0% Damage	0	BFS	0	0% Damage	0
		1.5% Damage	0			1.5% Damage	0
		3% Damage	1			3% Damage	0
		Uncoated bar	1			Uncoated bar	1
	1	0% Damage	0		1	0% Damage	0
		1.5% Damage	0			1.5% Damage	0
		3% Damage	1			3% Damage	1
		Uncoated bar	2			Uncoated bar	1
	2	0% Damage	0		2	0% Damage	0
		1.5% Damage	1			1.5% Damage	1
		3% Damage	1			3% Damage	1
SF		Uncoated bar	2	FA		Uncoated bar	1
	0	0% Damage	0		0	0% Damage	0
		1.5% Damage	1			1.5% Damage	0
		3% Damage	1			3% Damage	0
		Uncoated bar	0			Uncoated bar	1
	1	0% Damage	0		1	0% Damage	0
		1.5% Damage	0			1.5% Damage	0
		3% Damage	0			3% Damage	1
		Uncoated bar	0			Uncoated bar	1
	2	0% Damage	0		2	0% Damage	0
		1.5% Damage	0			1.5% Damage	1
		3% Damage	0			3% Damage	1
						Uncoated bar	1

*Corrosion rating: 0: No corrosion; 1: Minor corrosion; 2: Minor to moderate corrosion; 3: Moderate corrosion

CHAPTER 5

CONCLUSIONS AND RECOMMENDATIONS

5.1 CONCLUSIONS

In this study, the performance of fusion-bonded epoxy-coated (FBEC) bars with varying surface damages, embedded in plain and blended cement concrete specimens with varying chloride contaminations and exposure temperatures was evaluated. The effect of surface damage to the FB epoxy was investigated by preparing concrete specimens with 1.5 and 3% surface damage in plain and blended cement concrete specimens contaminated with 0, 1 and 2% were prepared. From the data developed in this investigation, the following conclusions could be drawn:

1. Time to cracking was the least in the concrete specimen with the uncoated steel bars. The highest time to cracking was noted in the FBEC bars without any damage. However, it decreased with the extent of surface damage. For similar bar type, the time to cracking decreased with the extent of chloride contamination.
2. Among blended cements, silica fume cement exhibited better resistance to corrosion and its projected time to cracking was 1.5 times that in the plain cement concrete. Similarly, silica fume cement concrete performed better than the blast furnace slag and fly ash cement concretes.

3. The data on the corrosion current density indicated very low reinforcement corrosion in the concrete specimens prepared with undamaged FBEC bars. As expected, the I_{corr} values on the uncoated steel bars were very high. In these bars, the I_{corr} increased with increasing the chloride contamination and temperature.

4. While the I_{corr} values in the undamaged FBEC bars were very low; they tended to increase with increasing surface damage, temperature and chloride contamination. The effect of FBE coating damage on the corrosion of underlying metal was more predominant than that of the chloride contamination.

5. With increasing temperature, the I_{corr} values in all types of bars and blended cements are increased. Among the blended cements, the concrete specimens prepared with silica fume exhibited very low I_{corr} values compared to the specimens prepared with plain and other blended cement concrete specimens.

6. At room temperature, the concrete specimens prepared with ordinary plain cement contaminated with up to 1% chloride, the surface damage to the FBE coating should be less than 3%. However, when the structures are to be exposed to high chloride contamination, resulting in a chloride concentration of 2% by weight of cement, the surface damage should be less than 1.5%.

7. When the structures are exposed to high temperature and chloride contamination, silica fume cement should be used as it shows very low I_{corr} values even at 48°C.

8. For the concrete specimens prepared with plain, fly ash and blast furnace slag cements contaminated with 0%, 1%, and 2% chlorides in uncoated and bars having damages of 1.5% and 3%, active reinforcement corrosion, indicated by an I_{corr} value of more than 0.3 μA/cm², was observed at temperatures of 35°C and 48°C.

9. In the concrete specimens with FBEC bars having surface damage of 1.5% and 3%, the I_{corr} values were less than 0.3 μA/cm² at room temperature with 0% and 1% chloride contamination when the specimens were prepared with blended cements. However, in the concrete specimens contaminated with 2% chloride, by weight of cement, active reinforcement corrosion was noted in the concrete specimens with steel bars with a surface damage of 3% in plain, fly ash and blast furnace slag cements.

10. The chloride concentration was the highest, at all depths, in the plain cement concrete specimens while it was the least in the silica fume concrete specimens. This indicates that the diffusion of chloride ion was more in the plain cement concrete than in the blended cement concretes.

11. Corrosion was not noted on the uncoated steel bars in the plain cement concrete specimens contaminated with 1% chloride and exposed to 23°C. Minor corrosion was noted on the uncoated steel bars in the plain cement concrete specimens with 2% chloride concentration and exposed to 35°C. Minor to moderate corrosion was

noted on the uncoated and FBEC steel bars with 3% damage in the plain cement concrete specimens with 2% chloride exposed to 48°C.

5.2 RECOMMENDATIONS

Based on the out come of the study the following recommendations are made:

1. Avoid damage to FBEC bars as much as possible.
2. Use blended cements to improve the corrosion-resistance of FBEC steel bars. Blended cements with 7.5% silica fume, 70% blast furnace slag or 30% fly ash are preferable.
3. When concrete structures are to be exposed to a temperature of 48 °C silica fume cement concrete with up to 2% chloride contamination and 3% surface damage to FBEC steel bars can be used. For similar exposure temperature and chloride contamination, the limit on surface damage to FBEC steel bars should be 1.5%.

REFERENCES

1. Shameem, M., Maslehuddin, M., Saricimen, H. and Al-Mana, A. I., "Extending the Life of Reinforced Concrete Structures in the Arabian Gulf Environment," *Proceedings, Structural Faults and Repairs Conference*, London, July 1995, pp. 115- 126.

2. Malasheski, G. J., Maurer, D. A., Mellot, D. P. and Arellano, J. L., *Bridge Deck Protective Systems*, PENN DOT Research Project 85-17, 1986.

3. Pfeifer, D. W., Landgren, J. R. and Zoob, A., *Protective Systems for New Prestressed and Substructure Concrete*, FHWA Report No. RD-86/193, 1987.

4. Al-Gahtani A.S., " Environmental Consideration for the Use of Epoxy-Coated Rebars (FBECR) in the Gulf Region," *Proceedings, Symposium on performance of Concrete Structures in the Arabian Gulf Environment*, KFUPM, Nov, 15-17, 1998, pp. 21-36.

5. Pourbaix, M., "Application of Electrochemistry in Corrosion Science and Practice," *Corrosion Science*, Vol. 14, 1974, pp. 22-28.

6. Page, C. L., "The Mechanics of Corrosion Protection in Reinforced Concrete Marine Structures," *Nature*, Vol. 258, 1975, pp. 514-515.

7. Leek, D. S. and Poole, A. B., "The Breakdown of the Passive film on High Yield Mild Steel by Chloride Ions," *Corrosion of Reinforcement in Concrete*, edited by Page, Treadaway and Bamforth, Elsevier Applied Science, London, 1990, pp. 65-73.

8. Sagoe-Crentsil, K. K., and Glasser, F. P., "Analysis of the Steel Concrete Interface", *Corrosion of Reinforcement in Concrete*, edited by Page, Treadaway and Bamforth, Elsevier Applied Science, London, 1990, pp. 74-86.

9. Maslehuddin, M., Saricimen, H. and Al-Mana, A. I., "Performance Evaluation of Concrete in the Arabian Gulf," *Proceedings, Deterioration and Repair of Reinforced Concrete in the Arabian Gulf*, Oct. 1993, Bahrain, pp. 233-246.

10. Maslehuddin, M. and Al-Amoudi, O. S. B., "Corrosion of Reinforcing Steel in Concrete, its Monitoring and Prevention," *Proceedings, Symposium on Corrosion and its Control*, 16-18 May 1992, Riyadh, pp. 110- 125.

11. Hoar, T. P., "The Anodic Behavior of Metals," *Corrosion Science*, Vol. 7, 1967, pp. 341-355.

12. Chao, C. Y., Lin L. F. and MacDonald, D. D., "A Point Defect Model for Anodic Passive Films. Part I: Film Growth Kinetics, Part II: Chemical Breakdown and Pit Initiation," *Journal of Electrochemical Society*, Vol. 128, 1981, pp. 1187-1194.

13. Alvarez, M. G. and Galvele, J. R., "The Mechanics of Pitting of High Purity Iron in NaCl Solutions," *Corrosion Science*, Vol. 24, 1984, pp. 27-48.

14. Rasheeduzzafar, Hussain, S. E. and Al-Saadoun, S. S., "Effect of Tricalcium Aluminate Content of Cement on Chloride Binding and Corrosion of Reinforcing Steel in Concrete," *ACI Materials Journal*, Jan-Feb 1992, pp. 3-12.

15. Page, C. L. and Vennesland, O., "Pore Solution Composition and Chloride Binding Capacity of Silica-Fume Cement Pastes," Materials and Structures, Vol. 16, No. 91, 1983, pp. 19-25.

16. Tritthart, J., "Chloride Binding in Cement, II: The Influence of the Hydroxide Concentration in the Pore Solution of Hardened Cement Paste on Chloride Binding," Cement and Concrete Research, Vol. 19, No. 5, 1989, pp. 683-691.

17. Rasheeduzzafar, Hussain, S. E. and Al-Saadoun, S. S., "Effect of Cement Composition on Chloride Binding and Corrosion of Reinforcing Steel in Concrete," Cement and Concrete Research, Vol. 21, No. 5, 1991, pp. 777-794.

18. Mangat, P. S.,and Gurusamy, K., "Corrosion Resistance of Steel Fibers in Concrete under Marine Exposure," Cement and Concrete Research, Vol.18, No.1, January 1989, pp. 44-54.

19. Hausmann, D. A., "Steel Corrosion in Concrete, How Does It Occur?," Materials Protection, Vol. 6, Nov. 1967, pp. 19-23.

20. Gouda, V. K., "Corrosion and Corrosion Inhibition of Reinforcing Steel Immersed in Alkaline Solution," British Corrosion Journal, Vol. 5, 1970, pp. 198-203.

21. Mangat, P. S. and Molloy, B. T., "Influence of PFA, Slag and Microsilica on Chloride Induced Corrosion of Reinforcement in Concrete," Cement and Concrete Research, Vol. 21, No.5, 1991, pp. 819-834.

22. Al-Amoudi, O.S.B., Rasheeduzzafar, Abduljauwad, S.N., and Maslehuddin, M., "Corrosion of Reinforcing Steel in Sabkha Environment," Journal of King Saud University {ENGINEERING SCIENCES}, Special Issue of the Journal "Corrosion and Its Control," Vol. 8, 1996, pp. 37-50. Also published in: Preprint, Symposium on Corrosion and Its Control, King Saud University, May 1992, pp. 90-100.

23. Sagues, A. A., Powers, R.G., and Zayed, A.M., " Marine Environment Corrosion of Epoxy-Coated Reinforcing Steel," Corrosion of Reinforcement in Concrete, C.

Page, K Treadaway and P. Bamforth, Eds., Elsevier Applied Science, London-New York, 1990, pp 539-549.

24. Sagues, A. A., "Evaluation of Corrosion Rate by Electrochemical Impedance in a System with Multiple Polarization Effects," Paper No. 25, Corrosion 89, NACE, New Orleans Convention Center, New Orleans, Louisiana, April 17-21, 1989, 10p.

25. Zayed, A.M., and Sagues, A. A., "Corrosion at Surface Damage on an Epoxy coated Reinforcing Steel," Corrosion Science, Vol. 30, No. 10, 1990, pp 1025-1044.

26. Zayed, A.M., and Sagues, A. A., "Corrosion of Epoxy Coated Reinforcing Steel in concrete," Paper No. 379, Corrosion 89, NACE, New Orleans Convention Center, New Orleans, Louisiana, April 17-21, 1989, 20p.

27. Clear, K.C., Effectiveness of Epoxy-coated Reinforcing Steel, interim report, Canadian Strategic Highway Research Program (C-SHRP), Ottawa, Ontario, November 1992.

28. Sohanghpurwala, A., and Clear, K.C., "Effectiveness of Epoxy-Coating on Minimizing Corrosion of Reinforcing Steel in Concrete," Paper No. 890432, Transportation Research Board, 69th Annual Meeting, Washington, D.C., January 1990, 9 p.

29. Lee, H., and Neville, K., Handbook of Epoxy Resins, 2nd ed., McGraw-Hill, Inc., New York, NY, 1982.

30. Pike, R.G., Hay, R.E., Clifton, J.R., Beeghly, H.F., and Mathy, R.G., "Nonmetallic Coatings for Concrete Reinforcing Bars," Public Roads, Vol 37, No. 5, U.S Bureau of Public Roads, June 1973, pp 185-197.

31. Read, J,A., "FBECR- The Need for correct specification and quality control", Paper Presented at Symposium on FBECR at Sheffield University on Wednesday May 17, 1989, 23 p.

32. Gustafson, D.P., and Edgell, T.W., "Epoxy-Coated Rebars Provides Rehab Relief," Roads and Bridges, Vol. 27, No. 8, August 1989, pp 51-53.

33. McFadden, B.J., "Application and Fabrication of Epoxy-coated Reinforcing Steel" Paper No. 8; Seminar Reprints on Solving Rebar Corrosion Problems in Concrete, September 27-29, 1982, Chicago, III, NACE, Houston, TX, 1983, 6 p.

34. Neif, T., "Performance of Epoxy-Coated Bars," A seminar presentation at Wyndham Hotel, Austin, TX, November 2, 1991.

35. Robert, A.G., " Organic coatings: Properties, Selection and Use," NBS, Building Science Series 7, National Bureau of Standards, Washington, D.C., 1968.

36. Andrade, C., Holst, J.D., Nurnberger, U., Whiteley, J.D., and Woodman, N., "Protection Systems for Reinforcement," CEB Bulletin D' Information No. 211, Switzerland, February 1992.

37. McKeel, W.T., Jr., "Evaluation of Epoxy-Coated Reinforcing Steel," Report No. VHTRC 77-R56, Virginia Highway and Transportation Research Council, Federal Highway Administration, Charlottesville, Virgina, June 1977, 26 p.

38. Clifton, J.R., "Proection of Reinforcing Bars with Organic Coatings." Materials Performance, Vol. 15, No. 5, May 1976, pp 14-17.

39. Concrete Reinforcing Steel Institute, "CRSI Performance Research: Epoxy-Coated Reinforcing Steel," Interim Report, CRSI, Schaumburg, III, January 1992.

40. Poston, R.W., Improving Durability of Bridge Decks by Transverse Prestressing, Ph.D. Dissertation, Department of Civil Engineering, The University of Texas at Austin, Austin, TX, December 1984.

41. ACI Committee 222, Corrosion of Metals in Concrete, ACI 222R-85, ACI Manual of Concrete Practice , Part I, Materials and General Properties of Concrete, American Concrete Institute, Detroit, 1987, 30 p.

42. McKenzie, M., "The Effect of Defects on the Durability of Epoxy-Coated Reinforcement" Transportation Research Circular; Epoxy-Coated Reinforcement in Highway Structures, No. 403, ISSN0097-8515, National Research Council, Washington, D.C., March 1993, pp 17-28.

43. Sherman, M.R., Field Evaluation of Bridge Corrosion Protection Measures, A Master of Science Thesis, the University of Texas at Austin, TX, May 1993, 226 p.

44. Virmani, Y.P., Clear, K.C., and Pasko, T.J., Jr., Time-To-Corrosion of Reinforcing Steel in Concrete Slabs, V.5: Calcium Nitrite Admixture or Epoxy-Coated Reinforcing Bars as Corrosion Protection System, Report No. FHWA/RD-83/102, Federal Highway Administration, Washington, D.C Sepetember 1983, 71 p.

45. Swamy, R.N., Koyama, S., Arai, T., and Mikami, N., "Durability of Steel Reinforcement in Marine Environment," Concrete in Marine Environment Proceedings, 2nd International Conference, St. Andrews by the Sea, Canada, ACI SP 109, V.M. Malhotra, Ed., American Concrete Institute, Detroit, 1988, pp 147-161.

46. Baldwin, W.R., "An Update on Epoxy-Coated Reinforcing Steel," Paper No. 7, Seminar Reprints on Solving Rebar Corrosion Problems in Concrete, September 27-29, 1982, Chicago, III, NACE, Houston, TX, 1983, 4 p.

47. Munjal, S.K., Reviewed by Parrish, S., Evaluation of Epoxy-Coated Reinforcing Steel in Bridge Decks, Interim Report No. FHWA-MD-82/03, Maryland, March 1981, 137 p.

48. Smith, L.L., Kessier, R.J., Powers, R.G., "Corrosion of Epoxy-Coated Rebar in a Marine Environment," Transportation Research Circular; Epoxy-Coated Reinforcement in the Highway Structures, No. 403, ISSN 0097-8515, National Research Council, Washington, D.C., March 1993, pp 36-45.

49. Hamad, B.S., Jirsa, J.O., and D Abreu D Paolo, N.J., Effects of Epoxy Coating on Bond and Anchorage of Reinforcement in concrete Structures, Research Report No. 1181-1F, Center for Transportation Research, The University of Texas at Austin, Austin TX, November 1990, 56 p.

50. Clear, K.C., "Effectiveness of epoxy-coated reinforcing steel," Concrete International, May 1992, pp 58-62.

51. CRSI, "CRSI Comments," Concrete International, May 1992, pp 59-64.

52. ENR, "Top Researcher's Switch Shakes Bridge Deck Design," Engineering News Record, the McGraw-Hill Construction Weekly, June 15, 1992.

53. Clear, K.C., “Effectiveness of Epoxy-Coated Reinforcing Steel (C-SHRP Report: Executive Summary”, Transportation Research Circular: Epoxy-Coated Reinforcement in Highway Structures, No. 403, ISSN 0097-8515, National Research Council, Washington, D.C., March 1993, pp 66-67.

54. Standard Specifications for Epoxy Coated Reinforcing Bars, ASTM A 775/A 775M-93, American Society for Testing & Materials, Philadelphia, 2004, 6 pp.

55. Alley, J., “Epoxy-Coated Rebar Benefits’ Minnesota deck,” June 1993.

56. Weyers, R.E. and Cady, P.D., “Deterioration of Concrete Bridge Decks from corrosion of Reinforcing Steel,” Concrete International, Jan. 1987.

57. Treadway, K.W.J. and Davies, H., “Performance of Fusion-Bonded Epoxy-Coated Steel Reinforcement,” The Structural Engineer. Vol. 67, No. 6, March 1989, pp. 99-108.

58. Swamy, R.N., “Epoxy-Coated Steel Reinforcement,” American Concrete Institute, March 1980.

59. Sagues, A. A and Powers, R.G., "Effect of Concrete Environment on the Corrosion Performance of Epoxy-Coated Reinforcing Steel," Corrosion 90, Las Vegas, Paper No. 311, 1990, pp. 311/1-311/15.

60. Burke, D.F., "Performance of Epoxy-Coated Rebar, Galvanized Rebar, and plain Rebar with calcium Nitrite in a Marine Environment," Proceedings, International Conference on Corrosion and Corrosion Protection of Steel in Concrete, University of Sheffield, July 24-28, 1994, pp. 1254-1266.

61. Burke, D.F., "Epoxy-Coated Rebar in Marine Concrete," The Military Engineer, Aug-Sept. 1994, pp. 10-12.

62. Sakai, K. and Shinichi, S., "Ten-Year Exposure Test of Pre-Cracked Reinforced concrete in a marine Environment," Proceedings, 3rd International Conference on Durability of Concrete, Nice France American concrete Institute, Detroit, Michigan, (SP-145), 1994, pp. 353-369.

63. Nielsen, N.M., "Epoxy-Coated Rebar-State of the Art," Proceedings, 4th International Conference on Deterioration and Repair of Reinforced Concrete in the Arabian Gulf, Bahrain Society of Engineer, Bahrain, Vol. 1, 1993, pp. 409-418.

64. Smith, L.L., Kessler, R.J. and Powers, R.G., "Corrosion of Epoxy-Coated Rebar in a Marine Environment," Transportation Research Circular No. 403, National Research Council, March 1993, pp. 36-45.

65. Rasheeduzzafar, Dakhil, F.H., Bader, M.A and Khan, M.M., "Performance of Corrosion Resisting Steels in Steels in Chloride-Bearing Concrete," ACI Materials Journal, Vol. 89, No. 5, Sept-Oct. 1992, pp. 439-448.

66. Sagues, A. A., Mechanism of Corrosion of Epoxy-Coated Reinforcement Steel in Concrete (Final Report), Report prepared for Florida Department of Transportation in cooperation with the Federal Highway Administration, State Project No. 99700-7504-119 WP 1 05050543, 1991.

67. S. Erdogdu, T.W.Bremner and I.L. Kondartova., "Accelerated Resting of Plain and Epoxy-Coated Reinforcement in Simulated Seawater and Chloride Solution," Cement and Concrete Research, Vol. 31, 2001, pp. 861-867.

68. Elleithy, W.M, Alfarabi M.Sharif, Omar S B Al-Amoudi, Mohammed Maslehuddin and Abul Kalam Azad., "Effect of Holidays and Surface Damage to FBEC on Reinforcement Corrosion," Construction and Building Materials, Vol. 12, 1998, pp. 185-193.

69. Darwin, A.B., and Scantlebury J.D., "Retarding of Corrosion Process on Reinforcement Bar in Concrete with an FBE coating," Cement & Concrete Composites, Vol., 24, 2002, pp. 73-78.

70. Al-Amoudi, O. S. B., Maslehuddin, M and Mohammed Ibrahim "Long term Performance of Fusion-Bonded Epoxy-Coated Steel Bars in chloride-Contaminated Concrete", ACI Material Journal, Vol. 101, No. 4, July-August 2004, pp. 303-309.

71. A.M Neville, Properties of Concrete, 4th ed., Pearson Education, Singapore 1995. pp 75-85.

72. Mehta, P.K., and Aiticin, P.C. "Principles Underlying Production of High Performance Concrete. Cement," Concrete and Aggregates, Vol.12, No.2, pp. 70-78.

73. Feldman, R.F. "Pore Structure Formation during Hydration of Fly Ash and Slag Cement Blends. Proceedings," Symposium on Fly Ash Utilization in Cement and Concrete, Material Research Society, Boston, 1981, pp. 124-133.

74. Mehta P.K. "Influence of Pozzolanic Admixtures on the Transition Zone in Concrete Presented at the International Seminar on Industrial By-Products and the Durability of Concrete, Chalmers University of Technology, 1986.

75. Sheetz, B.E., M. Grutzeck, D.W. Stickler and D.M. Roy. "Effect of Composition of Additives upon Micro Structure of Hydrated Portland Cement Composites," Proceedings, 3rd International Conference on Cement Microscopy, Houston, 1981, pp. 307-318.

76. Mehta, P.K. and O.E. Gjorv, "Properties of Portland Cement Concrete Containing Fly Ash and Condensed Silica Fume," Cement and Concrete Research, Vol. 12, No.5, pp. 1982, 587-595.

77. Delage, P. and P.C. Aitcin, Effect of Cocndensed Silica Fume on the Porosity of Filed Concrete Industrial and Engineering Chemistry Product Research and Development, 1985, Vol. 22.

78. Manmohan D. and P.K Mehta, "Influence of Pozzolanic Slag and Chemical Admixtures on Pore Size Distribution and Permeability of Hardened Cement Pastes. Cement," Concrete and Aggregates, 1981, Vol. 3, No.1, pp.63-67.

79. Nyame, B.K and J.M. Illston, Capillary Pore Structure and the Permeability of Hardened Cement Paste. Proceedings, 7th International Congress on the Chemistry of Cement, Paris, 1986, Vol. 3, pp. VI. 181-VI. 186.

80. Hussain, S.E, Mechanism of High Durability Performance of Blended Cements, Ph.D. Thesis, King Fahd University of Petroleum and Minerals, Dhahran, Saudi Arabia, 1991.

81. Kumar, A., S. Komarneni and D.M. Roy, "Diffusion of Ca+ and Cl^- through Sealing Materials," Cement and Concrete Research, Vol. No.17, 1987, pp. 153-160.

82. Li, S., and D.M. Roy, "Investigation of Relations between Porosity, Pore Structure, and Cl^- Diffusion of Fly Ash and Blended Cement Pastes," Cement and Concrete Research, 1986, Vol. 16, No. 3, pp.749-759.

83. Kawamura, M., O.A. Kayyali and M.N. Haque, "Effects of Fly Ash on Pore Solution Composition in Calcium and Sodium Chloride Bearing Mortars," Cement and Concrete Research, 1988, Vol. 18, No.5, Sept, pp. 763-773.

84. Khan, C.N.S.A, The Effect of Temperature and Salt Contamination on Corrosion of Reinforcing Steel in OPC and Blended Cement Concretes, M.Sc. Thesis, Department of Civil Engineering, King Fahd University of Petroleum and Minerals, Dhahran, Saudi Arabia, 1993.

85. Maslehuddin, M., Al-Mana, M. Shamim and H. Saricimen, "Effect of Sand Repalcemnet on the Early-age Strength Gain and Long-term Corrosion-Resisting characteristics of Fly Ash Concrete," ACI Materails Journal, Jan.-Feb., 1989, pp. 58-62.

86. Byfors, K, "Influence of Silica Fume and Fly Ash on Chloride Diffusion and pH Values in Cement Paste," Cement and Concrete Research, 1987, Vol. 17, pp, 115-130.

87. Al-Amoudi, O.S.B., Studies on Soil-Foundation Interaction in the Sabkha Environment of Eastern Province of Saudi Arabia, Ph.D. Dissertation. King Fahd University of Petroleum and Minerals, Dhahran, Saudi Arabia, 1992.

88. Uhlig, H.H., Corrosion and Corrosion Control, Jhon Wiley and Sons, New York, 1983.

89. Maslehuddin, M., N. R. Jarrah, O.A Ashiru and A.I. Al-Mana, "Corrosion of steel in Alkaline Media", Proceedings, 6th Middle East Corrosion Conference, Bahrain, 1994, Jan. pp. 597-611.

90. Holmes, C.W. and S.G. Brundle, "The Deterioration of Reinforced Concrete through Chloride Attack," Proceedings, 2nd International Conference on Deterioration and Repair of Reinforced Concrete in the Arabian Gulf, Bahrain, 1987, pp. 469-487.

91. Benjemin, S.E and J.M. Sykes, “The Effect of Temperature on the Pitting Corrosion of Iron in OPC Mortars,” Proc., 3rd International Conference on Deterioration and Repair of Reinforced Concrete in the Arabian Gulf, Bahrain, 1989, pp.573-580.

92. Benjamin, S.E and J.M. Sykes, “Chloride-Induced Pitting Corrosion of Swedish Iron in ordinary Portland Cement Mortars and Alkaline Solutions and Effect of Temperature,” in Page, Treadaway and Bamforth (Eds): Corrosion Reinforcement in Concrete. Elsevier Applied Science, London, 1990, pp.59-64.

93. Schieβl, P.and M.Raupach, ”Influence of Concrete Composition and Microclimate on the critical Chloride Content in Concrete,” Corrosion of Reinforcement in Concrete, Page, Treadaway and Bamforth, Editors, Elsevier Applied Science, London, 1990, pp. 49-54.

94. Baumel, A. and H. J. Engel, “Korrosion von stohl in beton, Archive fur das Eisenhuttenwesen,” 1959, Vol. 30, pp. 417-428.

95. Henriksen, J.F., “The Corrosion and Protection of Steel in Saturated Ca(OH)2 Contaminated with NaCl. Corrosion Science,” 1980, Vol. 20, pp. 1241-1249

96. Gjorv O.E and O. Venesland, “Sea Salts and Alkalinity of Concrete,” Journal of American Concrete Institute, 1976, Vol. 73, No. 9, pp. 512-516.

97. Ogura, K. and T. Ohama, “Pit Formation in the Cathodic Polarization of Passive Iron: Effects of Anions,” Corrosion Science, Vol. 37, No. 10, p. 572.

98. Uhlig, H.H., Corrosion and Corrosion Control, John Wiley and Sons, NewYork, 1983.

99. American Society for Testing and Materials. Half-Cell Potentials of Uncoated Reinforcing Steel in Concrete, ASTM C876-87. Philadelphia: ASTM, 1987.

100. Jones, Denny A., Principles and Prevention of Corrosion; Macmillan New York, 1992.

101. Escalante, E., Ito, S., and Cohen. M., “ Measuring the Rate of Corrosion of Steel in Concrete”, Annual Report NBSIR 80-2012, National Bureau of Standards, Gaithersburg, Md., March 1980, pp.1-26

102. Escalante, E., Whitenton, E., and Qui, F., “Measuring the Rate of Corrosion of Reinforcing Steel in Concrete”, Final Report NBSIR 86-3456, National Bureau of Standards, Gaithersburg, Md., Oct. 1986 pp1-27.

103. Clear, K.C., “Measuring Rate of Corrosion of Steel in Field Concrete Structures”, Transportation Research Record, 1211, pp.28-36.

104. Stern, M., and Geary, A.L., “A Theoretical Analysis of the Shape of the Polarizing Curves”, Journal of Electrochemical Society, Vol. 104, 1957, pp. 56-63

105. Mansfield, F., “Polarization Resistance Measurements: Experimental Procedure and Evaluation of Data”, Electrochemical Techniques for Corrosion, NACE, Houston, 1977, pp. 18-26

106. Gonzalez, A.M., Feliu, S., Andrade, C., and Rodriguez, I., “On-site Detection of Corrosion of Reinforced Concrete Structures”, Materials and Structures, Vol. 24, 1991, pp. 346-350.

107. Wheat, H.G., and Z. Eliezer. “Some Electrochemical Aspects of Corrosion of Steel in Concrete.” Corrosion, Vol. 41, No. 11 (Nov. 1985); pp 640–645.

VITAE

Name: Mohammed Ismail

Date of Birth: 2nd February 1979

Nationality: Indian

Bachelor Degree: Bachelor of Engineering in Civil Engineering from Osmania University (2001), Hyderabad, AP, INDIA.

Masters Degree: Master of Science in Civil Engineering (March 2005), from King Fahd University of Petroleum and Minerals, Dhahran, Saudi Arabia.

E-mail ID: ismailzaheer@yahoo.com